Development of new dendritic ligands for copper mediated Atom Transfer Radical Polymerization (ATRP) of methyl methacrylate.

By

Lucky Moni

A thesis submitted in partial fulfillment of the

Requirement for the degree of

Doctor of Philosophy

In the Department of Chemistry

University of the Western Cape (UWC)

UNIVERSITY *of the*
WESTERN CAPE

Supervisor: Professor S.F. Mapolie

November 2007

Revised May 2008

Declaration

I, the undersigned, hereby declare that the work titled "**Development of new dendritic ligands for copper-mediated Atom Transfer Radical Polymerization (ATRP) of methyl methacrylate"** is my own original work and that I have not previously in its entirety or in part submitted it at any university for a degree and all the sources I have used or quoted have been indicated and acknowledged by means of complete references.

.....

Lucky Moni

Acknowledgements:

It has been a longest journey, many people contributed in different ways and I would like to extend my sincere thanks to all of them but I will mention the few: I say thanks to;

- **My supervisor: Prof S.F. Mapolie** for tolerance, support, for providing skills and guidance, and for being a source of knowledge.
- Organometallics group (J. sibanyoni, M, Sibaca, S. Titinchi, H. Abbo, N (D). Malumbazo, N. Mungwe, J. van Wyk, R. Malgas, J. Mugo, Y. Tancu, N. Mketho and S. Ray) for being a special team, I will always remember you.
- Timothy Lesch, and W. Jackson for your patience and skills
- Prof J. Darkwa and *the group* for being a fountain of knowledge.
- Special friends: S. Nelana, T. Tamahane and M. Siguba. N. Radasi, S.B. Matyeli, T.M. Ngxola, P. Ntliziywana, S. Mbulungwana. M Putu, Z. Mavuso Y. Mndubu. B. Matyeli (my late cousin), S. Mbutalala, V. Mtshemla, T. Papo, and S. Gcelu.
- KoNcibana, OoNojaholo, OoNyembezana (ekhaya) Nama Qocwa OoZikhali (kulomama) nasebazalini bam uMr J.N. Moni noMrs N. Moni (Gxadasi) nasebantwaneni basekhaya uN. Moni (Mafungwashe), V (vuvu). Moni and S.T. Moni (Iphelo) ndithi beningumthombo wamandla ndiyazidla ngani.
- To all the people in the chemistry Department for allowing me to be part of them.

Lastly I want to extend my special thanks to National Research Foundation for financial assistance and UWC research committee for the financial support. Once again thanks to the University of the Western Cape for giving me an opportunity to better my life.

CONFERENCE CONTRIBUTION:

1 L.Moni. and S.F. Mapolie **2004**

Dendritic polyimines in Cu mediated ATRP of MMA

37th National Convention of the South African Chemical Institute. CSIR International convention center, Pretoria.

2 L. Moni and S.F. Mapolie **2004**

Dendritic ligand based catalysts in Cu mediated ATRP

Catalysis Society of South Africa, Potchefstroom

3 L. Moni and S.F. Mapolie **2005**

Dendritic ligand based catalysts in Cu mediated ATRP

Cape Organometallic Symposium. Cape Town.

4 L. Moni and S.F. Mapolie **2005**

Dendritic ligands in Cu copper catalyzed ATRP

Catalysis Society of South Africa, Midrand

5 L. Moni and S.F. Mapolie **2006**

Dendritic ligand based catalysts in Cu mediated ATRP

Organometallic and their applications (OATA). Cape Town.

6 L. Moni and S.F. Mapolie **2006**

Dendritic ligands in Cu copper catalyzed ATRP

15th international symposium on homogeneous Catalysis, Sun city

ABBREVIATIONS:

Ar	= aryl
ATRA	= atom transfer radical addition
ATRP	= atom transfer radical polymerization
Bu	= butyl
DAB	= diaminobutane
Et	= ethyl
G	= generation
GC	= gas chromatography
GPC	= gel permeation chromatography
h/hrs	= hour/hours
HMTETA	= 1,1,4,7,10,10-hexamethyltriethylenetetramine
HPEI	= hyperbranched polyethyleneimine
IR	= infra-red
L	= ligand
m	= monomer
Me	= methyl
M_n	= number average molecular weight
M_t	= transition-metal
M_w	= weight average molecular weight
MMA	= methyl methacrylate
NMR	= nuclear magnetic resonance

PDI = polydispersity index

PMDETA = N,N,N′,*N*′,*N*′′-pentamethyldiethylenetriamine

Ph = phenyl

R = alkyl or aryl

RAFT = reversible-addition fragmentation chain transfer

STY = Styrene

t = tertiary

TEMPO = 2,2,6,6 – tetramethyl – 1- piperdionyloxy

TMEDA = tetramethylethylenediamine

THF = tetrahydrofuran

X = halogen

ABSTRACT

A variety of nitrogen based dendritic ligands have been synthesized and used in copper mediated Atom Transfer Radical Polymerization (ATRP) of MMA. These ligands were derived from the commercially available Generation 1 polypropyleneimine dendrimer DAB-$(NH_2)_4$. The first set of ligands was synthesized by reacting DAB-$(NH_2)_4$ with aromatic aldehydes such as 2-pyridinecarboxyaldhyde and 4-t-butyl benzaldehyde to form imine functionalized dendrimers. Analogous secondary amine functionalized dendrimers were also synthesized by reducing the abovementioned imine functionalized dendrimers using sodium borohydride. The ligands produced were characterized by ^{13}C / ^{1}H NMR, and infra-red spectroscopy as well as elemental analysis to confirm its structure. The ligands were then used in copper mediated ATRP of MMA. The resulting polymer solutions were analyzed by Gas Chromatography (GC) to monitor the monomer conversion while the isolated polymers were analyzed by gel permeation chromatography (GPC) for molecular weight determination. Results showed that the primary and secondary amine and imine dendritic ligands were not efficient in promoting ATRP reactions. This led to the modification of DAB-$(NH_2)_4$ using methyl methacrylate to replace the peripheral amino groups of the DAB-$(NH_2)_4$ with tertiary amine groups. A second generation tertiary amine dendrimer was also synthesized in a similar fashion. The ligands obtained were then characterized using ^{13}C and ^{1}H NMR spectroscopy. The tertiary amine dendrimers were used in copper mediated

ATRP of MMA. The polymerization medium was analyzed over time using GC to monitor monomer conversion while GPC was used for molecular weight determination of the resulting polymers. The results obtained using the methyl methacrylate modified ligands indicated that in the case of MMA polymerization, these ligands essentially conformed to the requirements of a good ATRP system. However in the preliminary studies, when employed in copper mediated ATRP of styrene, these ligands did not perform well. Further investigation is needed to improve the performance of these ligands in styrene polymerization under ATRP conditions.

Chapter One:

INTRODUCTION AND LITERATURE REVIEW

Contents *Page*

Chapter Two:

SYNTHESIS AND CHARACTERIZATION OF POLYPROPYLIMINE DENDRIMER DERIVATIVES

Contents *Page*

Chapter Three:

G1-POLYPROPYLENEIMINE DENDRIMER AND ITS IMINE AND AMINE DERIVATIVES: ITS USE IN COPPER MEDIATED ATOM TRANSFER RADICAL POLYMERIZATION OF METHYL METHACRYLATE

Contents *Pages*

Chapter Four:

METHYL METHACRYLATE FUNCTIONALIZED GENERATION 1 AND 2 POLYPROPYLIMINE DENDRIMERS IN COPPER MEDIATED ATOM TRANSFER POLYMERIZATION OF METHYL METHACRYLATE

Contents *Page*

Chapter Five:

CHAPTER ONE:

Contents *Pages*

1.1 Introduction

Atom Transfer Radical Polymerization (ATRP) is a relatively new generation of free-radical process that has proven to be a possible solution to the problem of the instability of free-radicals, which ultimately lead to uncontrollable chain transfer or chain disproportionation reactions.[1] ATRP has fulfilled an important quest by synthetic polymer chemists, to gain control not only over the molecular weights and polydispersities of polymer chains but also over polymer architecture and the manipulation of polymer end groups.

The ATRP process has its roots in organic chemistry reaction namely Atom Transfer Radical Addition (ATRA),[2-6] which is sometimes called the Kharash addition. ATRP occurs in the presence of a catalyst system, which consists of a co-ordination metal complex in which the transition-metal is in a low oxidation state with an organic halide as an initiator. The reactivity of these catalysts is highly influenced by the type of ligands present in the co-ordination complex. Monodentate ligands produce polymers with unpredictable molecular weights and high polydispersities.[1] Bidentate ligands, on the other hand, produce polymers with predictable molecular weights and low polydispersities. Polydentate ligands in contrast produce polymers with well-defined molecular weights and very low polydispersities. In this chapter we review some of the recent developments in the area of ATRP.

1.2 Literature review

1.2.1 Controlled living polymerization in general

Polymers are long chain molecules made up of small repeat units (mers) called monomers[7]. The chains in the polymers are of different lengths depending on the degree of polymerization. These macromolecules are important mostly because of their physical properties, in contrast to low molecular weight molecules, which are important due to their chemical properties. An important feature of polymers in terms of its physical properties is their physical strength. Often this can be related to its bulk density together in conjunction with the molecular weight of the polymer. The density of a polymer is largely affected by the linearity of the chains as well as the stereo arrangements (tacticity) of substituents on the polymer backbone.[8] Different polymers have different physical and chemical properties and hence are applied differently. Thus polymers may have varying degrees of crystallinity (normally observed from their melting points) or amorphicity (observed from their glass transition temperatures).

Polymers were first produced by step-growth and chain-growth polymerization.[8] Step-growth polymerization is a condensation reaction of poly-functional organic monomers that usually involves the elimination of water or other small molecules as a by-product. According to Carothers, step-growth polymers are those in which the formula of the repeating unit lacks certain atoms that are present in the

monomer(s) from which it is formed or to which it may degrade[8] as shown in Figure 1.1.

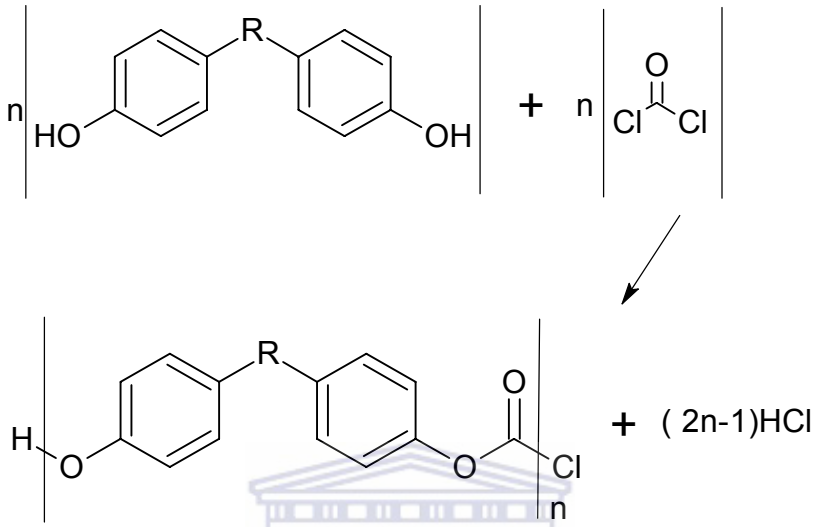

Figure 1.1: *Condensation polymerization*

Conventional chain-growth polymerization involves mainly the reaction of monomers containing a carbon-carbon double bond and features addition to the double bond without any loss of a small molecule (see Figure 1.2). This type of chain-growth polymerization consists of four elementary steps such as initiation, propagation, chain transfer and termination. This type of polymerization produces very high molecular weight polymers at a faster rate when compared to step-growth polymerization. It also requires an initiator with a reactive center for polymerization to occur.

Figure 1.2: *General addition polymerization*

The reactive center of the initiator may either be a free radical, a cation, or an anion. In the case where the reactive center is a cation, the polymerization will propagate by addition of the cationic reactive center to the C-C double bond of a large number of monomers. Such a reaction is known as cationic polymerization. In this process termination is also likely to occur when active centers undergo chain transfer. The initiators in this particular process are normally protic acids or Lewis acids.

In the case where the reactive center is an anion, the reaction proceeds by addition of anionic reactive center to the C-C double bond of the monomers and the reaction is called anionic polymerization. The greatest breakthrough in anionic polymerization occurred in 1956 where styrene as monomer was polymerized using an alkyl-lithium as an initiator and the reaction proceeded without termination or chain transfer to yield a polymer with low polydispersity and an active chain end (see eq 1). This active chain end is able to resume polymerization when a fresh monomer is added and because of this ability, it is called living anionic polymerization.[9]

$$C_4H_9Li + Styrene \rightarrow C_4H_9\text{-polystyrene}^-Li^+ \quad (1)$$

In the case where the active center is a free radical, in the presence of a monomer the active center will propagate by addition of an active radical to the C-C double bond of a large number of monomers. Such a reaction is called free radical polymerization. Free-radical polymerization is one of the older processes employed in the synthesis of polymers.[10] Free radical polymerizations are important for the industrial production of commodity polymers, which account for the major fraction of polymers produced commercially.

Free-radical polymerization offers many advantages such as its ability to polymerize a wide variety of monomers and the fact that it is easy to be performed in bulk, aqueous emulsion or suspension polymerization process. However, the high reactivity and instability of free-radicals which leads to uncontrollable transfer reactions or fast irreversible termination reactions *via* coupling or disproportion reactions has been a major draw-back to the free-radical polymerization process. This drawback has limited the use of the free-radical process in the production of polymers.[11]

One of the most important goals of synthetic polymer chemists is to gain control not only of the molecular weight and polydispersities of polymers but also their architecture and the nature of the end groups. Living ionic polymerization, in which neither transfer nor termination reactions take place, appear to be the best

technique to achieve these goals.[9] Polymers produced by this method have very narrow molecular weight distributions. In living ionic polymerization, molecular weight of the polymer is directly proportional to conversion and in free radical polymerization high molecular weight polymers are produced in the initial stages whereas in step-growth polymerization high molecular weight polymers are produced only as conversion approaches 100%.[12] These living ionic processes, anionic in particular, suffer from their sensitivity towards a number of reagents, particularly hydrogen active compounds such as water. This has made the industrial application of these living ionic systems difficult. Recently, controlled radical polymerization was reported in which the problem of fast termination of free radical polymerization was circumvented. Three types of radical polymerization processes have been reported.[13-15] The first one involves the reversible homolytic cleavage of a dormant chain end to form a radical chain end and a stable radical that cannot initiate any polymerization. An example of this type of polymerization involves TEMPO (2,2,6,6-tetramethyl-1-piperdinyloxy) free radical mediated polymerization of styrene[13] and the polymerization of acrylates catalyzed by cobalt porphyrin.[14]

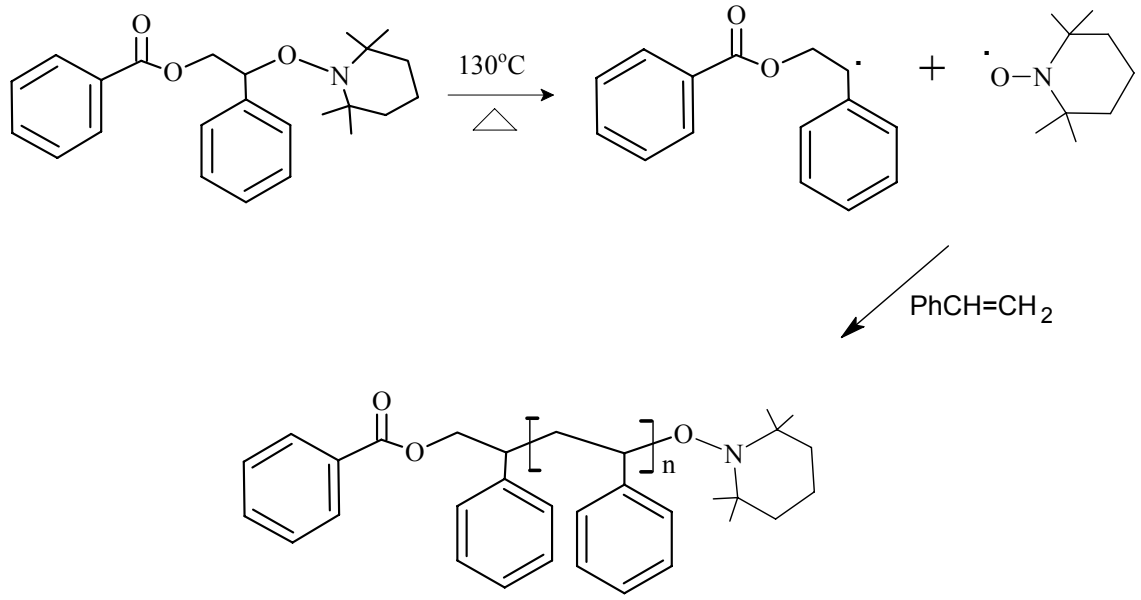

Figure 1.3: *Controlled living radical polymerization in presence of nitroxy*

The second type is based on bimolecular transfer of an end group between an active and dormant chain. This process was observed in the nitroxy mediated polymerization of styrene *(see Figure 1.3)*.[15] The only disadvantage of these two controlled radical polymerization methods is their limitation to a specific monomer.

The third type is based on reversible addition fragmentation chain transfer (RAFT) (Figure 1.4).[16] Its initiating system consists of a standard radical initiator and a dithioester-transfer agent. The terminal end of the dormant chain is a dithioester. The advantage of this system is its simplicity and the absence the catalyst. The major disadvantage of the RAFT system is the presence of low molecular weights radicals, which are available for termination reactions.

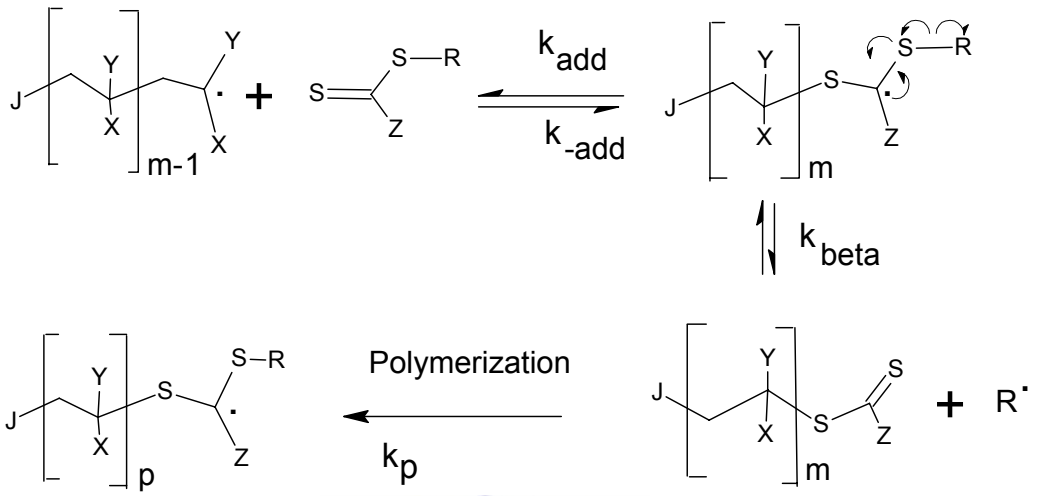

Figure 1. 4: *The RAFT mechanism*

1.2.2. Atom Transfer Radical polymerization(ATRP) and its roots

In 1995, Sawamoto and Matyjaszewski independently reported the use of transition metal coordinated systems as catalysts to achieve a controllable living radical polymerization process. Based on the mechanism of this polymerization process it was named Atom Transfer Radical Polymerization (ATRP).[1] The mechanism of ATRP proceeds via homolytic cleavage of a carbon-halogen bond catalyzed by the transition metal complex[17] (Scheme1.2). This process has its roots in organic synthesis in the form of Atom Transfer Radical Addition (ATRA) sometimes called Kharash addition[3] (Scheme 1.1).

The ATRP process uses a catalyst system that consists of a simple organic halide as an initiator, an electron donating compound as ligand and a transition metal salt in a low oxidation state as a catalyst. The mechanisms for both ATRA and ATRP are displayed in Schemes 1.1 and 1.2 respectively.

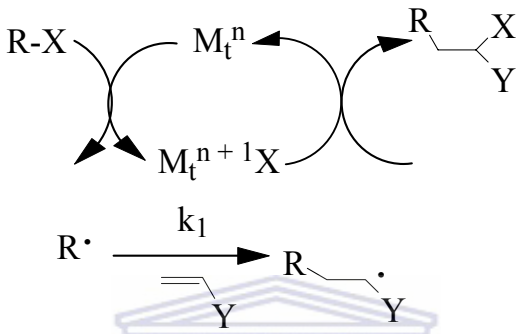

Scheme 1. 1: *Atom Transfer Radical Addition*

Initiation

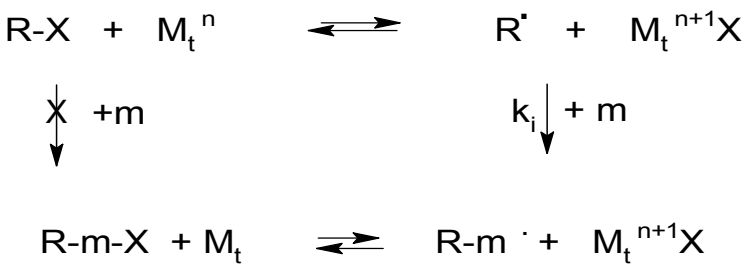

Propagation

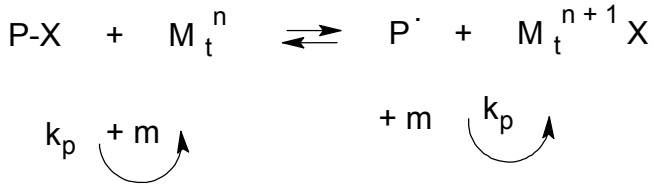

Scheme 1. 2: *Atom Transfer Radical Polymerization*

R-X in both schemes represents the alkyl halide which acts as the initiator and where **X** is a halide atom, **m** in Scheme1.2 represents for the monomer whereas **M** represents the transition metal atom with superscript **n** indicating the low oxidation state. In the ATRP mechanism, the first step involves the homolytic cleavage of the **R-X** bond forming the radical **R**$^{\cdot}$, simultaneously the halogen atom is transferred to the metal center resulting in an increase in the oxidation state of the transition metal. The **R**$^{\cdot}$ radical adds to the double bond of the vinyl monomer forming a propagating radical which then re-accepts the halogen atom, regenerating the original low oxidation state metal center. The reaction will proceed until most of the monomer is consumed.

It can be understood from this mechanism that many radicals existing at the same time might combine or disproportionate resulting in the termination of the process. In order to keep the concentration of radicals as low as possible and to minimize the bimolecular termination, the equilibrium between dormant and active radical species should be shifted to the dormant side. This is where other components of the catalyst system becomes important.[18] The catalyst is the central component of the ATRP process. It does not only affect the position of the equilibrium but also the dynamics of the exchange and as a result it controls the polymerization. Sawamoto's first catalyst system was based on $Ru(PPh_3)_3Cl_2$; however the effectiveness of this catalyst was only achieved if a sterically hindered aluminum alkyl or $Al(O^iPr)_3$ was used as a co-catalyst[19,20] (Scheme 1.3).

The use of the co-catalyst limited the choice of solvent and excluded the use of functionalized monomers, which are prone to reaction with the aluminum alkyl compounds.

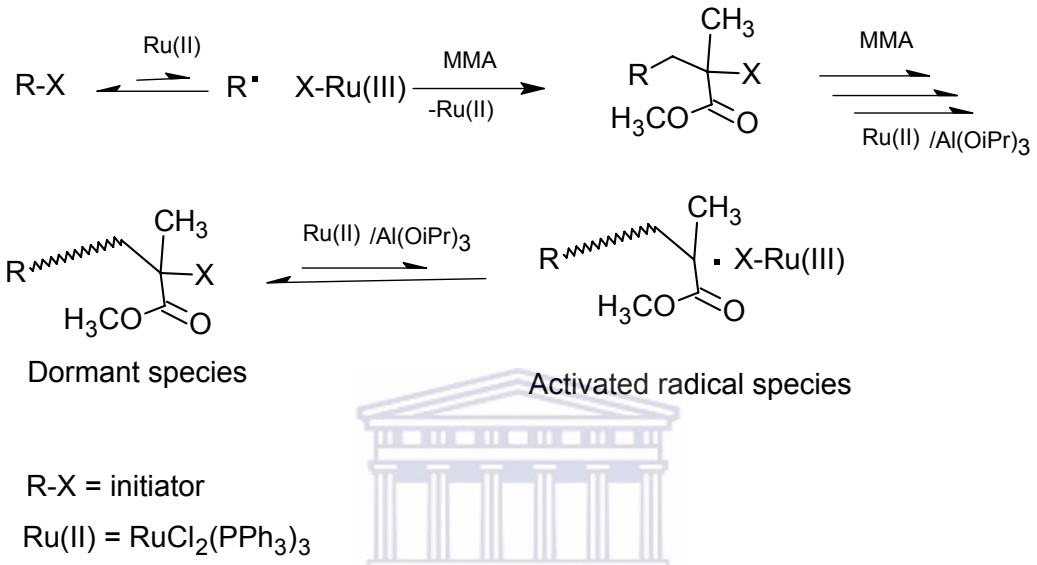

Scheme 1. 3: *Sawamoto's Ruthenium mediated ATRP*

In 1997 Sawamoto reported the ability of these ruthenium systems to work effectively in the presence of water and methanol, and the possibility of re-initiation after isolating the functionalized dormant polymer, which qualified this system as living polymerization process.[21-23] In 1999 Demonceau and coworkers reported a ruthenium system without the co-catalyst which performed efficiently in living polymerization as was expected.[24] On the other hand, Matjyaszewski the pioneer of ATRP reported the first catalyst based on a Cu(I) salt, bipyridine as a ligand and alkyl halide as an initiator but without a co-catalyst[25-29] (Scheme 1.4). The results were equally as good as Sawamoto's. This copper(I) mediated

system could polymerize a variety of vinyl monomers such as styrene, methyl methacrylate and methyl acrylate.

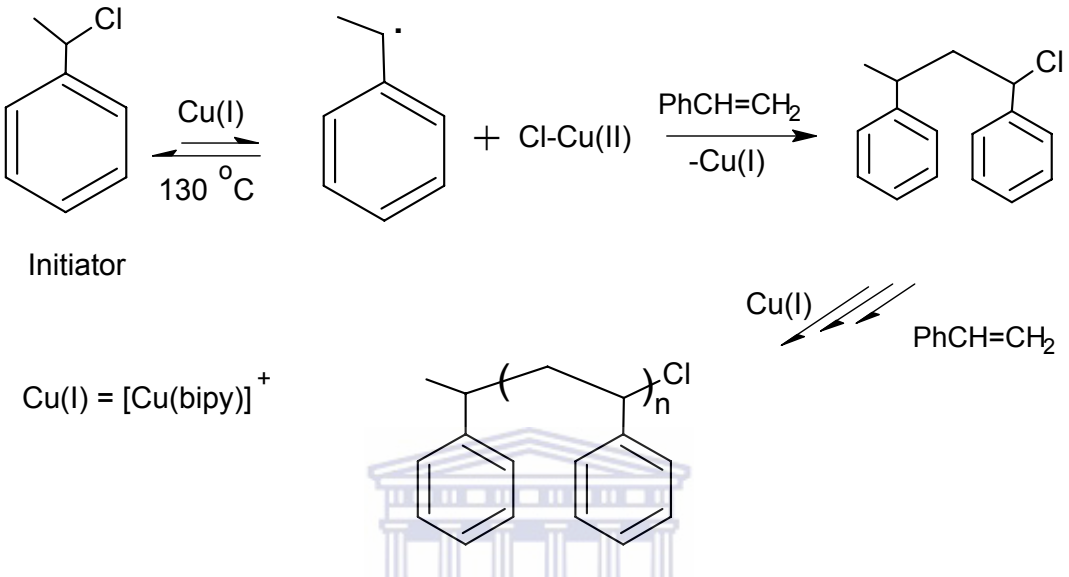

Scheme 1. 4: *Matyjaszewski's Copper mediated ATRP*

The choice of these two transition metals (Cu and Ru) by the above two researchers is attributable to the effectiveness of the two metals in the ATRA of sulfonyl chloride to olefins.[30,31]

1.2.3. Other transition metals in ATRP

The work of Sawamoto and Matajyszewski led to the investigation of many other transition metals which have performed well in other fields of chemical synthesis. The research included the investigation of transition metals such as rhodium, nickel, palladium, molybdenum, iron, rhenium and others in ATRP.

Rhodium, nickel[32], palladium[33], copper and ruthenium complexes were used as catalysts in the addition of alkyl halides to olefins, in the so-called Kharasch reaction, an example of an ATRA reaction. Since ATRP stems from ATRA, it therefore made sense to expect that complexes based on these transition-metals could also be active catalysts in the ATRP process.

This was indeed true as reported in the case of Ni[34-37], Pd[38], and Rh[39] but their catalytic activities were much lower than those of Copper and Ruthenium catalysts as was the case in ATRA reactions as well. Rhodium is well known as a catalyst in the hydroformylation process[40] and other homogeneous catalytic processes such as hydrogenation of alkenes[41], using, for example the Wilkinson's catalyst in particular. The application of this transition metal in ATRP was first realized 1996 when it polymerized styrene in the presence of arenesulfonyl chloride as an initiator[42] though, producing polymers with high polyderispersities and poor control of molecular weights. Different and more acceptable results as far as ATRP requirements are concerned were seen with methyl methacrylate as monomer. Thus, good control of polymerization and lower polydipersities were obtained.[43] In the development of oligomerization and polymerization processes nickel has been one of the major catalysts widely used industrially. With regards to ATRP, nickel as a catalyst has also been successfully used. Since nickel has a wide variety of possible oxidation states such as nickel(0-IV), zerovalent nickel was explored in ATRP. As early as 1990,

Otsu attempted ATRP with Nickel(0) but due to poor initiator efficiency poor results were obtained. Different types of ligands were tried with nickel such as [{$C_6H_3(CH_2NMe_2)_2$-o,o'}Br] a complex that was most reactive in the atom transfer addition reactions (ATRA), it performed well in ATRP but at temperatures not above 80^oC.[44] More work was done on transition metal mediated ATRP which included trying nickel mediated systems using triphenyl phosphines as ligands. As in the ruthenium mediated ATRP, $Al(O\text{-}^iPr)_3$ was used as a co-catalyst to improve controllability of polymerization.[45] Although triphenylphosphine was effective as a ligand its complexes were unstable and also not soluble enough. The use of tri-n-butylphosphine was thus a solution to the problem of solubility of the ligand.[46] Palladium in the form of the acetate or chloride salt with triphenyl phosphine as ligands also found application in the ATRP[38] although not much has been reported compared to Nickel.

Iron and ruthenium are metals of the same group in the periodic table and their behavior is expected to be similar. These two metals have received a thorough study in atom transfer radical addition (ATRA) reactions. Iron was first investigated after unusual results were obtained from a steel autoclave used to perform a polymerization reaction of acrylonitrile in carbon tetrachloride and chloroform. Adducts were obtained between the haloalkyl solvents and acrylonitrile but polymerization was also observed. The formation of adducts was explained as being caused by oxidation of Iron resulting from the corrosion of the autoclave which catalyzed the addition of those haloalkyls to the acrylonitrile

double bond.[47] This was the beginning of the investigation of iron in ATRA. Iron featured a great deal in ATRA and therefore it was expected that it should perform well in ATRP. Iron was then tried in ATRP and early experiments involved the use of tri-phenylphosphine as ligand in conjunction with a Fe(II) salt.[48,49] However, the polydisperisities of the polymers produced were high. In addition, even though $Al(O^iPr)_3$ was used to accelerate the polymerization there was no control of the molecular weight in the process.[50]

The investigation of iron in ATRP subsequently proceeded to the exploration of bulky nitrogen based ligands used with Fe(II) salts as catalysts and this resulted in more positive outcomes. These bulky ligands included nitrogen based ligands such as tri-n-butyl amine ($N(^nBu)_3$ and dialkylaminopyridine which were used with $FeBr_2$ salt as a catalyst by Gobelt and Matyjaszewski.[51]. This system, however failed to polymerize styrene.[52] α-Diimine ligands have also been used with $FeCl_2$[53] as a catalyst together with bulky nitrogen based ligands as shown in Figure1.5.[54] All these Iron mediated systems with bulky nitrogen based ligands except the Gobelt and Matyjaszewski ligand[53] mentioned above produced results that met the requirements of controlled living ATRP systems. The use of ligands which do not contain nitrogen or phosphorous was also attempted and they produced polymers with well-defined molecular weights and low polydispersities.[55,56]

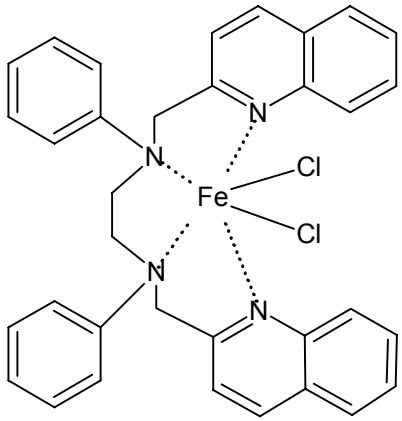

Figure 1.5: *Iron complex used as a catalyst in ATRP*

Molybdenum is usually employed in ATRA but has been applied in ATRP. Molybdenum, like many other transition metals, has been used widely as a catalyst in many chemical reactions. The first report of this metal in ATRP involved lithium molybdate(V) complexes which however performed very poorly, producing polymers with high polydispersities. This was ascribed to the extreme air-sensitivity of these lithium containing complexes.[57] Side reactions were also witnessed where lithium molybdate(V) reacted with initiators to produce lithium salts.

Approximately two years after the above publication, it was reported that Mo(III)/Mo(IV) with phosphine ligands could produce polymers under ATRP conditions. This publication provided better options where molybdenum complexes were easy to work with and better results obtained.[58] It was also reported in the same year by the same group that this Mo(III)/Mo(IV) system can accommodate two different ligands at same time and still produce better

results.[59] The preferred oxidation states of this transition metal are Mo(III)/Mo(IV) because it was believed that Mo(II)/Mo(III) do not provide enough radicals to sustain the polymerization.

Rhenium, a metal that is outside of the late transition elements which are popular metals in the field of catalysis, has shown its ability to produce polymers under the conditions of ATRP. It was reported in 1999 that rhenium(V) with phenyl-triphosphine as a ligand can be used as a catalyst in ATRP. The reaction had to be initiated with an alkyl iodide in the presence of additional aluminium triisopropoxide (Scheme1.5).[60] This catalyst was reported to induce polymerization at high temperatures, giving polymers with narrower polydisperisities. Low PDI's were favoured as temperatures were decreased to between 30^{o}C and 100^{o}C. There is still much of work that could be done on this catalyst in order to optimize it. It appears that these systems could not be quenched in the conventional manner used for ATRP systems but rather with 2,2' 6,6'-tetramethylpiperidine-N-oxyl(TEMPO) which is a radical source able to stop radical polymerization including ATRP.

Since copper has a proven record of good results under ATRP conditions especially with nitrogen based ligands so it will be the chosen a transition metal for this work. Some other transition metal may be tried under the ATRP condition but their results will only be reported in this thesis if they are better than what copper may produce. The most likely metal to be tried is nickel.

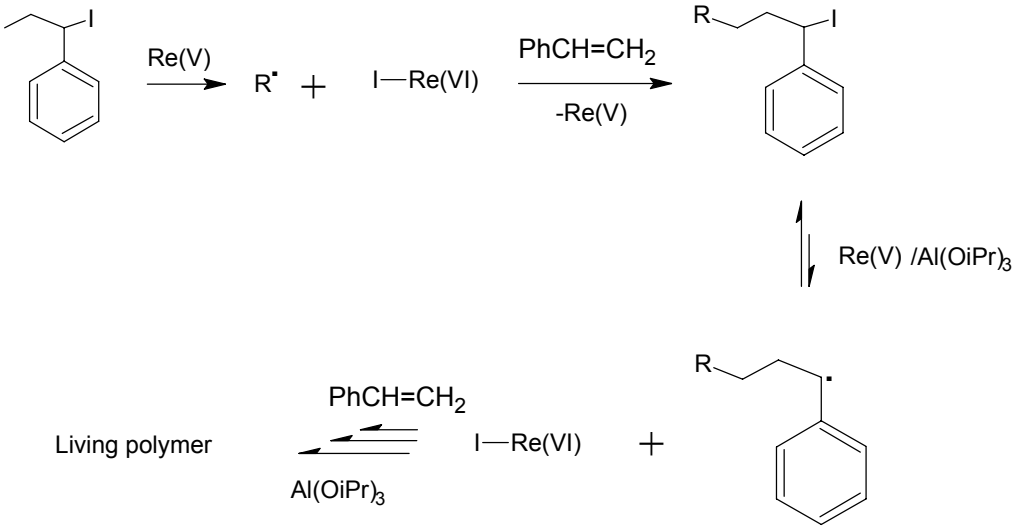

Scheme 1. 5: *Rhenium(V) mediated ATRP of styrene.*

1.2.4. Types of Ligands and their influence in ATRP catalysis

Besides being active as ATRA catalysts, nickel and palladium complexes together with iron complexes have found use in coordination polymerization where they were able to polymerize olefins.[61] These late transition metals were known previously to only oligomerize olefins due to facile chain termination *via* beta-hydride elimination.[62-63] However because of the newly designed diimine ligands, these late transition metals have been shown to be efficient catalysts for the polymerization of olefins. The influence of these ligands came about as a result of their bulkiness which retarded the rates of chain transfer.[64]

Even in the case of the ATRP process, the reactivity of the ATRP catalyst systems is highly influenced by the type of ligands used. The effect of the ligand extends to both the chemical structure and steric bulkiness of the ligand. Monodentate ligands such as pyridine produced polymers with unpredictable molecular weights with high polydispersities[65] that do not fulfill the requirements of ATRP. On the other hand, bidentate ligands such as 2,2-bipyridine, which was the first ligand to be used by Matjyaszewski in the polymerization of styrene, methyl methacrylate, and methyl acrylate, resulted in well-defined polymers with narrow molecular weight distribution. In an effort to improve the efficiency of these catalyst systems, other ligands have been explored mostly having a large number of chelating sites. These include alkylpyridine methylamine[65,66] and phenanthroline derivatives[67], as well as substituted terpyridines.[68] All of these ligands gave well-defined molecular weights and narrow molecular weight distributions under ATRP conditions. However, another factor that negatively affected the efficiency of these aromatic compounds as ligands in metal mediated ATRP was their poor solubility in the reaction medium. The need to improve solubility led to use of 4,4-diheptyl-2,2-bipyridine[42] which is soluble in common organic solvents. This improved the control of polymerization and led to a dramatic improvement in the polydispersities of polymers produced. The solubility of these organic compounds was attributed to the long chain alphatic substituents. Aromatic ligands have been very popular in co-ordination polymerization especially diimine compounds because of their bulkiness which positively enhanced the use of nickel, palladium, iron and cobalt catalysts to

polymerize olefins.[70] In ATRP, however bulkiness is less important, this is evident in the case of bipyridine, which produced polymers when used as a ligand in copper mediated ATRP process but failed to polymerize olefins in co-ordination polymerization. In ATRP the bulkiness of the ligand reduces the rate of activation, as the metal center is less accessible to the halogen atom.[71] Bulkiness that also has some rigidity might completely deactivate the catalyst by blocking access of the halogen atom to the metal center. As much as bipyridine was an effective ligand, solubility of Cu(II) species with these aromatic ligands was a problem and this led to the modification of the structure of bypyiridine using different substituents as shown in Figure 1.6.

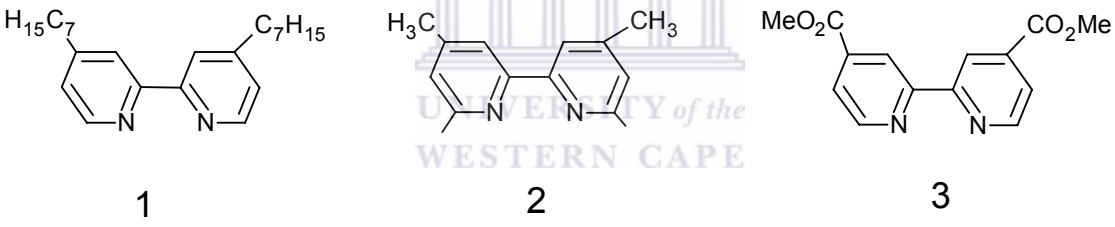

Figure 1. 6: *Modified 2'2-bipyridine ligands*

The ligands with electron withdrawing substituents such as (3) were found to be unsuccessful in the ATRP. Increasing the number of chelating sites also improves the performance of a ligand. Polydentate ligands such as MeTREN [tris(2-dimethylamino)-ethylamine], TMEDA- (Tetramethylethylenediamine), PMDETA(N,N,N,N,N-pentamethyl diethylene triamine) and HMTETA (1,1,4,7,10,10-hexamethyltriethylenetetramine) (Figure1.7) proved to be a solution to the solubility problem posed by aromatic ligands and they are also

less rigid which also allows easy access of the halogen atom to metal center. The use of these ligands led to production of polymers with well-defined molecular weights and very low polydispersities.[72]

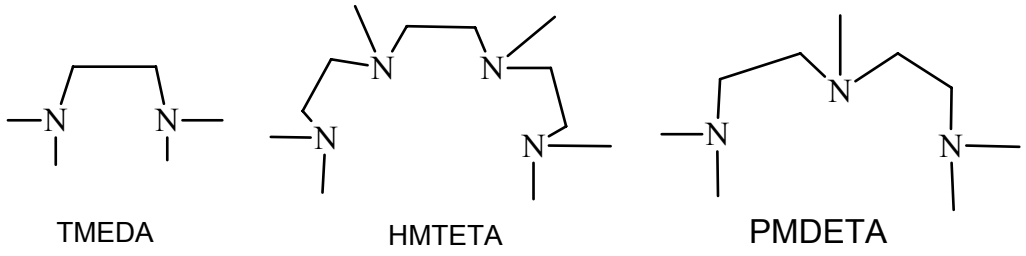

Figure 1 .7: *Polydentate nitrogen based aliphatic ligands used by Matyjaszweski*

In ATRP, nitrogen based compounds proved to be the most efficient ligands compared to other types of ligands. Therefore focus of this work is combining the bulkiness and the flexibility of the aliphatic chains hoping to achieve good solubility, less hindrances and good control of polymerization. In 2006 this family of nitrogen based ligands was expanded by introduction of hyperbranched macroligands reported by Frey and coworkers.[73] These macroligands carried the flexibility provided aliphatic carbon chains and the multi-chelating sites in the form of nitrogen atoms. These macro-ligands produced polymers with low polydispersities and well defined molecular weights. This work will make reference to these macroligands of Frey and the ligands of Haddleton as most of the ligands synthesized although are dendrimers of different kind have some resemblance in certain group or substituents. Haddleton and coworkers in 1997 acknowledged that although Brookhart's ligands performed well in the polymerization of ethylene they were not tried in ATRP at the time. In 2007, a

report in which a ligand of Brookhart's type was released. The ligands produced well define polymers with lower polydispersities.[74] These polydentate ligands provide electronic properties similar to those found in diimine functionalized ligands.

It is clear from the foregoing discussion that ligands which are nitrogen based are the most commonly used ligands in ATRP and it is suggested that changing the structural designs would have an impact on the performance of the ligands. Exploitation of structural design of nitrogen based ligands in the ATRP has to be linked with fact that copper has been the most effective transition metal in ATRP thus far and copper is the only transition metal in the fore-mentioned transition metals that has not been used with ligands such as sulfur, oxygen or phosphorus for ATRP. Phosphorus ligands have also contributed significantly in ATRA and ATRP.

The special characteristic of dendrimers is the easiness to modify its surface. This characteristic can be exploited by modifying the surface functionalities using substituents which a have proven ability of acting as ligands in the successful ATRP processes. This work is built around this thought about dendrimers.

1.3 Objectives of this work

Prominent researchers in the field polymer synthesis state that the key to tailoring the reactivity of the catalyst for ATRP is the choice of the ligand. They

further assert that multidentate nitrogen based ligands perform well in copper mediated ATRP by providing the desired reactivity.[73] However, not all multidentate ligands are suitable in ATRP. It is shown in a paper by Matyjaszewski *et al*[73] that if there are more than two carbons linking two coordinating nitrogens atoms in the ligand higher polydispersities and less control are observed. In most ligands especially the nitrogen based ones they commonly have less than three carbon atoms between chelating nitrogen atoms and that is in agreement with the observation by Matyjasezweski. The question that arises is, should the ligands with propylene linkers be ignored as potential ligands for ATRP systems?

The aim of this work is to synthesize new ligands based on a multidentate dendrimeric organic compounds starting from the commercially available polyethylenepropylimine dendrimer, (DAB$(NH_2)_4$) and to evaluate these in copper mediated ATRP of methylmethacrylate (MMA). The modification of this dendritic ligand will take two forms as indicated below:

- Modification of multidentate dendrimer (DAB$(NH_2)_4$) using aromatic substiuents.
- Modification of this multidentate dendrimer (DAB$(NH_2)_4$) using flexible aliphatic substituents.

Although the main objective of this work is to develop the new dendritic nitrogen based ligands for copper mediated ATRP of MMA, it will also be of interest to evaluate the effect of the length of the aliphatic linker between the two chelating

nitrogen atoms on the performance of the multinuclear ligands in copper mediated ATRP.

1.4 Scope of the thesis

The work described in this thesis deals with the synthesis of polydentate nitrogen based compounds to be used as ligands in the Copper mediated ATRP of methyl metacrylate. All of the ligands are derived from commercially available generation-1 dendrimers of polypropyleneimine tetra amine ($DAB(NH_2)_4$). Copper complexes will not be isolated but an in situ approach will be followed. ^{1}H, ^{13}C NMR and infra-red(IR) spectroscopy, gas chromatography (GC), gel permeation chromatography (GPC) and elemental analysis are core analytical techniques used in this work.

1.5 Structure of the thesis

Conventional free radical polymerization is a widely applied method for producing polymers. Chapter one, gives a brief theoretical background of living ionic polymerization and their limitations. Types of Living radical polymerization mainly based on TEMPO and nitroxy radical polymerization are briefly discussed. This chapter presents the emergence of atom transfer radical polymerization (ATRP) in the year 1995 and its relationship with the old atom transfer radical addition (ATRA) is also discussed. The role of different transition metals in ATRP is explained. The contribution and the influence of different types of ligands in

ATRP are also presented with more emphasis on multidentate nitrogen based ligand.

In Chapter two, different types ligands were synthesized by modifying the commercially available polypropyleneimine dendrimer DAB-$(NH_2)_4$ with aromatic substituents *via* a condensation reaction between amino groups at the periphery of the dendrimer and a suitable aldehyde. The products were characterized by NMR spectroscopy, elemental analysis and IR spectroscopy. The other set of ligands with methyl methacrylate at periphery of the dendrimer was synthesized and fully characterized. The set of ligands were expanded to include the Generation 2 dendrimer and synthesized in a similar fashion as generation 1.

The aromatic functionalized dendrimers synthesized in Chapter two were used in Chapter three in the ATRP of methyl methacrylate. The kinetic studies of this polymerization were conducted to establish whether these ligands did help to promote living and controlled ATRP. The kinetic results were calculated from percentage conversions obtained from Gas chromatography (GC) and molecular weights from Gel Permeation Chromatography (GPC). The kinetic result were reported in graphs and discussed thereafter.

In Chapter four, the methyl methacrylate functionalized dendritic ligands were used in the ATRP of methyl methacrylate. Kinetic studies were conducted using GC for conversion and molecular weights of the resulting polymers were

determined using GPC. The ligands were also applied in the preliminary ATRP of styrene. The mixed halide based catalyst systems were the only set of active catalyst used in these reactions. In Chapter 5, the conclusion about the overall performance of these ligands is outlined.

1.6 References:

1. Wang, J. ; Matyjaszewski, K. *Macromolecules*. **1995**, 28, 7901.
2. Bellus, D. *Pure Appl. Chem*. **1985**, 57, 18273.
3. Kharasch, M.S. ; Jensen, E.V. ; Urry, W.H. *Science*. **1945**, 102, 128.
4. Kharasch, M.S. ; Jensen, E.V. ; Urry, W.H. *J.Am. Chem.Soc.* **1945**, 67, 1626.
5. Kharasch, M.S. ; Jensen, E.V. ; Urry, W.H. *J. Org. Chem.* **1938**, 2, 288.
6. Hey, D.A.; Waters, W.A. *Chem. Rev.* **1937**, 21, 169
7. Billmeyer, F.W.; *Text book of polymer Science*. Wiley: New York 3rd ed. **1989.**
8. Odian, G., *Principles of Polymerization*. Wiley & Sons Inc, 3rd ed. **1991**.
9. Szwarc, M. Living Polymer. *Nature*. **1956**, 178, 1168.
10. Curran, D.P. *Synthesis*. **1988**, 489.
11. Flory, P.J., *Principles of Polymer Chemistry* . Cornell Univ. Press. Ithaca NY, **1953.**
12. Webster, O. *Science*. **1991**, 251, 887.
13. Georges, M. K.; Veregin, R. P. N.; Kazmaier, P. M.; Hamer, G. K.; Saban, M. *Macromolecules*. **1994**, 27, 7228.

14. Waland, B. B.; Pszmik, G.; Mukerjee, S. L.; Fryd, M.; *J. Am. Chem. Soc*. **1994**, 116, 743.

15. Li, I.; Howell, B. A.; Matyjaszewski, K.; Shigemoto, T.; Smith, P. B.; Priddy, D. B. *Macromolecules* **1995,** 28, 6692.

16. Wang, J. S.; Gaynor, S.; Matyjaszewski, K. *Macromolecules*. **1995**, 28, 8051.

17. Patten, T.E. ; Matyjaszewski, K. *Acc. Chem. Res*. **1999**, 30, 2216.

18. Takahashi, H. ; Ando, T. ; Kamigaito, M. ; Sawamoto, M. *Macromolecules*. **1999**, 32, 6461.

19. Ando, T. ; Kato, M. ; Kamigaito, M. ; Sawamoto, M. *Macromolecules*. **1996**, 29, 1070.

20. Kato, M. ; Kamigaito, M. ; Sawamoto, M. ; Higashimura, T. *Macromolecules*. **1995**, 28, 1721.

21. Ando, T. ; Kamigaito, M. ; Sawamoto, M. *Tetrahedron*. **1997**, 53, 15445.

22. Takahashi, H. ; Ando, T. ; Kamigaito, M. ; Sawamoto, M. *Macromolecules*. **1999**, 32, 3820.

23. Nashikawa, T. ; Ando, T. ; Kamigaito, M. ; Sawamoto, M. *Macromolecules*. **1997**. 30. 2244.

24. Simal, F. ; Demonceau, A. ; Noels, A.F. *Angew. Chem. Int. Ed. Engl*. **1999**, 38, 538.

25. Haddleton, D.M.; Jasieczek , C.B.; Hannon, M. J.; Shooter, A.J. *Macromolecules*. **1997**, 30, 2190.

26. Wang, J.S. ; Matyjaszewski, K. *J .Am. Chem. Soc*. **1995**, 117, 5614.

27. Patten, T.E. ; Xia, J. ; Abernathy, J. ; Matyjaszewski, K. *Science*. **1996**, 272, 866

28. Percec, V. ; Barboiu, B. *Macromolecules*. **1995**. 28. 7970.

29. Percec, V. ; Barboiu, B. ; van der Sluis, M. *Macromolecules*. **1998**, 31, 4053.

30. Asscher, M.; Vofsi, D. *J. Chem. Soc*. **1964**, 4962.

31. Kamigata, N.; Sawada, H.; Kobaya, M. *Tetrahedron lett*. **1979**, 159.

32. Lee, G. M.; Weinreb, S. M.; *J. Org. Chem*. **1990**, 55, 1281.

33. Tsuji, J.; Sato, K.; Nagashima, K. *Chem. Lett*. **1981**, 1169.

34. Moineau, G. ; Minet, M. ; Teyssie, P. ; Jerome, R. *Macromolecules*. **1999**, 32, 8277.

35. Wang, J. ; Sheares, V.V. *Macromolecules*. **1998**, 31, 6769.

36. Uegaki, H. ; Kamigaito, M. ; Sawamoto, M. *J. Polym. Sci. Part A ; Polym. Chem*. **1999**, 37, 3003.

37. Moineau, G.; Minet, M.; Dubois, Ph.; Teyssie, Ph. ; Senninger, T. ; Jerome, R. *Macromolecules*. **1999**, 32, 2735.

38. Lecomte, Ph.; Drapier, I.; Dubois, ph,; Teyssie, Ph. ; Jerome, R. *Macromolecules*. **1997**, 30, 7631.

39. Petrucci, M.G.L.; Lebuis, A.M.; Kakkar, A.K.; *Organometallics*. **1998**, 17, 4966.

40. Masters, C.; **1981** *Homogeneous transition-metal catalysis: a gentle art*. Chapman and Hall, London.

41. Liprandi, D.; Quiroga, M.; Cagnola, E.; L'Argentiere, P. *Ind. Eng. Chem. Res*. **2002**, 41, 4906.

42. Percec, V. ; Barboiu, B. ; Neumann, A. ; Ronda. J.C. ; Zhao, M. *Macromolecules*. **1996**, 29, 3665.

43. Moineau, G. ; Granel, C. ; Dubois, Ph. ; Jerome, R. ; Teyssie, Ph. *Macromolecules*. **1998**, 31, 542.

44. Haddleton, D.M. ; Crossman, M.C. ; Dana, B.H. ; Duncalf, D.J. ; Heming, A.M. ; Kukulj, D.; Shooter, A.J. *Macromolecules*. **1999**, 32, 2110.

45. Uegaki, H. ; Kotani, Y. ; Kamigaito, M. ; Sawamoto, M. *Macromolecules*. **1997**, 30, 2249.

46. Uegaki, H.; Kotani, Y.; Kamigaito, M. ; Sawamoto, M. *Macromolecules*. **1998**, 31, 6756.

47. Minisci, F. *Acc. Chem. Res* **1975**, 8, 165.

48. Xia, J. ; Paik, H. ; Matyjaszewski, K. *Macromolecules*. **1999**, 32, 8310.

49. Kotani, Y.; Kamigaito, M.; Sawamoto, M. *Macromolecules***. 2000**, 33, 3543.

50. Ando, T.; Kamigaito, M.; Sawamoto, M. *Macromolecules*. **1997**, 30, 4507.

51. Matyjaszewski, K.; Wei, M.; Xia, J.; McDermott, N.E. *Macromolecules*. **1997**, 30, 8161.

52. Gobelt, B.; Matyjaszewski, K.; *Macromol. Chem. Phys*. **2000**, 201, 1619.

53. Gibson, V. C.; O'Reilly, R. K.; Reed, W.; Wass, D. F.; White, A. J. P.; Williams, D. J.; *Chem. Comm*. **2002**, 1850.

54. Ibrahim, K.; Yliheikkila, K.; Abu-surrah, A.; Lofgren, B.; Lappalainen, K.; Leskela, M.; Repo, T.; Seppala, J. *Eu. Pol. J*. **2004**, 1095.

55. Teodoreaux, M. ; Gaynor, S.G. ; Matyjaszewski, K. *Macromolecules.* **2000**, 33, 2335.

56. Kotani, Y.; Kamigaito, M.; Sawamoto, M. *Macromolecules*. **1999**, 32, 6877.

57. Brandts, J. A. M.; Geijn, P.; Faassen, E. E.; Boersma, J.; Koten, G. *J. Organomet. Chem.* **1999**, 584, 246.

58. Kotani, Y.; Kamigaito, M.; Sawamoto, M.; *Macromolecules*. **1999**, 32, 2420.

59. Stoffelbach, F.; Claverie, J.; Poli, R. *C.R. Chimie*. **2002**, 5, 37.

60. Kotani, Y.; Kamigaito, M.; Sawamoto, M.; *Macromolecules*. **1999**, 32, 2420.

61. Britovsek, G. J. P.; Gisbson, V. C.; Kimberley, B. S.; Maddox, P. J.; Mctavish, S. J.; Solan, G. A.; White, J. P. A.; William, D. *Chem. Comm*. **1998**, 849.

62. Chiefari, J.; Chang, Y. K.; Ercole, F.; Kristina, J.; Jeffery, J.; Le, T. P. T.; Mayadunne, R. T. A.; Meijis, G, F.; Moad, C. L.; Moad, G.; Rizzardo, E.; Thang, S. H. *Macromolecules*. **1998**, 31, 5559.

63. Rix, F.; Brookhart, M.; *J. Am. Chem. Soc*. **1995**, 117, 217.

64. Johnson,L.K.; Killian, C.M.; Brookhart, M. ; *J. Am. Chem. Soc*. **1995**, 117, 6414.

65. Xia, J.; Gaynor, S.G.; Matyjaszewski. *Macromolecules*. **1998**, 31, 5958.

66. Haddleton, D.M. ; Crossman, M.C. ; Jasieczek, B.C. ; Hannon, A.M.J. ; Shooter, A.J. *Macromolecules*. **1997**, 30, 2190.

67. Destarac, M. ; Bessiere, J.M. ; Boutevin, B. *Macromol. Rapid commun*. **1997**, 18, 967.

68. Kiclkelbick, G. ; Matyjaszewski, K. *Macromol. Rapid commun*. **1999**, 20, 341.

69. Matyjaszewski, K. ; Patten, T.E. ; Xia, J. *J. Am. Chem. Soc*. **1997**, 119, 674.

70. Britovsek, G. J. P.; Gibson, V. C.; Kimberley, B. S.; Maddox, P. J.; McTavish, S. J.; Solan, G. A.; White, A. J. P.; Williams, D. J. *Chem. Commun.* **1998**, 849.

71. Matyjaszewski, K.; Gobelt, B.; Paik, H.; Horwitz.C.P. *Macromolecules*. **2001**, 34, 430.

72. Xia, J. ; Gaynor, S.G. ; Matyjaszewski, K. *Macromolecules*. **1997**, 30, 7697.

73. Shen, Z.; Chen, Y.; Frey, H.; Styria, S.E. *Macromolecules*. **2006**, 39, 2092.

74. O'Reilly, R.K.; Shaver, M.P.; Gibson, V.C. *Inorganica Chimica Acta*. **2006**, 359, 4417.

75. Xia, J. ; Zhang, X. ; Matyjaszewski, K, *Polym. Mater. Sci. Eng*.**1999**, 80, 453.

CHAPTER TWO:

Contents *Pages*

2.1 Introduction

Dendrimers are macromolecules with core and hyper-branched structures that extend in a highly organized fashion out to the terminal groups[1]. These terminal groups provide a possibility to modify the surface of these macromolecules.[2] It is because of the ease of modification of the surface that these macromolecules find so many applications in different fields of chemistry such as drug delivery and catalysis.[2]

This advantage of modification of the terminal groups of dendrimers have been exploited by many researchers including Noble(IV) and coworkers in their work on surface-confined monomers on electrode surfaces where they substituted primary amine terminal groups of the diaminobutane poly(propylimine) dendrimer (DAB) as shown in Scheme 2.1. [3]

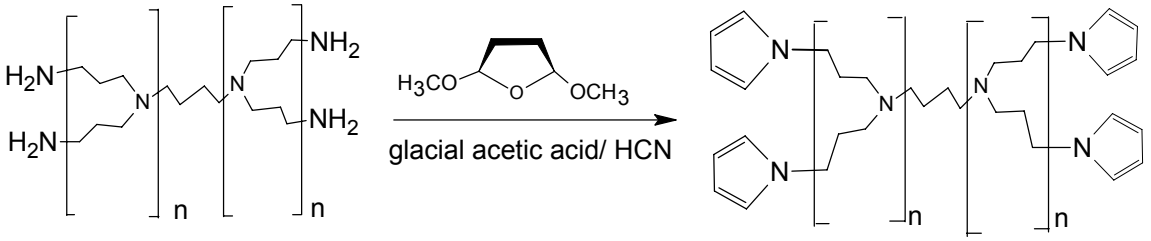

DAB-$(NH_2)_{n+1}$
n = 1-3

DAB-$(pyr_z)_{n+1}$

Scheme 2.1 *The synthesis pyrrole-terminated poly(propylene imine) dendrimer*

These macromolecules have been used in drug delivery[4], and they have also functioned as crosslinkers in polymeric membranes.[5] Their potential catalytic

properties were realized when they were exploited in the form of metallodendrimers.[6] The focus of this chapter is on modifying the primary amino groups of the diaminobutane dendrimer depicted in Figure 2.1. At first, the terminal primary amino groups were converted to imine functional groups by a reaction with 2-pyridyl carboxyaldehyde or 4-tert-butylbenzylaldehyde. The imine functional groups were subsequently reduced to secondary amine terminal groups. In another experiment, the amino groups of DAB-$(NH_2)_4$ was modified by reaction with methyl methacrylate via a Michael addition reaction. The same reaction was performed with the generation 2 polypropyleneimine dendrimer, (DAB-$(NH_2)_8$).

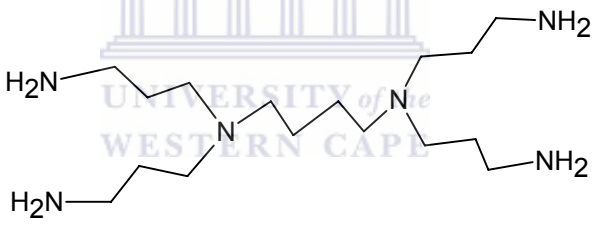

DAB-$(NH_2)_4$ **L1**

Figure 2.1 *The structure of polypropyleneimine (DAB-$(NH_2)_4$) generation 1 dendrimer*

2.2 Results and Discussion

2.2.1 Synthesis and reduction of 2-Pyridylimine functionalized DAB (py-DAB)(L 2) dendrimer and its amine derivative 2-Pyridylamine functionalized DAB dendrimer (py-DABH)(L 3):

This compound was synthesized according to the procedure reported by Smith and Mapolie.[6] The synthesis of this compound was carried out via the condensation reaction of 2-pyridyl carboxyaldehyde with DAB-$(NH_2)_4$ (Figure 2.1) and involved stirring of the reagents at room temperature for two days in the presence of magnesium sulphate as a dehydrating agent (Scheme 2.2). The product (**L2**) was obtained as a brown oil and characterized by ^{1}H NMR and the chemical shifts are shown in Table 2.1. The ^{1}H NMR spectrum is displayed in Figure 2.2 and the details are discussed under section 2.2.1.1.

The product (**L2**) was reduced using sodium borohydride in refluxing ethanol for five hours (Scheme 2.3)[7] producing **L3**. The newly produced ligand was obtained as an orange brown oil and characterized by ^{1}H NMR spectroscopy (Figure 2.3). The chemical shifts are shown in Table 2.1. The spectrum is discussed under section 2.2.1.1. The identity of both the parent compound **L 2**, and its derivative **L 3** was further confirmed by IR spectroscopy**.**

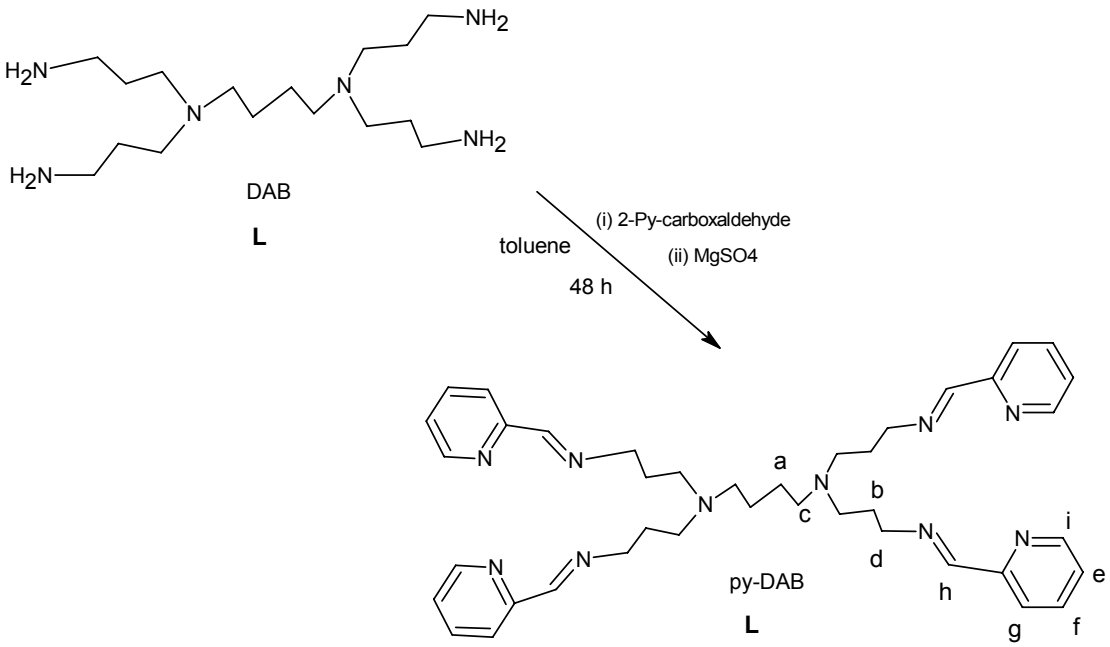

Scheme 2.2: *Synthesis of py-DAB (**L 2**)*

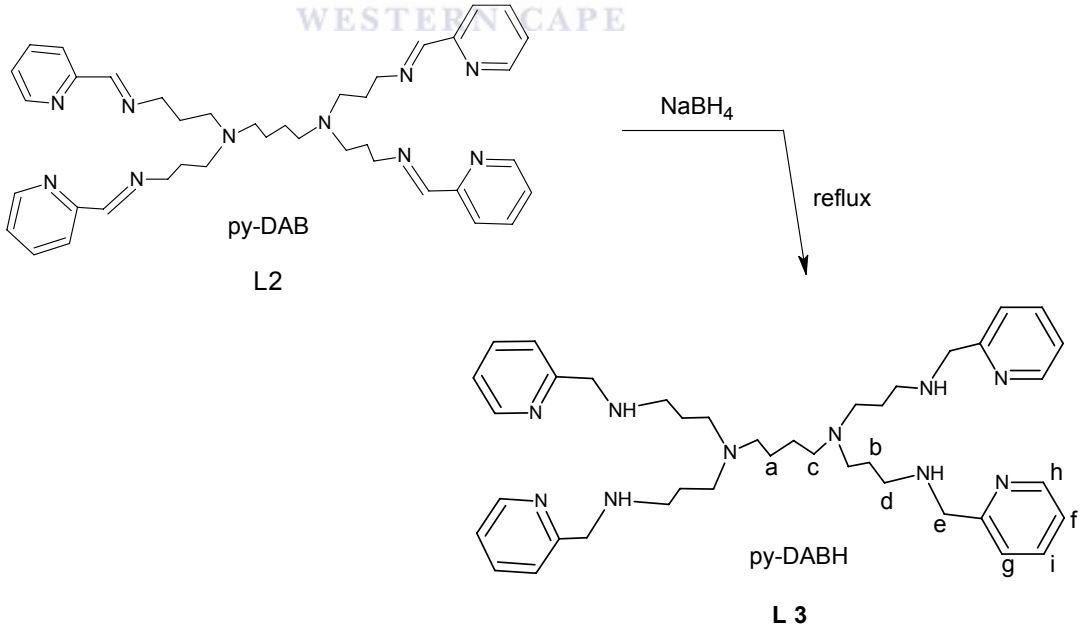

Scheme 2.3: *Reduction of py-DAB (**L 2**) to py-DABH (**L 3**)*

2.2.1.1. The ^{1}H NMR data of (L 2) and (L 3)

The chemical shifts corresponding to the structural assignments in Scheme 2.2 and 2.3 are displayed in Table 2.1. The ^{1}H NMR spectra of the respective compounds are shown in Figures 2.2 and 2.3. The data in Table 2.1 also serves to confirm the shifts in peaks which occurred when **L 2** was converted to **L 3**.

Table 2.1: The ^{1}H NMR spectral assignments for **L2** and **L3**

Proton	**Chemical shift (ppm) Py-DAB (L2)**	**Chemical shift (ppm) Py-DABH (L3)**
a	1.42 (s)	1.34(s)
b	1.89 (t) (*J = 7.4Hz*)	1.63 (t) (*J = 7.2Hz*)
c	2.34-2.56 (m)	2.32-2.46 (m)
d	3.68 (t) (*J = 6.6Hz*)	2.60 (t) (*J = 6.8Hz*)
e	7.14-7.30 (m)	3.84 *(s)*
f	7.71 (t) (*J = 8 Hz*)	7.07-7.13 (m)
g	7.96 (d) (*J = 6Hz*)	7.26-7.24 (m)
h	8.36 (s)	7.54-7.63 (t) (*J = 7.6Hz*)
I	8.61(d) (*J = 8Hz*)	8.505(d) (*J = 4.8Hz*)

The structural designations in Scheme 2.2 and the chemical shifts in the second column of Table 2.1 refer to the ^{1}H NMR spectra in Figure 2.2 below. The singlet peak at δ = 1.42 ppm is attributable to the methylene group protons **a** which are a

part of the diaminobutane core of **L2** as shown in Scheme 2.1; whereas the triplet at δ = 1.89 ppm arises from the methylene protons **b** between tertiary nitrogen and the imine nitrogen. The multiplet observed in the region δ = 2.34-2.56 ppm is attributable to the methylene protons **c** adjacent to the tertiary nitrogen at the core whereas the peaks in the region δ = 3.64-3.71 ppm are due to the methylene protons **d** adjacent to the imine nitrogen. The peaks in the region δ = 7.14-7.97 ppm are attributed to the pyridyl ring protons **e**, **f** and **g**. The singlet at δ = 8.36 ppm is due to the imino proton **h**. This peak is presented in bold in the chemical shifts in Table 2.1 because its disappearance is used to confirms the conversion of **L2** to **L3** this is indicative of the success of the reduction reaction. The doublet at δ = 8.61 ppm was assigned to the pyridyl proton **i** adjacent to nitrogen of the pyridine ring. These results exactly match the published chemical shift values which mean we have successfully synthesized **L 2**.[8] The next step was to reduce **L2** to **L3**, which is just a conversion of an imine to an amine. The ^{1}H NMR spectrum of **L3** is displayed in Figure 2.3 and the corresponding peak designations are shown on the structure of py-DABH in Scheme 2.3. It can be observed from Table 2.1 that the pattern for the chemical shifts is the same for both **L2** and **L3** except for a slight shift in some peaks. The only notable difference is the appearance of a singlet at δ = 3.84 ppm due to the methylene protons adjacent to the newly formed secondary amine group and the absence of the peak at δ = 8.36 (s) ppm which was due to the imino proton in **L2**. The chemical shifts confirm the successful conversion **L2** to **L3**.

2.2.1.2. The IR spectral data of py-DAB(L2) and py-DABH(L3)

The successful reduction of **L2** to **L3** was further confirmed by infra-red (IR) spectroscopy. As these two compounds were both oils the IR measurement was performed as a neat oil between NaCl plates and the spectra are shown in Figures 2.4 and 2.5 for **L2** and **L3,** respectively. From the IR spectrum of **L2** the stretching frequency due to ν(C=N) which appears at 1648 cm^{-1} is worth noting because when reduction occurs the imine functional group will be converted to the amine group that will result in the disappearance of this stretching frequency. The IR spectrum of **L3** in Figure 2.5 confirms the successful conversion **L2** to **L3** as suggested by the absence of the stretching frequency at 1648 cm^{-1} due to ν(C=N). Evidence for the formation of **L3** was further supported by the presence of ν(N-H) stretching frequency at ν= 3286 cm^{-1} and a sharp band at 1590 cm^{-1} due to ν(N-H) bending vibration in Figure 2.5.

2.2.2. Synthesis of 4-t-butyl phenylmethylimine functionalized DAB dendrimer (^{t}Bu-DAB) (L4) and its amine derivative 4-t-butyl phenylmethylamine functionalized-DAB (^{t}Bu-DABH) (L5)

The synthesis of **L4** involves the condensation reaction of 4-t-butyl-benzylaldehyde with **L1** at room temperature for 3 days in the presence of magnesium sulphate as a dehydrating agent (Scheme 2.4). The product was isolated as a white powder and characterized by ^{1}H and ^{13}C NMR spectroscopy. The spectra are displayed in Figure 2.6 and 2.7 respectively.

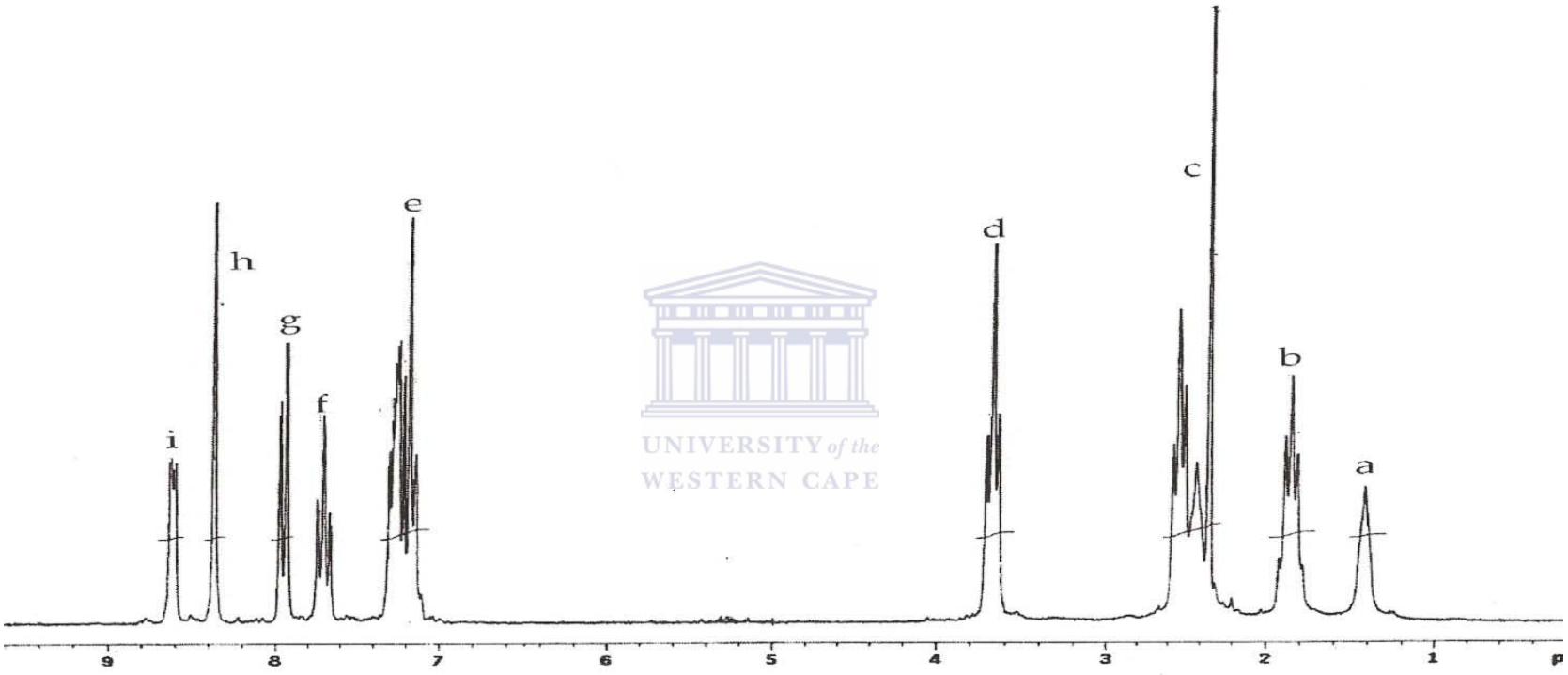

Figure 2.2: *The ^1H NMR spectrum of* ***L2***

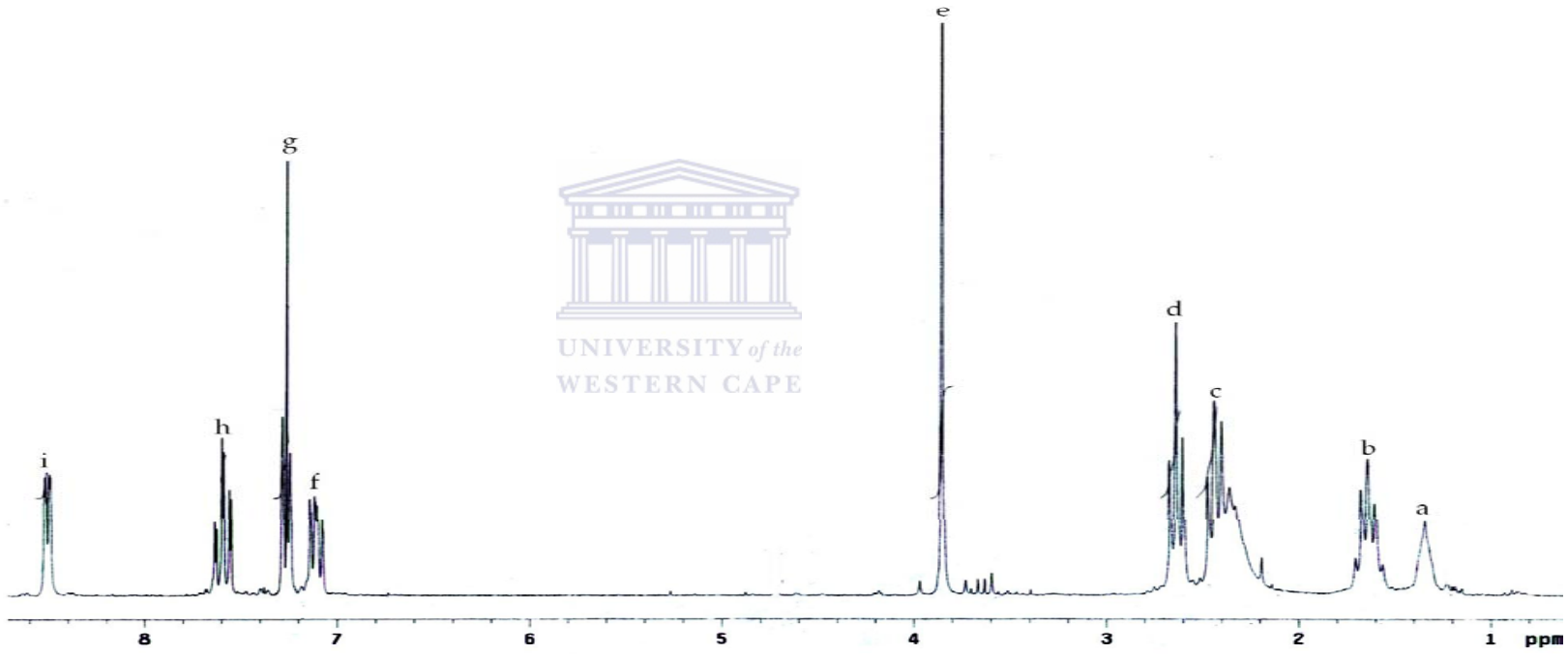

Figure 2.3: *The ^{1}H NMR spectrum of* ***L3***

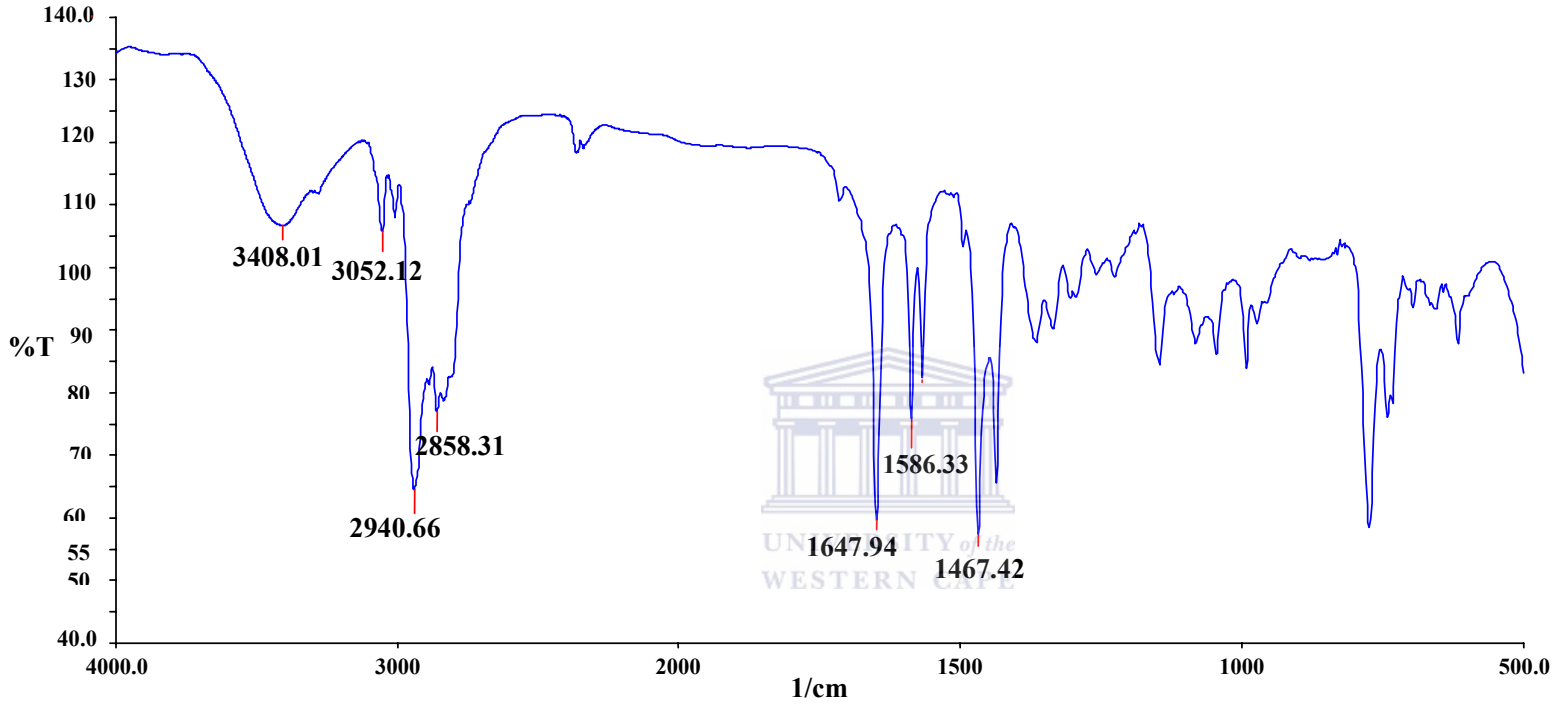

Figure 2.4: *The infra-red spectrum of* ***L2***

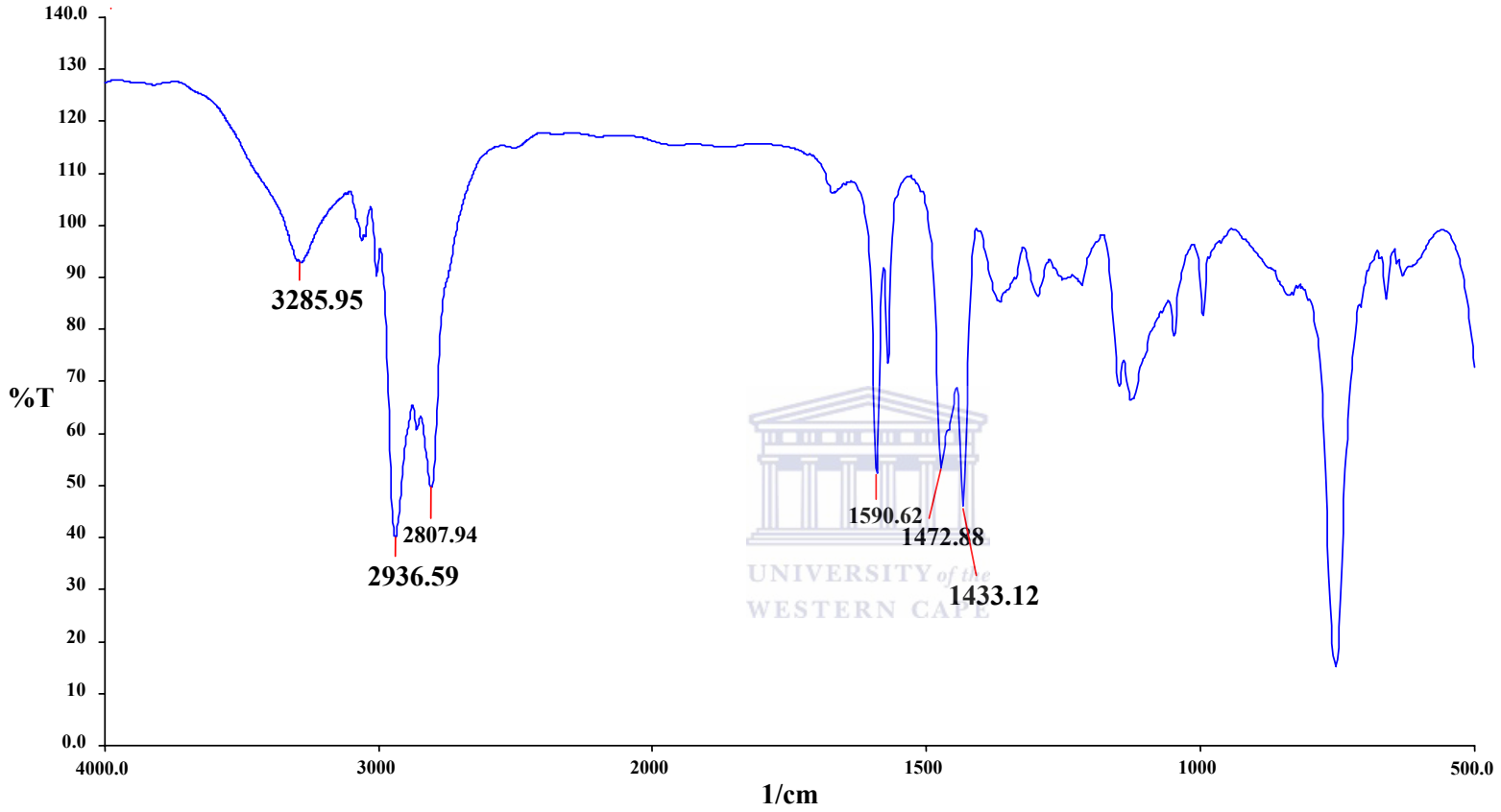

Figure 2.5: *The infra-red spectrum of* ***L3***

The results were further confirmed by elemental analysis and the composition data is displayed in Table 2.4. IR spectroscopy was also performed and the spectrum is depicted in Figure 2.9. **L4** was then reduced using sodium borohydride in refluxing ethanol for 10 hours (Scheme 2.4). The product was a faint yellow oil which was characterized by ^{1}H NMR spectroscopy. The chemical shifts are shown in Table 2.4 and the spectrum is displayed in Figure 2.8. The identity of the compound was further confirmed by IR spectroscopy and the spectrum is shown in Figure 2.10.

2.2.2.1. ^{1}H NMR data of (L4)

^{1}H NMR spectroscopy was used in the characterization of ^{t}Bu-DAB (**L4**) and the chemical shifts corresponding to the designations of the **L4** structure in Scheme 2.4 are reflected in Table 2.2. The chemical shifts in Table 2.2 refer to ^{1}H NMR spectrum in Figure 2.6 . The singlet observed at δ = 1.31 ppm is attributable to the methyl protons **a** of the tertiary butyl substituent on the benzene ring of **L4**. The singlet at δ = 1.42 ppm is associated with the internal methylene group protons **b** of the diaminobutane core, whereas the broad singlet at δ = 1.84 ppm arises from the internal methylene protons **c** of the diaminobutane branches. The other broad singlet observed at δ = 2.48 ppm was assigned to the methylene group protons **d** adjacent to the tertiary nitrogen of the diaminobutane core whereas the methylene proton **e** adjacent to the imino nitrogen resonated as a triplet at δ = 3.61 ppm. The doublet at δ = 7.41 ppm and δ = 7.63 ppm belong to the benzene ring protons **f** and **g** respectively.

The singlet at δ = 8.24 is attributable to the imino proton **h**. This singlet is significant because when this compound is reduced to **L5** it disappears.

Table 2.2 The ^{1}H NMR spectral assignments for **L4**

Proton	Chemical shift (ppm)
a	1.31 (s)
b	1.42 (s)
c	1.84 (broad, singlet)
d	2.48 (br, singlet)
e	3.61 (t) (*J = 6 Hz*)
f	7.41 (d) (*J = 7 Hz*)
g	7.63 (d) (*J = 6.6 Hz*)
h	8.24 (s)

.

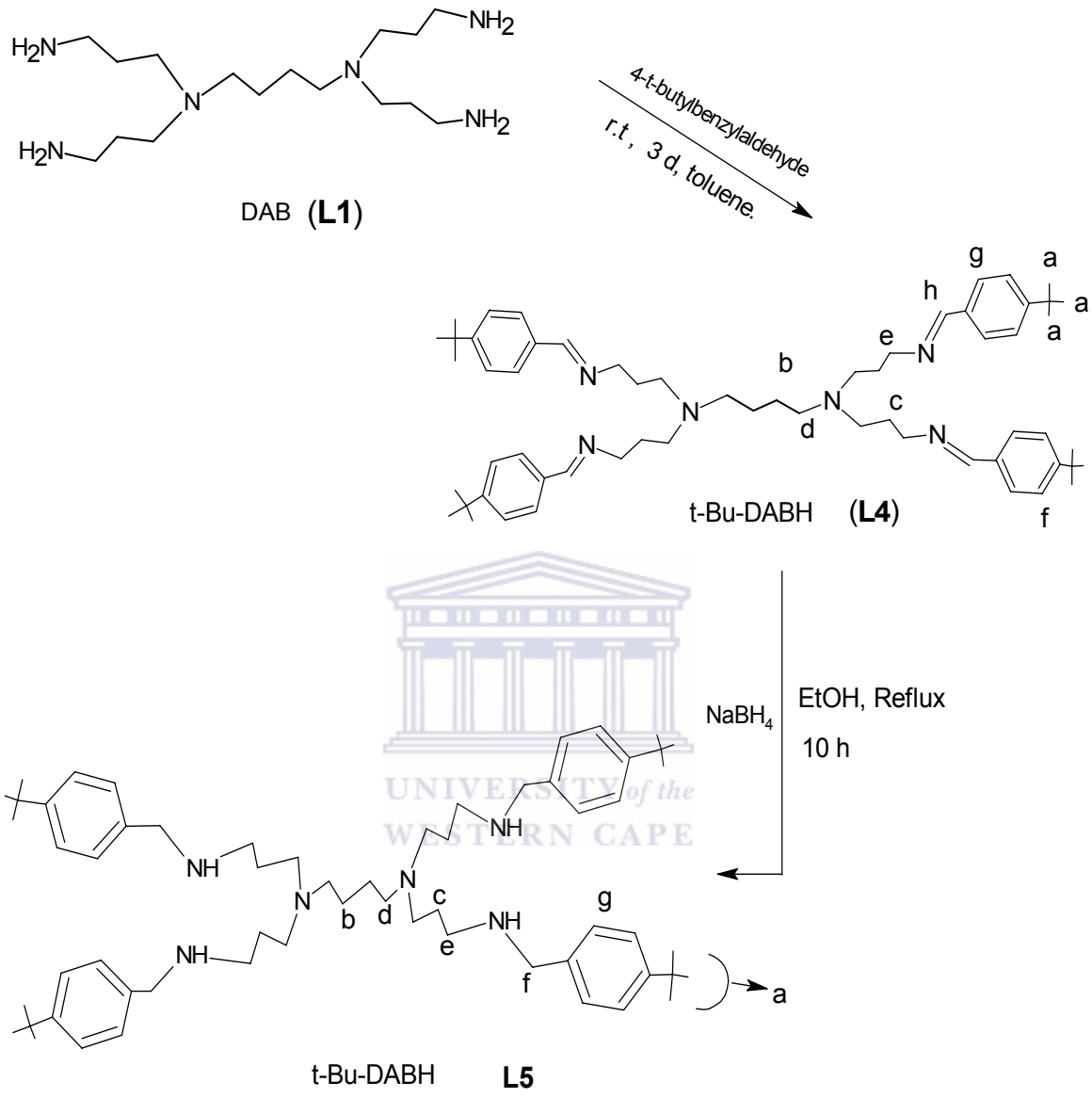

Scheme 2.4: *The synthesis of ^{t}Bu-DAB and its reduction to ^{t}Bu-DABH*

2.2.2.2. The ^{13}C NMR results of ^{t}Bu-DAB (L4)

The ^{13}C NMR data for ^{t}Bu-DAB (**L4**) structure with labels corresponding to the chemical shifts of carbons in Scheme 2.4 is displayed in Table 2.3.

Table 2.3. ^{13}C NMR data for **L4**

Carbon	Chemical shift (ppm)
1	25.16
2	34.77
3	133.69
4	125.42
5	127.77
6	153.69
7	160.71
8	59.00
9	31.17
10	54.06
11	51.68
12	28.41

The ^{13}C NMR spectral data in Table 2.3 and the spectrum displayed in Figure 2.7 further confirms the structure of ^{t}Bu-DAB. The peak at δ = 25.16 ppm is associated with the methyl carbons of the tertiary butyl substituent. The peak at δ = 28.41 ppm is assigned to the methylene carbon **12** at the center between the two tertiary nitrogen at the core of the dendrimer.

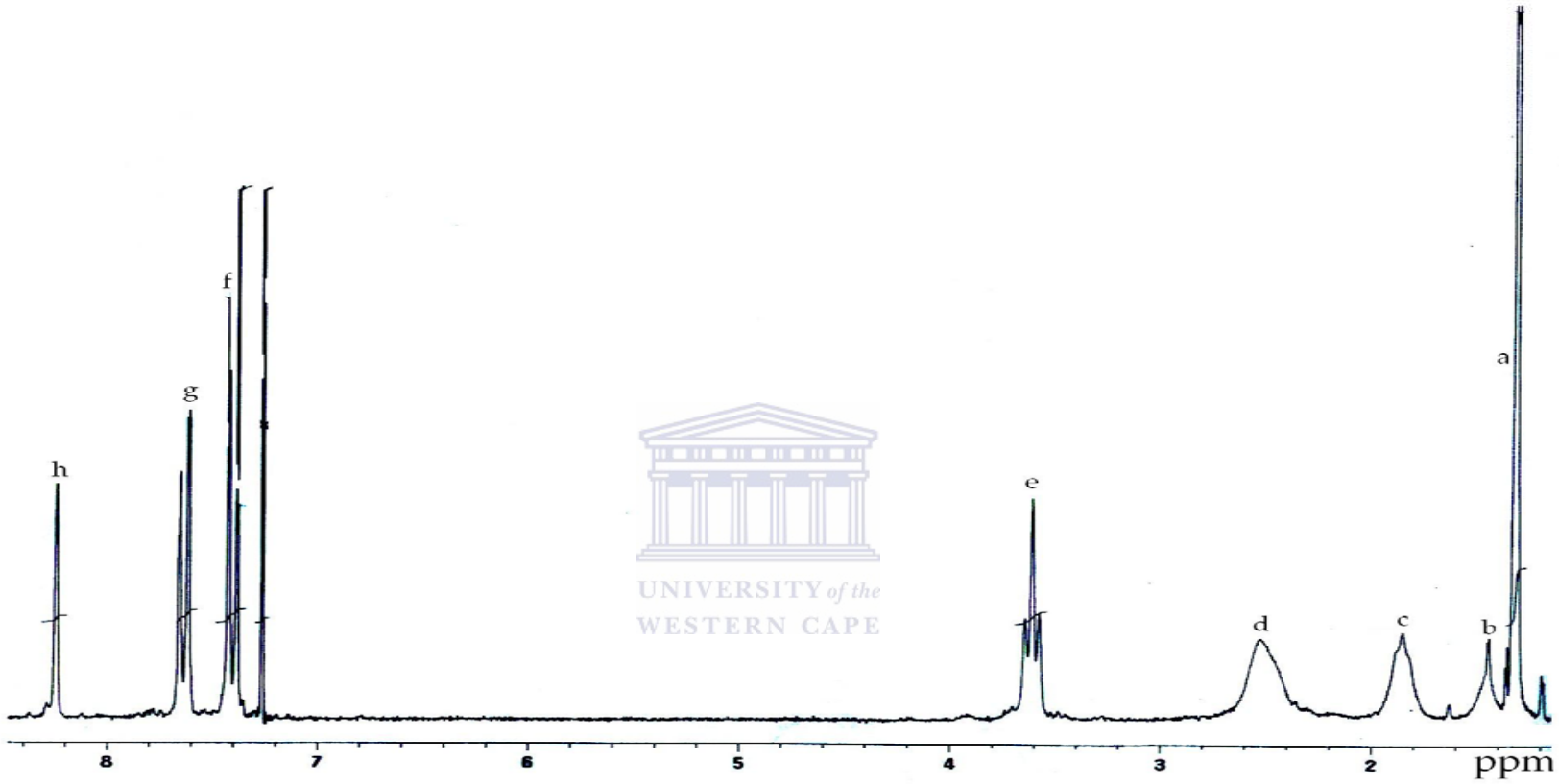

Figure 2.6: *The ^1H NMR spectrum of* ***L4***

The peak observed at δ = 31.16 ppm is associated with the methylene carbons **9** of the C3 carbon branches. The peak at δ = 34.77 ppm is due to the tertiary carbon **2** of the tert-butyl substituent. The peak at δ = 52.68 ppm is assigned to methylene carbon **11** adjacent to the tertiary nitrogen at the core of the dendrimer. The peak at δ = 54.06 ppm is associated with the methylene carbon **10** on the branch adjacent to the to tertiary nitrogen of the core of the dendrimer. The peak at δ = 59.70 ppm is due to methylene carbon **8** adjacent to the imine group. The peaks at δ = 125.42 ppm, 127.77 ppm, 133.69 ppm and 153.69 ppm were assigned to the carbons **4, 5, 3**, and **6** respectively of the benzene ring. The peak at δ = 160 ppm belonged to the imine carbon **7**.

2.2.2.3. Elemental analysis of ^{t}Bu-DAB (L4)

The structural information of **L4** obtained from the ^{1}H and ^{13}C NMR spectroscopy was further confirmed by elemental analysis and the data obtained is shown in Table 2.4.

Table 2.4 Elemental analysis data of **L4**

^{t}Bu-DAB	%C	%H	%N
calculated	80.66	9.93	9.41
experimental	80.64	10.02	9.33

The composition data in Table 2.4 centered above correctly confirms the success of the synthesis of **L4** and allowed reduction of this compound to its amine derivative to take place as reported in the next section.

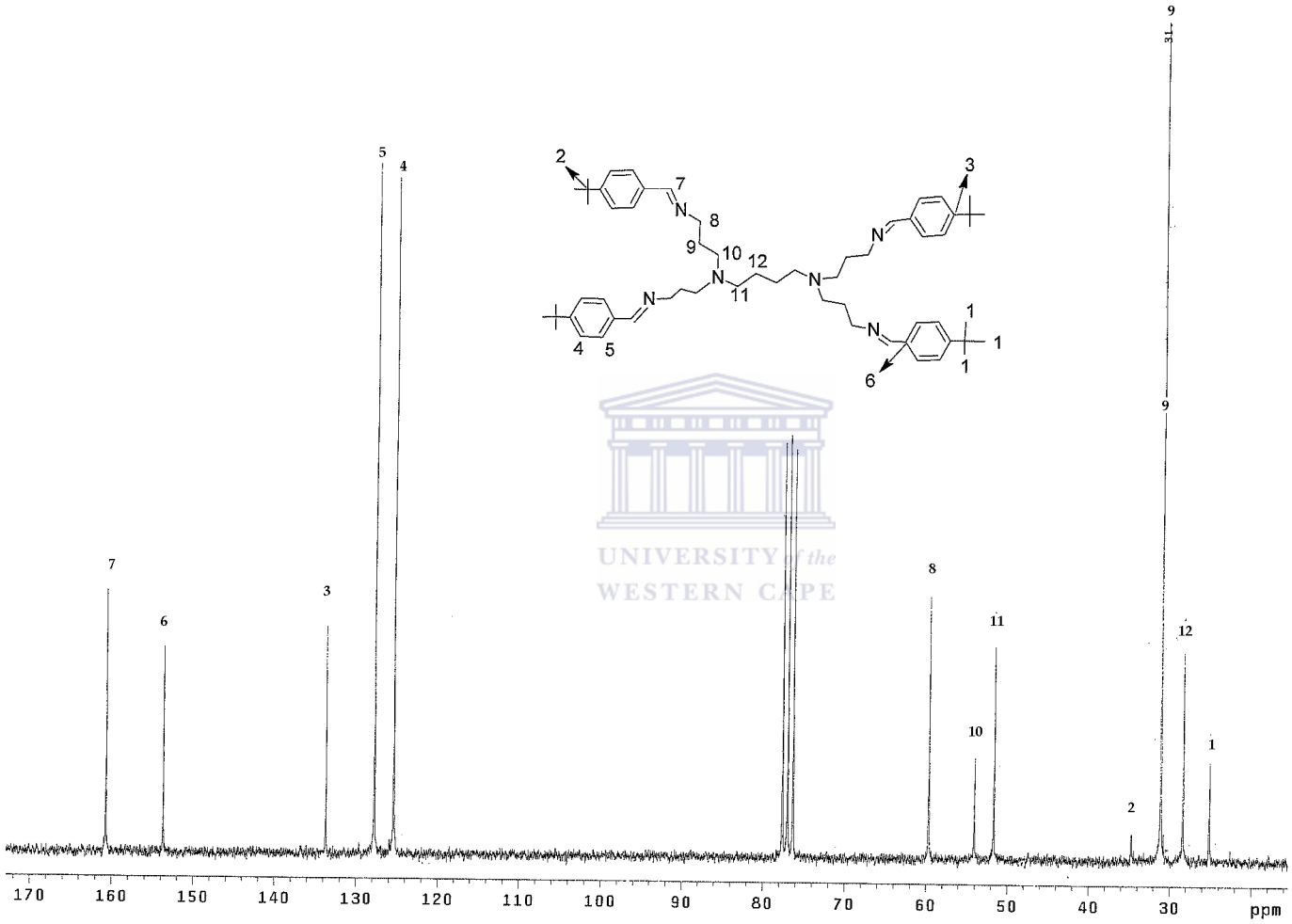

Figure 2.7: *The ^{13}C NMR spectrum of* ***L4***

2.2.3. Reduction of ^{t}Bu-DAB (L4) to ^{t}Bu-DABH (L5)

After **L4** was successfully synthesized and fully characterized, the step that followed was to reduce it to **L5**. The synthetic route for this compound is displayed in Scheme 2.4. This compound was characterized by ^{1}H NMR spectroscopy, the spectral data is provided in Table 2.5 and is compared with that of the parent molecule that is **L4.** The spectrum of **L5** is shown in Figure 2.8. In addition, the structural information obtained from IR spectroscopy, was also compared with that of the parent molecule **L4** and the IR spectra for both starting material (**L4**) and the product (**L5**) are displayed in Figures 2.9 and 2.10 respectively.

2.2.3.1. The ^{1}H NMR data of (L5)

The corresponding structural designations are displayed in Scheme 2.4 for data in Table 2.5 and the ^{1}H NMR spectrum is displayed in Figure 2.8 for **L5**.

Table 2.5 ^{1}H NMR spectral data for **L4** and **L5**

Proton designations	Chemical shifts (ppm) (**L4**)	Chemical shifts (ppm) (**L5**)
a	1.31 (s)	1.29 (s)
b	1.42 (s)	1.61 (t) (*J = 2 Hz*)
c	1.84 (br, s,)	1.97 (s)
d	2.48 (br, s,)	2.44 (t) (*J = 4.2 Hz*)
e	3.61 (t) (*J = 6 Hz*)	2.6 (t) (*J = 2 Hz*)
f	7.41 (d) (*J = 7 Hz*)	3.7 (s)
g	7.63 (d) (*J = 6.6 Hz*)	7.21-7.35 (m)
h	8.24 (s)	---

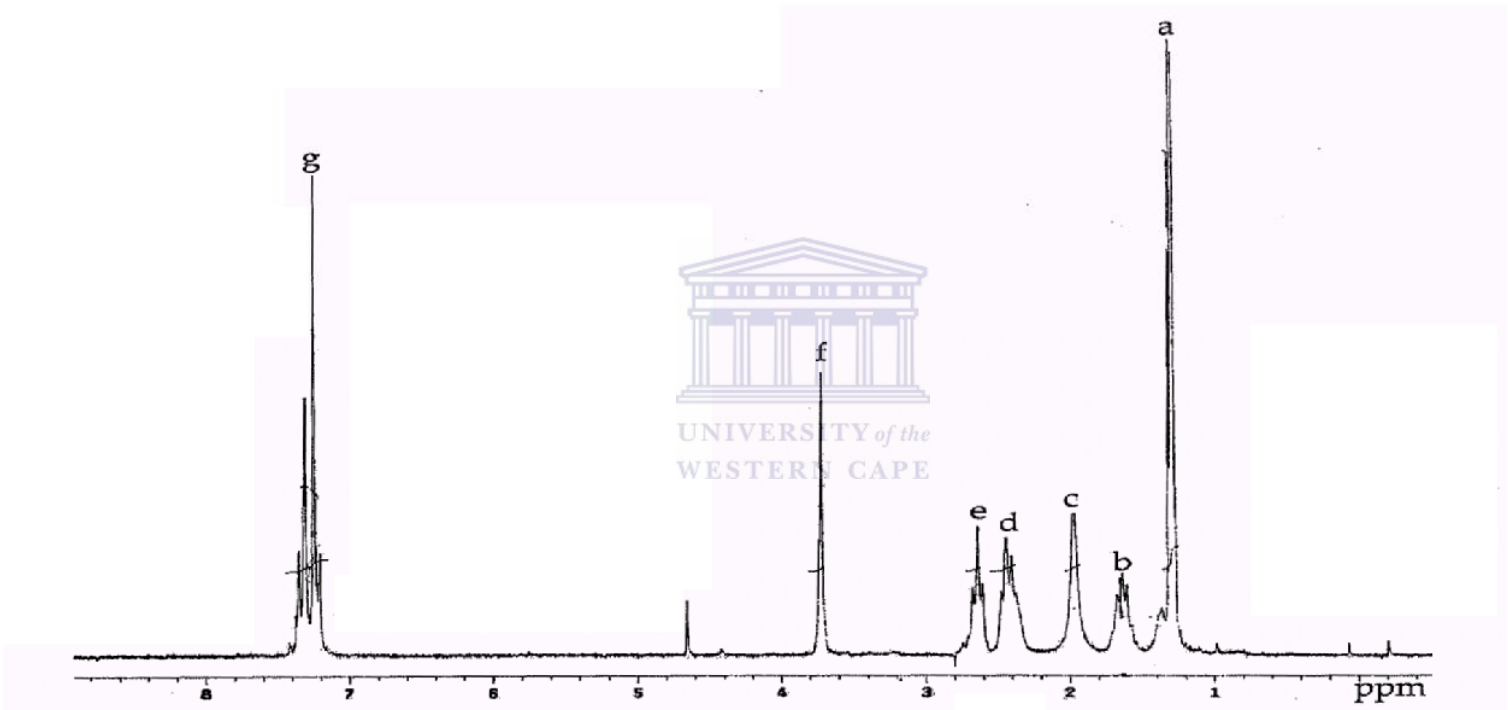

Figure 2.8: *^{1}H NMR spectrum of* ***L5***

The labeling of the structures **L4** and **L5** shown in Scheme 2.4 and the chemical shifts in the second column of Table 2.6 refer to the ^{1}H NMR spectrum in Figure 2.8. The chemical shifts in the ^{1}H NMR spectrum of **L5** follow a similar pattern to that of **L4** which was fully discussed under section 2.2.2.1. The point to note in the case of the ^{1}H NMR spectrum of **L5** is the imino proton signal peak observed at δ = 8.24 ppm in the spectrum of **L4** and the appearance of the singlet at δ = 3.70 ppm in the ^{1}H NMR spectrum of **L5** due to amine protons which is an indication of successful conversion the imine to the amine.

2.2.4. Comparison of IR data of ^{t}Bu-DAB (L4) and ^{t}Bu-DABH (L5) spectra

The successful conversion of **L4** to **L5** was confirmed by infra-red (IR) spectroscopy. **L4** is a solid compound. The IR spectrum was recorded as a nujol mull between two NaCl plates (Figure 2.9). **L5** was obtained as an oil and the IR spectrum was recorded as a neat oil between NaCl plates (Figure 2.10).

The same argument used in the case of **L2** and **L3** applies in this case because the bands to note in the transformation of the imine to the amine is υ(C=N) converted to υ(C-NH) displayed in the spectral data in shown in Figure 2.9 and 2.10 respectively. The other band that confirmed the presence of an amine is υ(N-H) which appeared at 1512cm^{-1}.

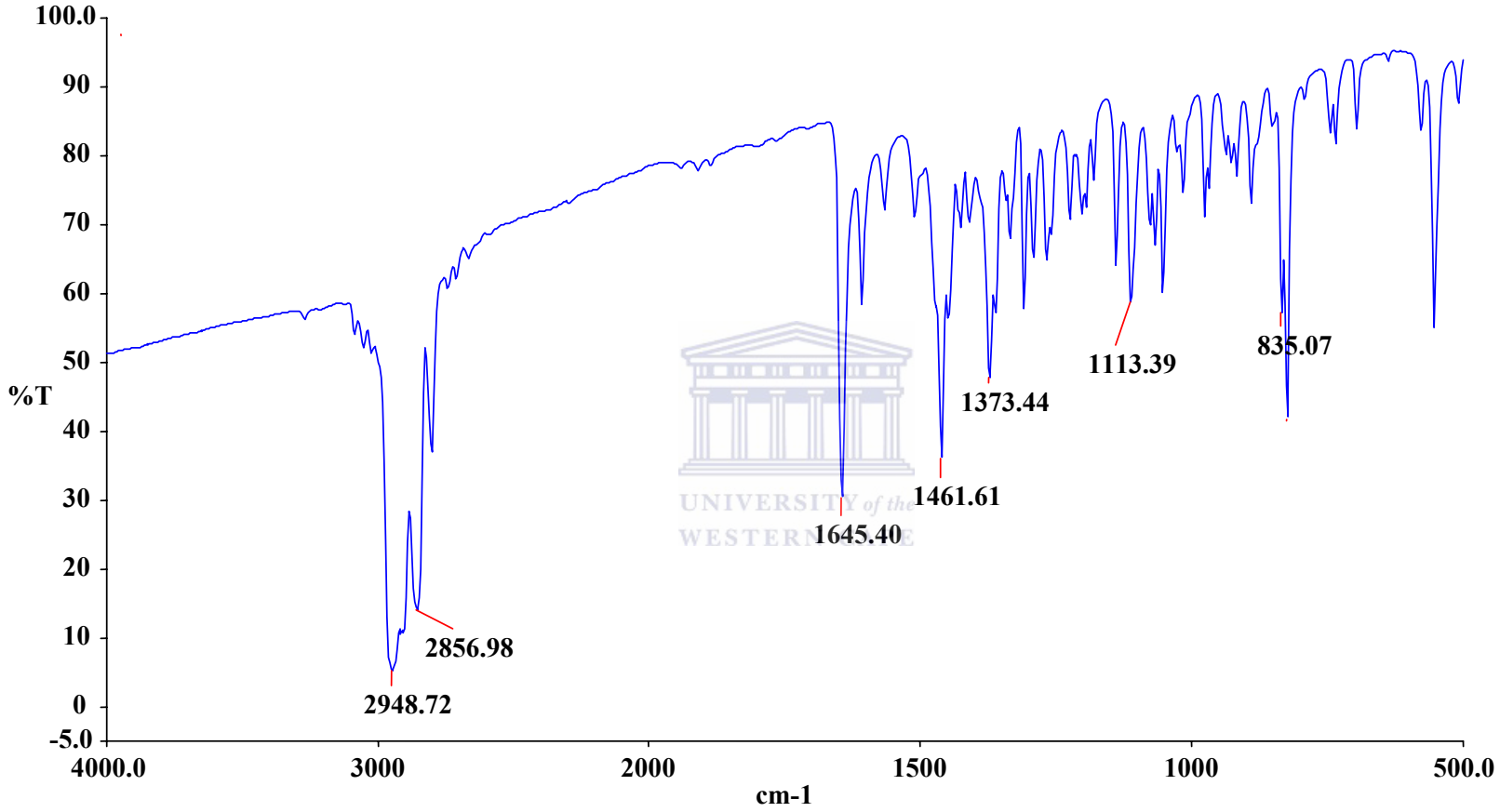

Figure 2.9: *The IR spectrum of* ***L4***

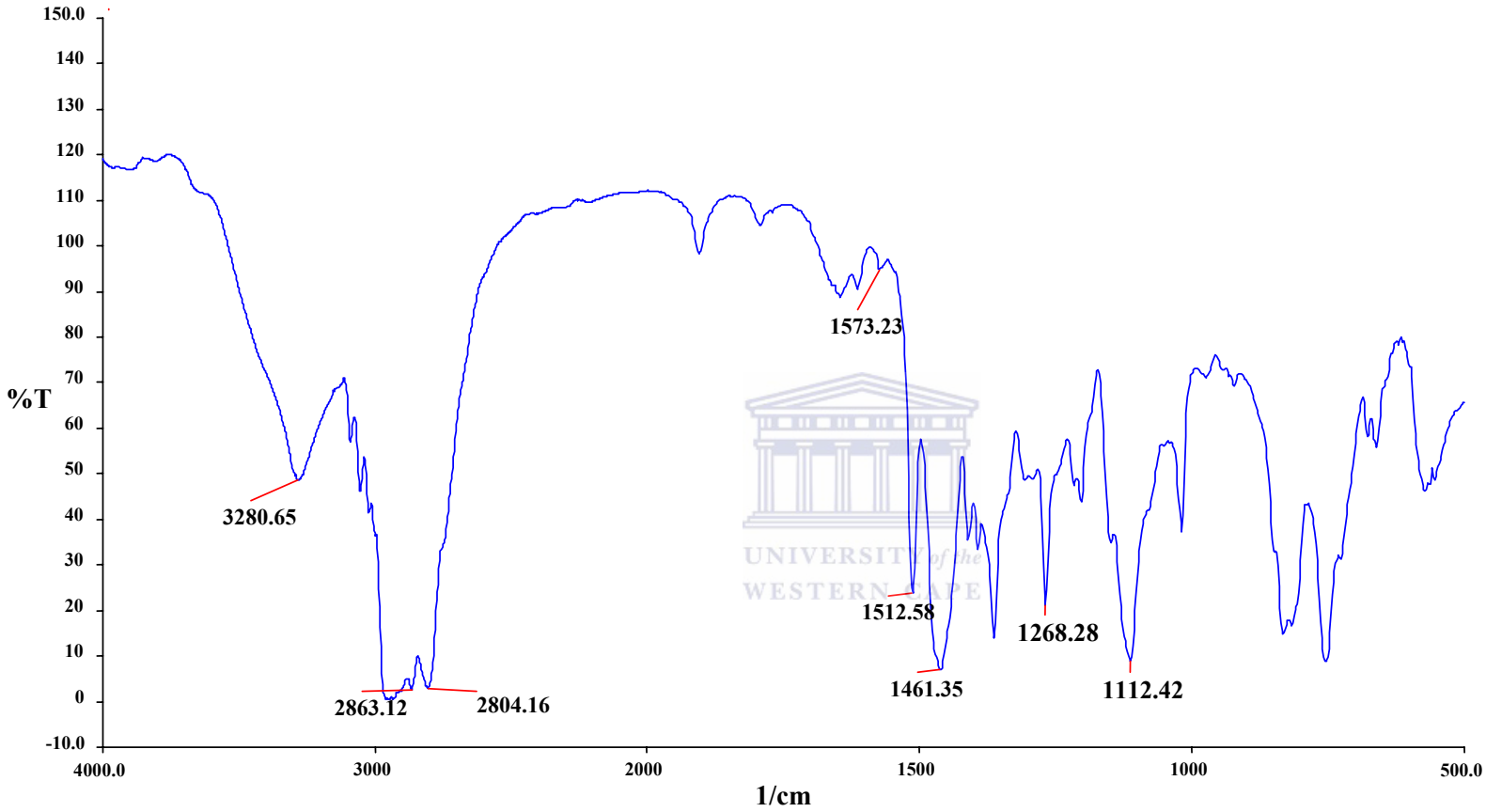

Figure 2.10: *The IR spectrum of* ***L5***

2.2.5. Synthesis of 1st generation of methyl methacrylate functionalized DAB dendrimer (L6).

Attempts to convert the 2° amine ligands (**L1,L3** and **L5**) reported in the previous section to 3° amines were not successful. Various attempts to alkylate the 2° amines with a range of alkylating agents failed. We therefore had to resort to an alternative approach to obtain 3° amine functionalized dendrimers. This involved the direct alkylation of the amino groups of the G1 dendrimer, DAB-$(NH_2)_4$ (**L1**) via a Michael addition reaction with methyl methacrylate. This is shown in Scheme 2.5.

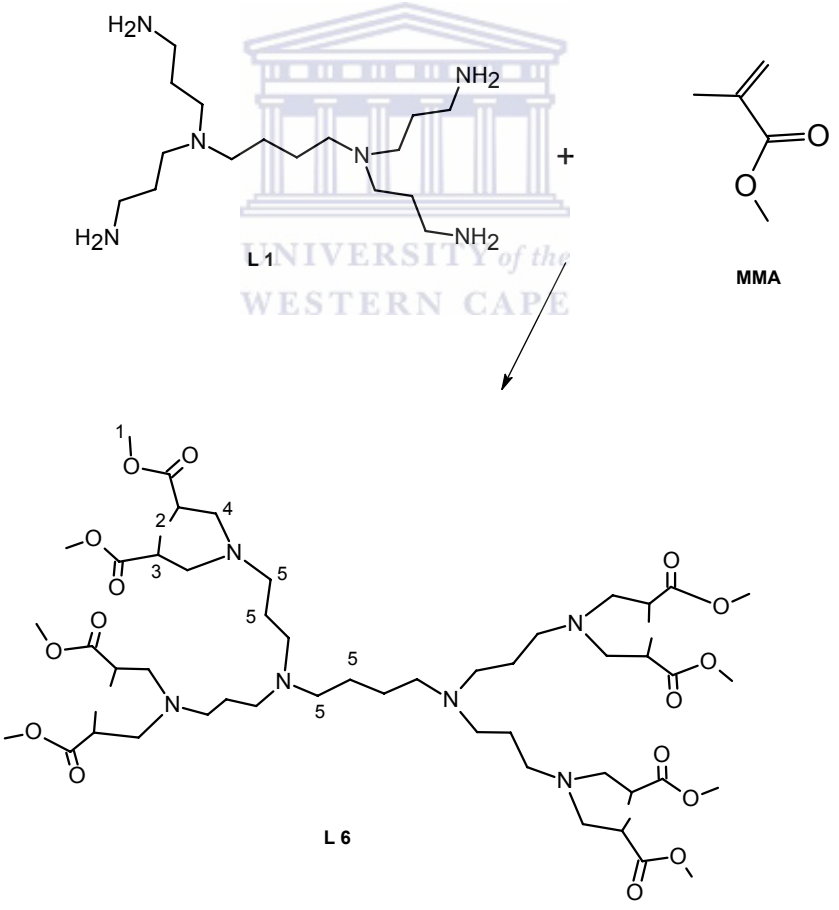

Scheme 2.5: *Synthesis of Methyl methacrylate functionalized* ***L 6***

2.2.5.1. Characterization L6

The ligand **L6** was synthesized following the procedure outlined by Frey and coworkers[8] with some modifications to the reported procedure. The reaction proceeded *via* a Michael addition of methyl methacrylate (MMA) to the amino groups of the polypropylenimine dendrimer (**L1**). This reaction took place in tetrahydrofuran (THF) for a total of 72 hours. The product **L6** was isolated as a brownish oil. This oil was analyzed by ^{1}H and ^{13}C NMR spectroscopy and the spectra are displayed in Figures 2.12 and 2.13 respectively. Figure 2.11 shows the proton NMR spectrum of **L1** which was used in the synthesis of **L6**. The labeling in the proton NMR spectrum in Figure 2.12 corresponds to the designations in **L6** structure in Scheme 2.5. The significant peaks in the proton NMR spectrum in Figure 2.12 are at δ = 3.66 ppm a singlet labeled **1** attributed to the proton **1** of the methoxy group, at δ = 1.12-1.15 ppm is a doublet labeled **2** associated with the proton **2** of methyl group at the gamma position to the carbonyl group and the multiplet labeled **3** at δ = 3.20-3.40 ppm associated with methine proton **3** at the beta position to carbonyl group. The peaks labeled **5** in this spectrum are attributed to the methylene peaks of **L6** at the core similar to the signals found in the spectrum of **L1** (see Figure 2.11)**.**

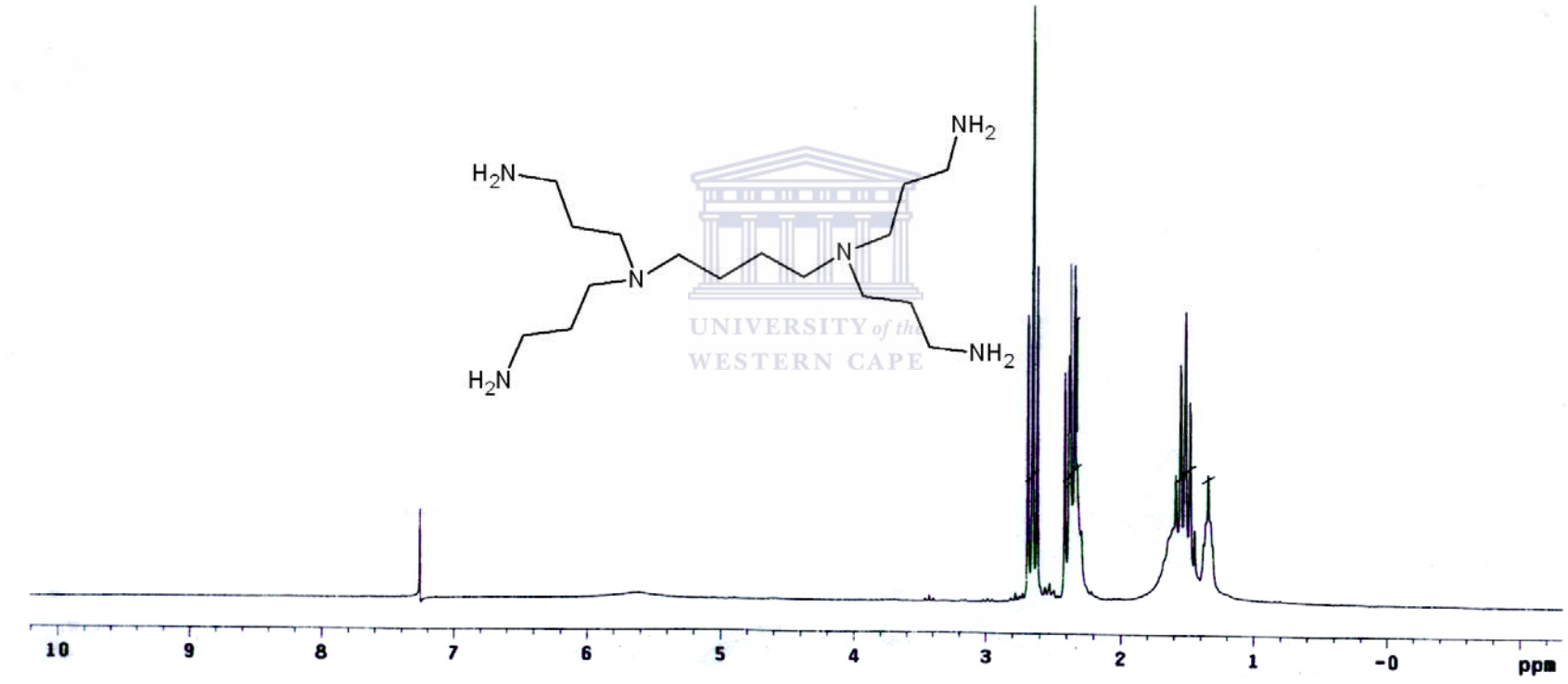

Figure 2.11: *Proton NMR of* ***L1***

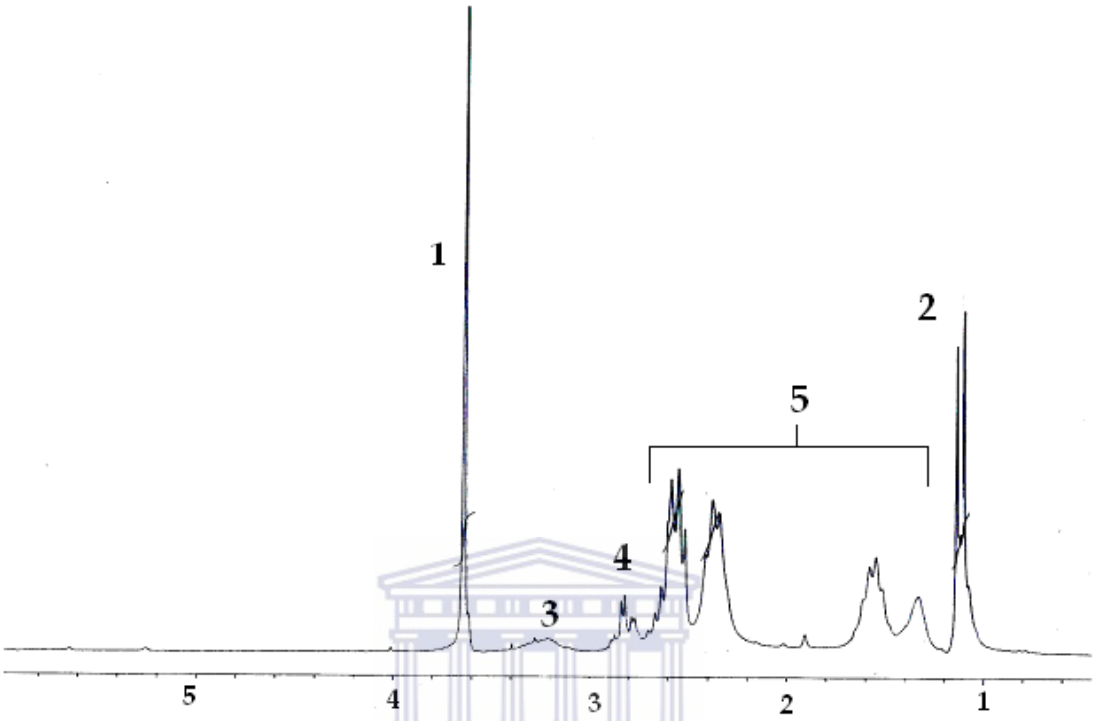

Figure 2.12: *Proton NMR spectrum of* ***L6***

The methine proton labeled as **3** is originally a proton attached to carbon of the vinyl double bond carbon of the monomer and normally expected to absorb down-field but owing to the reaction between the vinyl double bond of monomer and the primary amines of the dendrimer it shifted up field. A similar trend is observed for the protons labeled **2** and **4** in that both are shifted up-field. The only group left unaffected by this Michael-addition reaction is the methoxy group. The results were confirmed by the ^{13}C NMR spectrum displayed in Figure 2.13. The ^{13}C NMR spectrum shows all the expected peaks at the relevant chemical shifts and it confirms successful synthesis of **L6**.

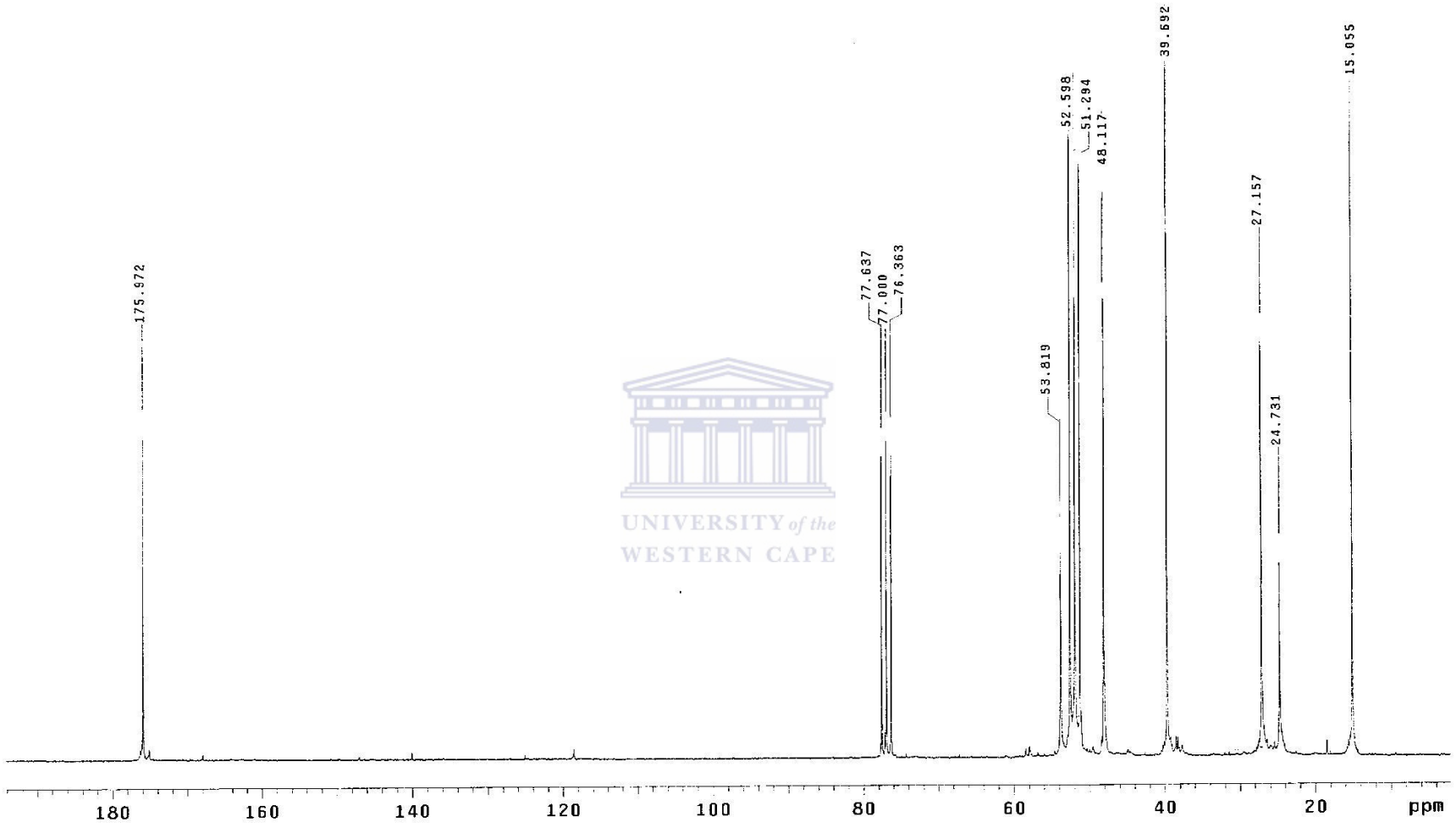

Figure 2.13: *^{13}C NMR spectrum of* ***L6***

2.2.6. Synthesis of 2nd generation methyl methacrylate functionalized DAB(L7)

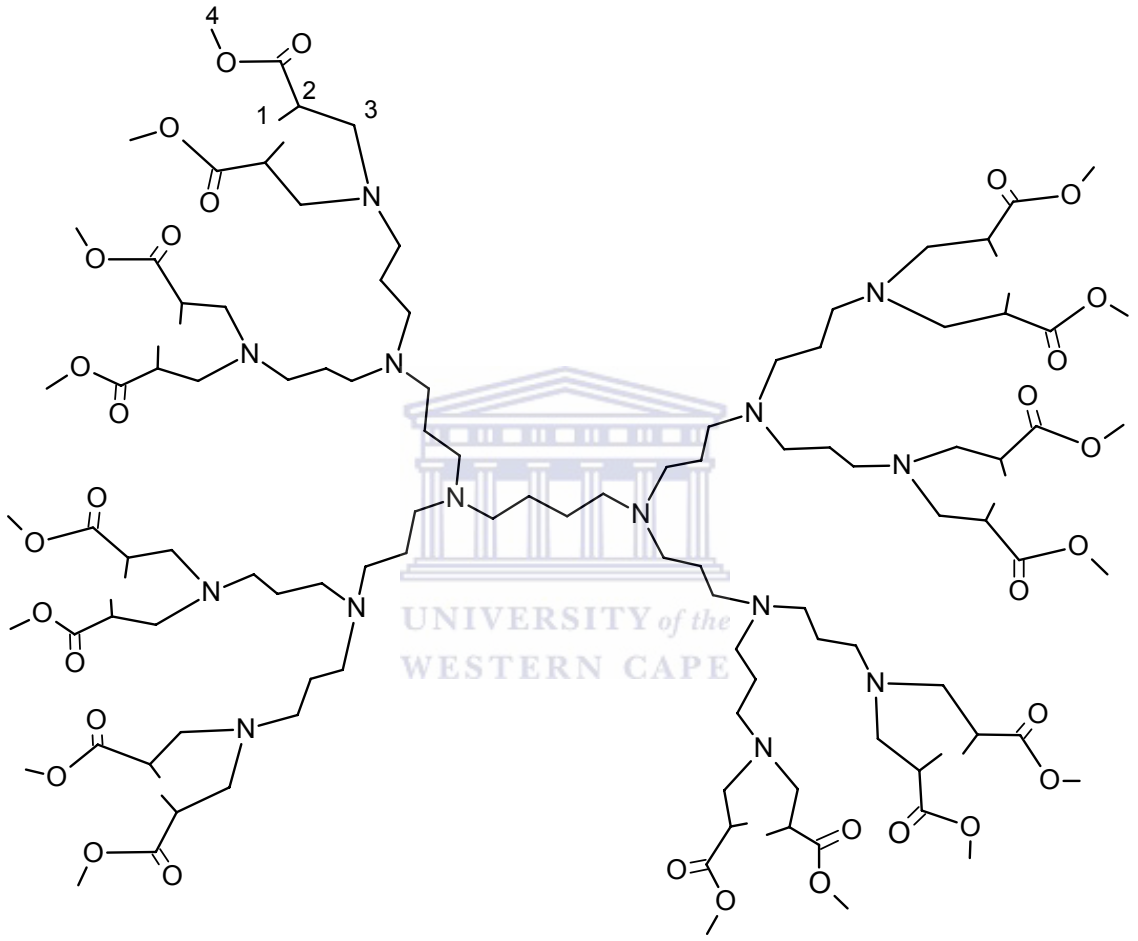

Figure 2.14: *The structure of MMA functionalized generation 2 DAB (**L7**)*

The ligand **L7** (Figure 2.14) was synthesized following the same procedure as outlined in Scheme 2.5. The reaction mixture was stirred for 4 days instead of 2 days as was the case for the generation 1 analogue. The product was isolated as

a yellow-brown viscous oil, which was soluble in chloroform and in warm toluene and p-xylene.

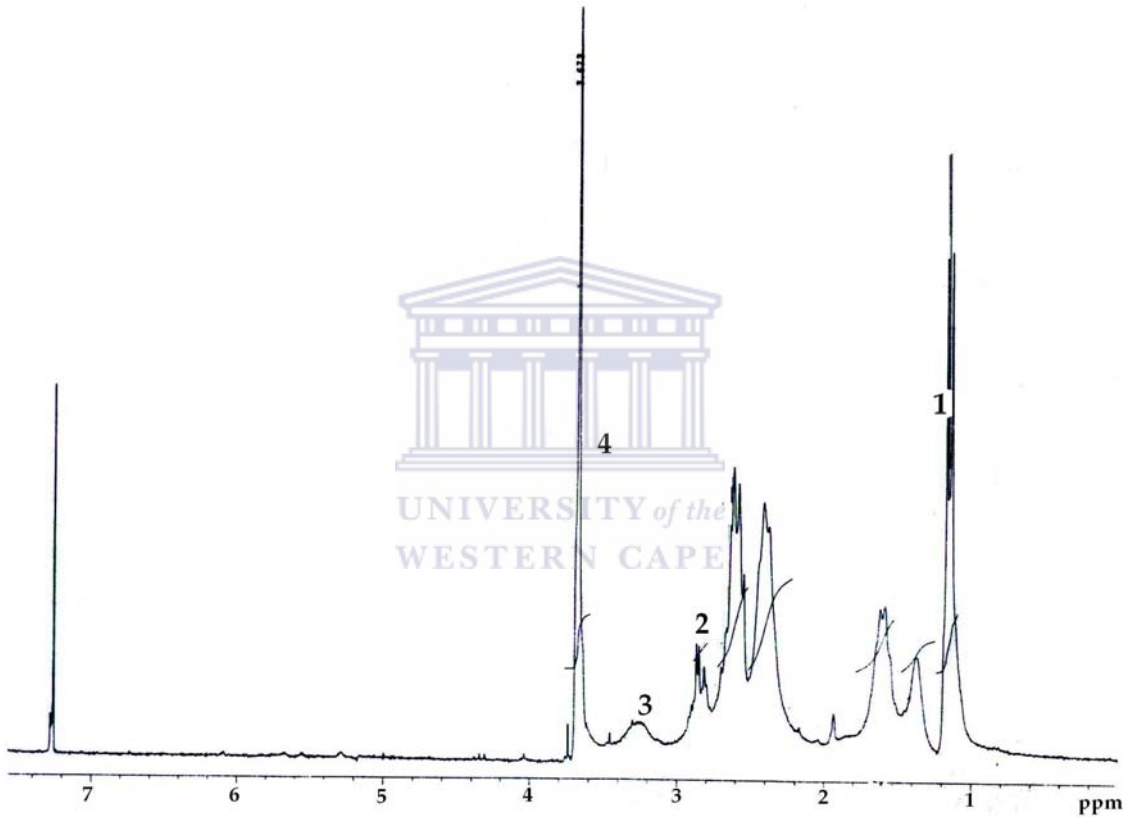

Figure 2.15: *Proton NMR of* ***L7***

2.2.6.1. Characterization L 7

The proton NMR spectrum displayed in Figure 2.15 shows that the methyl methacrylate functionalized G-2 dendrimer was successfully synthesized. The proton NMR spectrum also shows similar peak absorptions as those found in the

spectrum of the generation 1 compound. As can be observed, the chemical shift at δ = 3.44 ppm labeled as **3** is attributed to the methine proton **2** whereas the chemical shift at δ = 3.68 ppm labeled as **4** is associated with protons of the methoxy group at the surface of the functionalized dendrimer. The peak at δ = 2.85 ppm labeled as **2** is attributed to the methylene proton **3** between the carbonyl group and the tertiary amine at the periphery of the dendrimer and the doublet at δ = 1.14 -1.16 ppm is due to methyl protons of the methyl methacrylate group at the periphery of the dendrimer.

2.3. Conclusions

The synthesis of **L4** which was based on the commercially available dendrimer $DAB(NH_2)_4$ was accomplished very successfully. This is confirmed by the data obtained from the ^1H and ^{13}C NMR spectroscopy, Elemental analysis and IR spectra and NMR spectroscopy provided full information about the identity of this compound. IR spectroscopy confirmed the presence of C=N functional group. **L4** together with **L2** were successfully transformed to amine using a reducing agent to form **L5** and **L3** respectively. The hyperbranched ligands **L6** and **L7** were also successful synthesized and characterized. These two ligands were obtained as viscous oils which are stable in air.

2.4. Experimental

Materials

2-pyridylcarboxyaldehyde, $DAB(NH_2)_4$, and 4-t-butylbenzylaldehyde, were purchased from Sigma Aldrich and were used without further purification. Sodium borohydride was also purchase from Sigma Aldrich. Solvents: toluene, dichloromethane, chloroform and ethanol were purchased from Kimix Chemicals, South Africa.

Purification of solvent:

Toluene: Purified by distillation over sodium benzophenone ketyl under nitrogen.

Ethanol: Purified by distillation over dry magnesium turnings/iodine

Dichloromethane: Purified by distillation over calcium hydride under nitrogen atmosphere.

2.4.1. Synthesis of py-DAB(L2)[9]

This experiment was conducted following the procedure outlined by Smith et al. A clean round bottom flask equipped with a magnetic stirrer bar was charged with $MgSO_4$(about 3 g) in freshly dried toluene (60 ml), 2-pyridylcarboxyaldehyde (0,270 g 2,532 mmol) followed by drop-wise addition of **L1** (0.200 g 0,633mmol) in dry toluene (5 ml). The reaction mixture was stirred at room temperature for 2 days. After two days the mixture was filtered by gravity and the solvent removed by rotary evaporator. The resulting oil was dissolved in dichloromethane (20 ml) and then washed with water (7x50 ml). The organic layer was dried over $MgSO_4$

and then filtered off. The filtrate was concentrated on a rotary evaporator to produce a brown oil with a yield of 80%.

2.4.2. Synthesis of py-DABH (L3)

This compound was synthesized following the general procedure outlined by Kessar and the co-workers.[7] A solution of **L2** (0,36 g 0.5 mmol) in ethanol (20 ml) was refluxed with excess sodium borohydride (0.08 g for 5 hours. The solvent was then evaporated and residual $NaBH_4$ was decomposed with water (10 ml). The mixture was extracted with chloroform and the organic layer was dried over $MgSO_4$. The $MgSO_4$ was filtered off and the filtrate was taken to dryness on the rotary evaporator yielding an orange-brown oil, (yield 0.32 g, 89%).

2.4.3. Synthesis of tb-DAB (L4)

A clean round bottom flask equipped with a magnetic stirrer bar was charged with $MgSO_4$ (ca. 3,00 g) in freshly dried toluene (60 ml). 4-t-Butylbenzylaldehyde (0,412 g 2,53 mmol) was added followed by drop-wise addition of **L1** (0.200 g 0,632 mmol).The reaction was stirred at room temperature for 4 days. The mixture was filtered by gravity followed by removal of the solvent using a rotary evaporator. The resulting oil was dissolved in dichloromethane (20 ml) and then washed with water (4x100 ml). The organic layer was dried over $MgSO_4$ and then filtered off. The filtrate was concentrated on a rotary evaporator to yield a light yellow oil. The oil was then dissolved in hexane and allowed to stand at -5^oC overnight. A white solid was formed and it was filtered off and allowed to dry. The

product had a melting range of 85°C-87°C. The yield was 0.28 g (70%). This product was stable in air and at room temperature.

2.4.4. Synthesis of ^{t}Bu-DABH (L5)

A solution of ^{t}Bu-DAB (0.50 g 0.66 mmol) in ethanol (20 ml) was refluxed with excess sodium borohydride (0.10 g) for 10 hours. The solvent was then evaporated and the residual $NaBH_4$ was decomposed with water (10 ml). The mixture was extracted with chloroform. After drying with $MgSO_4$, the filtrate was evaporated using a rotary evaporator and the resulting in a light yellow oil yield of 0.46 g (92%). This oil was stored in the fridge at about °C.

2.4.5. General procedure for functionalization of polypropyleneimine dendrimer DAB-$(NH_2)_4$ *via Michael addition of methyl methacrylate*[9]

(synthesis of L6 an L7).

An oven dried Schlenk tube equipped with a magnetic stirrer bar and a condenser was charged with DAB-$(NH_2)_4$ in freshly distilled THF and freshly distilled methyl methacrylate at a mole ratio of two to one relative to the amine groups. The mixture was stirred for 24 hours at room temperature and then at 60 °C for 2 days (4 days for generation 2). The mixture was then evaporated on a rotary evaporator. The resulting product (oils in this case) was dissolved in chloroform (50 ml) and extracted with water (10 x 100 ml) to remove the un-reacted starting dendrimer. The organic layer was taken to dryness on a rotary evaporator. The resulting oil was dried under vacuum for 2 to 3 day to remove

excess methyl methacrylate. The yields were 90% for generation 1 and 66% for generation 2.

2.5. References:

1. Santos, D.S.; Cardoso, M.R.; Leite, F.L.; Aroca, R.F.; Mattoso, L.H.C.; Oliveira, N.O.; Mendorca, C.R. *Langmuir*. **2006**, 22, 6177.
2. Paloos, C.M.; Tsiourvas, D, Sideratou, Z.; Tziveleka, L. **2004,** 5, 524.
3. Noble (IV), C.O.; McCarley, R.L. *Org. Lett*. **1999**, 1, 1021.
4. Lim.V.; Kim, T.; Lee, W.J.; Kim, S.; Kim, H.; Kim, k.; Park, J. *Bioconjugate. Chem*. **2000**, 13, 1181.
5. Shoa, L.; Chung, T.; Goh, S.H.; Pramoda, P. J. *Membrane* Sc. **2004**, 238, 155.
6. Smith, G.S.; Chen, R.; Mapolie, S.F. *J. Organomet. Chem*. **2003**, 673, 111.
7. Kessar, V.S.; Gupta, Y.P.; Balakrishnan, P.; Sawal, K.K.; Mohammad, T.; Dutt, M. *J. Org .Chem*. **1988**, 53, 1708.
8. Shen, Z.; Chen, Y.; Frey, H.; Stiriba, S.E. *Macromolecules*. **2006**, 39, 2092.

Chapter Three:

Contents *Pages*

3.1. Introduction

Nitrogen based ligands have played a central role in Atom Transfer Radical Polymerization (ATRP) systems. Such ligands have been commonly used in the form of tertiary amines with copper(I) salts as catalysts, mostly by Matyjaszewski and coworkers.[1-4] Imine ligands have also been successfully used but they are not as common as is the case with multidentate tertiary amines.[5,6] The structural design of these nitrogen based ligands plays a very influential role in their performance as catalyst components in ATRP systems. Ligands with bulky and flexible structures have attracted attention because of their improved solubility.[1] This has resulted in these substituted ligands giving fairly good results under ATRP conditions. The efficiency of these bulky and flexible ligands was reported by Matyjaszewski *et al* who used ligands such as TMEDA (Tetramethylethylenediamine), PMDETA (*N,N,N,N,N*-pentamethyl diethylene triamine), and HMTETA (1,1,4,7,10,10-hexamethyltriethylenetetramine) (see Figure 3.1) to produce polymers with predetermined molecular weights and low polydispersities.[1] In contrast, high molecular weights and high polydispersities were obtained when bulky ligands such as unsubstituted terpyridines were used as ligands under ATRP conditions. This was attributed to the rigidity of the ligand structure which disfavours a tetrahedral structure for Cu(I) and forces Cu(II) to adopt a relatively stable trigonal bipyramidal or square pyramidal structures.[7]

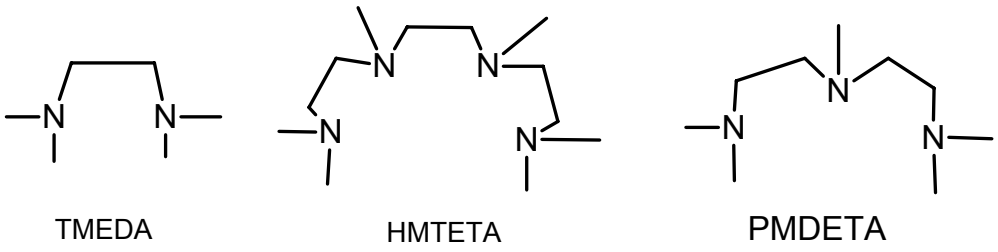

Figure 3.1: *Polydentate nitrogen based aliphatic ligands used by Matyjaszweski*

The effectiveness of tertiary amine ligands was also observed in the case of Ni(II) mediated ATRP systems. Nickel is more popular with phosphorus based ligands as far as ATRP is concerned.[8,9] The complex displayed in Figure 3.2 is known as one of the best in ATRA. However, when it was evaluated in the ATRP of styrene at high temperature, it failed to produce any polymer.[10] This nickel complex nonetheless successfully polymerized methyl methacrylate when the temperature was lowered and polymers with low polydispersities were produced. Despite the relative success of this nickel complex, no other nickel(II) complexes with tertiary amines have subsequently been reported to be useful in ATRP.

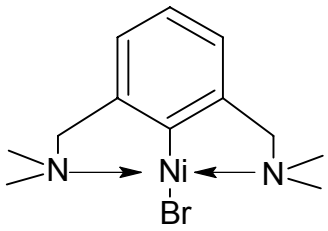

Figure 3.2: *The structure of Ni{ o,o' -$(CH_2NMe_2)_2$- C_6H_3 }Br*

Nickel complexes have recently resurfaced in the field of ATRP but with imine based ligands. These nickel complexes were again used to polymerize styrene.[11]

The structural design of these imine based ligands for the synthesis of as complexes with nickel were extensively exploited in alpha-olefin polymerization by researchers such Brookhart and Gibson independently.[12,13] The ligand shown in Figure 3.2, to the best of our knowledge, has only been used with nickel in ATRP and not with any other metal.

In this work we attempted ATRP reactions involving copper metal salts as a catalysts using polyamines as ligands with different structural designs. The use of amines in this project was guided by the work of Matjyaszewski although in his work he used tertiary amines as ligands[14]. Our ligands differed from his in that some were primary and others secondary amines. In addition many of the ligands were bulky and are also based on a dendritic scaffold. We had hoped that by incorporating them into dendrimers they would exhibit improved behaviour. These ligands are derived from the polypropyleneimine diaminobutane, Generation-1 dendrimer, DAB-$(NH_2)_4$ which is a multidentate nitrogen based ligand. DAB-$(NH_2)_4$ and is commercially available. All the new dendrimers were synthesized and characterized as reported in Chapter 2 of this thesis. All the ligands derived from DAB-$(NH_2)_4$ (**L1**) discussed in this chapter are displayed in Figure 3.3.

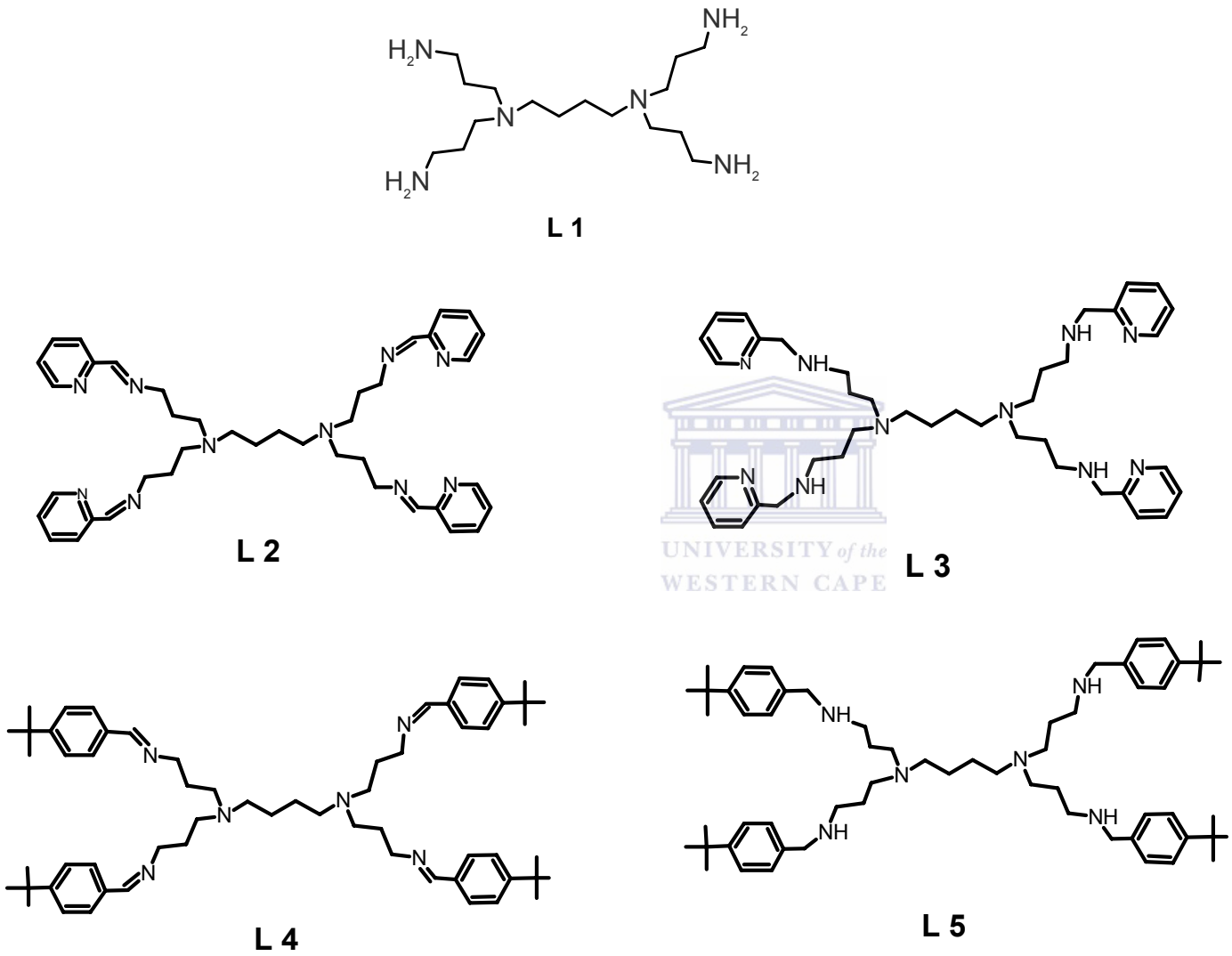

Figure 3.3: *The chemical structures of DAB(**L1**)and its derivatives*

3.2. Results and Discussion

The molecular weights of polymers obtained were experimentally measured by Gel Permeation Chromatography (GPC) and the results are compared to the theoretical calculated molecular weights and the calculations of these molecular weights are guided by the general formula given in equation 1,

$$M_n = (\Delta[M]/[R\text{-}X]_o)/(MW)_o \times \text{Conversion} + (MW)_{R\text{-}X} \qquad [1]$$

where M_n is the average number molecular weight of the polymer, [M] is the monomer concentration at time t, R-X is the initiator, $(MW)_o$ original molar mass of the monomer and $(MW)_{R\text{-}X}$ is the molar mass of the initiator.[1-4]

It is well known that the use and the subsequent value of polymers are mainly influenced by their physical properties. The physical properties of polymers are in turn influenced by their molecular weight distribution. The latter is indicated determined or measured by the polydisperisity index. The broader the molecular weight distribution, the higher the polydisperisty index of the polymer. The polydispersity of the polymer is calculated from the formula given in equation 2,

$$M_w/M_n = 1 + k_p[RX]_o/k_d[M_t^{II}X]\{(2/p - 1)\} \qquad [2]$$

where k_p and k_d are rate constants for propagation and diffusion respectively, $[M_t^{II}X]$, the concentration of the high oxidation state metal salt and p is the conversion of a monomer to polymer.[7]

3.2.1. Copper Mediated ATRP of Methyl Methacrylate in Solution

3.2.1.1 Amine dendrimers (L1, L3, L5) as ligands in copper mediated ATRP

3.2.1.1.1. ***L1*** *in copper mediated ATRP*

The first ligand tested in these ATRP systems was the commercially available DAB-$(NH_2)_4$ **L1** with copper bromide using methyl methacrylate as monomer. The reaction was performed in freshly distilled *p*-xylene as a solvent at 90^{o}C under ideal conditions of ATRP as shown in Scheme. 3.1.

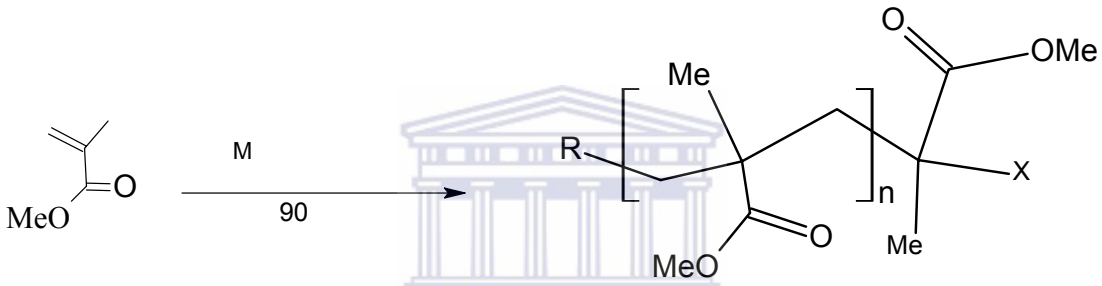

MMA **R-PMMA-X**

M

DAB = **L1**

R-X = 2-ethylbromoisobutyrate

Scheme 3.1: *Copper mediated ATRP of methyl methacrylate*

The colour of the mixture at time zero was light green which resembled the colour observed with PMDETA.[1] The reaction was initiated by 2-bromoethylisobutyrate at a ratio of 1:1:100, of initiator to copper to monomer ratio. This experiment proceeded for 45 minutes before the reaction mixture was observed to gel. The polymer product isolated from this reaction had a relatively high molecular weight (see Table 3.2) that exceeded the targeted molecular

weight of 10 000 g/mol. This was indicative of uncontrollable free radical polymerization. Since the molecular weight was higher than the target of 10 000 g/mol and as the molecular weight distribution was also higher than 1.5, it was clear that the specifications for controlled polymerization had not been met. The polymerization rate slowed down when the ratio of metal to ligand to monomer was changed to 1:1:200. In this case a conversion of about 66% was reached after 6 hours. The polymerization was repeated more than three times and the representative set of results is displayed in Figure 3.4.

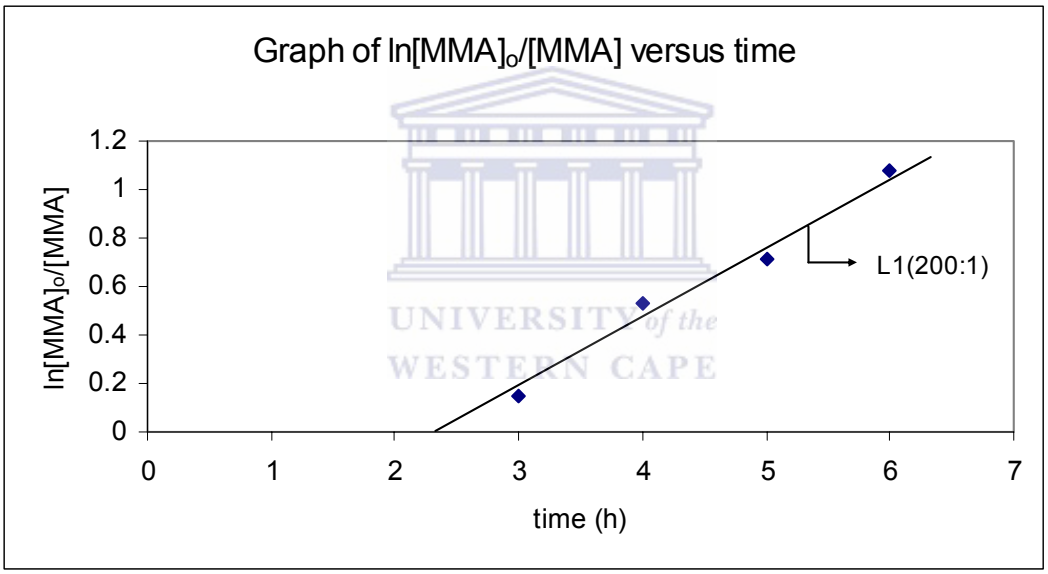

Figure 3.4: *Kinetic plot for the polymerization of MMA with 2-Ethyl- bromoisobutylrate as an initiator and CuBr/L1 in p-xyene (33% v/v) at 90°C at ratio of [MMA]/[initiator]/[CuBr]/[**L1**] = 200:1:2:1.*

The kinetic results of the polymerization of MMA were plotted as $\ln[MMA]_o\backslash[MMA]$ versus time graph (Figure 3.4) where $[MMA]_o$ = concentration of the monomer at time = zero and the [MMA] is the concentration of the monomer at time = t. A straight line graph was obtained which represents a *pseudo*-first

order kinetic plot, indicative of a constant concentration of propagating radicals and therefore minimal termination reactions as required for a controlled ATRP system. Despite the pseudo-first order reaction the molecular weights were higher than predicted and the high polydispersities also ranged from 1.42 to 1.66 (see Table 3.1). These results seem to indicate that one of the components of our catalyst system was not suitable to promote controlled ATRP. All of the components except **L1** had previously been applied in effective ATRP systems.[1] It therefore suggested that **L1** could be influencing the results negatively. The failure of **L1** to perform as desired was attributed to the possible inability to form the necessary active complexes in the different oxidation states of copper during polymerization. Alternatively if these complexes existed, they were far too stable to promote the reaction. This seems to be supported by the fact that induction times were too long as observed in Figure 3.4. The longer induction periods could have been caused by the presence of impurities or side reactions in our catalyst system which might have resulted in a retarded initiation process for our catalyst system. A most probable side-reaction to occur could involve the reaction of peripheral amine groups of the dendrimer with the methyl methacrylate monomer via addition to the vinyl double bond. If this happens a fair amount of MMA could be used up in the reaction with amino groups of **L1** that will lead to reduction of the monomer concentration initially present which at the end affect the outcome. Another side reaction could involve the peripheral amine groups with the 2-ethylbromobutyrate initiator catalyzed or promoted by the copper salt.[15] The filtrate obtained after precipitating and separating the polymers

was analyzed to ascertain if there was any product resulting from any of the possible reactions mentioned above. No unexpected species were observed. The most likely reaction was between the peripheral amine groups of **L1** and methyl methacrylate via a Micheal addition. A similar reaction was reported to be possible by Dubber and Lindhorst[16] where the authors showed the reaction of an amine with methyl acrylate (in Scheme 3.2)

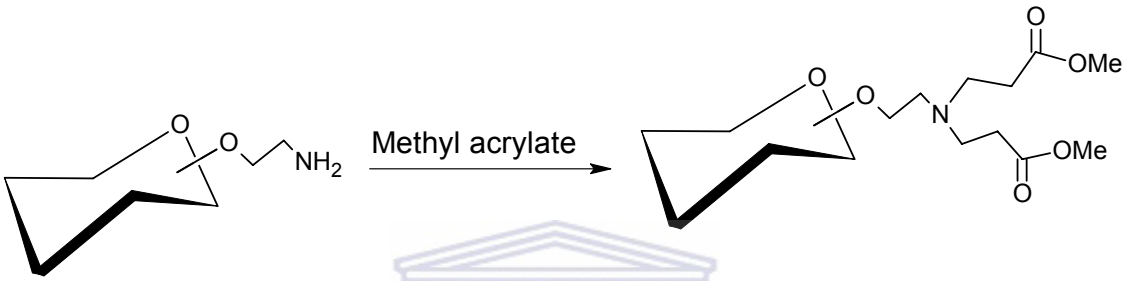

Scheme 3.2: *Reaction of methyl acrylate with primary amine via Michael addition*

After failing to identify any other kind of side reaction product and having only observed uncontrolled radical polymerization, it was discovered in the literature that there was a report discussing other possible reasons for uncontrollable ATRP.[14] This report was a paper by Matyjasewszki and coworkers explaining that "linker between the two coordinating nitrogens is crucial" meaning that if two coordinating nitrogen atoms of a polydentate ligand are separated by more than two methylene carbon atoms, they are likely to produce polymers with high polydispersities and high molecular weights under the ATRP condition.[14] This paper went further to provide examples of such ligands. These examples are shown below in Figure 3.5. Examining the chemical structures of these ligands in Figure 3.5 it can be seen that all of these ligands are bidentate. Since (**L1**) is

multidentate, it was therefore hoped that a positive outcome would be obtained. As demonstrated by the experimental results obtained in our labs, this was not the case. To provide more insight, the results obtained in our study were compared to those reported by Matyjaszewski el al. [14] This data is shown in Table 3.1 in compared with data in Table 3.2.

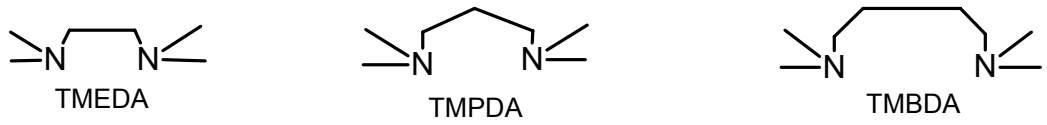

Figure 3.5 The chemical structures of TMEDA, tretramethyl propyl diamine (TMPDA) and tetramethyl butyl diamine (TMBDA)

Table 3.1: *Literature conversion and GPC data*[14]

Ligand	monomer	time(h)	conv(%)	$^{a}M_{n(cal)}$	$^{b}M_{n(GPC)}$	M_w/M_n
TMEDA	MMA	2.75	65.7	13140	12140	1.39
TMPDA	MMA	1.40	30.1	6020	16460	1.44
TMBDA	MMA	0.50	3.00	600	65390	2.00

^{a}Mn(cal) = theoretical molecular weights, ^{b}Mn(GPC) = experimental molecular weight. Conditions: 50%(v/v) anisole, 90^{o}C: $[MMA]_O/[2\text{-EBiB}]_o$ = 200;[2-EBiB]o/[CuBr]o/[ligand]o = 1/1/1

The above results from Matjyaszewski *et al,*[14] show the non-compliance of TMPDA and TMBDA as ligands in ATRP reactions. These two ligands produced molecular weights ($M_{n(GPC)}$) that are much higher than the theoretical molecular weights (M_{ncal}) whereas TMEDA with two carbon atoms between two coordinating nitrogen atoms produced experimental molecular weights of which were lower than the theoretical molecular weights, something acceptable for a controlled ATRP system. The literature results in Table 3.1 were compared to our

experimental results when **L1** was used as a ligand at different ratios of ligand to metal to initator. The results are displayed in Table 3.2. It is clear from these results that the ATRP requirements were not met for our system because the molecular weights obtained from GPC are much higher than the theoretical molecular weights calculated from the conversions. In addition, the polydispersities are far above the 1.5 limit.

*3.2.1.1. 2. **L3** as a ligand in copper mediated ATRP*

In the process of modifying **L1,** it was decided that this ligand should be chemically modified with the aim to increase its bulkiness and electronic properties. This was achieved by incorporating aromatic functionalities such as pyridine-amine units on the periphery to produce **L3**. The aromatic groups were also expected to influence the electronic properties of the ligand.[17] However it should be remembered that the solubility may be compromised by these changes. ATRP of MMA was performed with **L3** as a ligand at ratio of 1:2:1:200 (initiator to metal to ligand to MMA) at 90^{o}C in freshly dried p-xylene as solvent. The reaction gave a green color at the beginning which is common for amines and it went dark green as the reaction progressed. There was no observable difference in the solubility of **L3** compared to **L1**. As the reaction progressed and samples withdrawn there was no observable change in viscosity, except in the last sample. This observation signaled a slow reaction with low conversion as confirmed by the kinetic plot displayed in Figure 3.6.

Table 3.2: *Conversion of MMA and GPC data for **L1** as ligand in MMA polymerization*

[L1]:[M_t]:[Monomer]	time(h)	conv(%)	[a]$M_{n(cal)}$	[b]$M_{n(GPC)}$	M_w/M_n
1:1:100	0.45	81	8265	14170	1.87
1:2:100	2	36	3945	10831	1.52
	4	40	4145	11011	1.41
	8	46	4795	12357	2.80
	12	50	5235	12916	3.10
1:2:200	2	13	2795	18945	1.93
	3	14	2995	22871	2.22
	4	41	8395	24419	2.35
	5	51	10395	24156	2.35
	6	66	13395	24968	2.40
1:2:300	6	10	3195	21665	3.92
	9	18	5595	29302	3.39
	12	57	17295	31356	3.88

[a]Mn(cal) = theoretical molecular weights, [b]Mn(GPC) = experimental molecular weight. Conditions: 33%(v/v) p-xylene, 90^{o}C:[2-EBiB]o/[CuBr]o/[ligand]o = 1/2/1

.The graph in Figure 3.6 shows a perfectly straight line which indicates a low concentration of radicals produced which should indicated a reduce occurrence of termination reactions. However, the experimental molecular weights ($M_{n(GPC)}$)

were higher than the theoretical molecular weights ($M_{n(cal)}$) and the polydispersities were also higher than 1.5. The graph also shows a very long induction period even worse than that for **L1** (see Figure 3.4). The latter which had an induction period just above two hours compared to four hours observed for **L3**.

Table 3.3 *Conversions of mma and GPC data for **L3** as ligand in mma polymerization*

[L3]:[Mt]:[Monomer]	time(h)	conv(%)	[a]$M_{n(cal)}$	[b]$M_{n(GPC)}$	M_w/M_n
1:2:100	4	43.7	4565	24583	2.21
	5	50.7	5265	54050	3.00
	7	63.5	6545	56855	3.65
	10	70.1	7205	60191	3.56
1:2: 200	4	2.0	595	34754	1.77
	6	10.0	2195	38738	1.67
	8	24.0	4995	41657	2.01
	12	39.0	7995	52928	1.43

[a]Mn(cal) = theoretical molecular weights, [b]Mn(GPC) = experimental molecular weight. Conditions: 33%(v/v) p-xylene, 90^{o}C:[2-EBiB]o/[CuBr]o/[ligand]o = 1/2/1

The bulkiness caused by the presence of aromatic groups on the ligand structure could also have played a role in the slow formation of active species indicated by a long induction period. The bulkiness may have restricted the rate of the halogen exchange since it is known that the halogen transfer from the transition

metal salt should be close to diffusion controlled.[7] If Equation 2 is applied it can be seen that if there is no halogen transfer between the oxidation states of a metal salt high polydispersities will be observed.

$$M_w/M_n = 1 + k_p[RX]_o/k_d[M_t^{II}X]\{(2/p -1)\} \quad [2]$$

where k_p and k_d are rate constants for propagation and deactivation, respectively, $[M_t^{II}X]$ the concentration of the high oxidation state metal salt and p the conversion.[7]

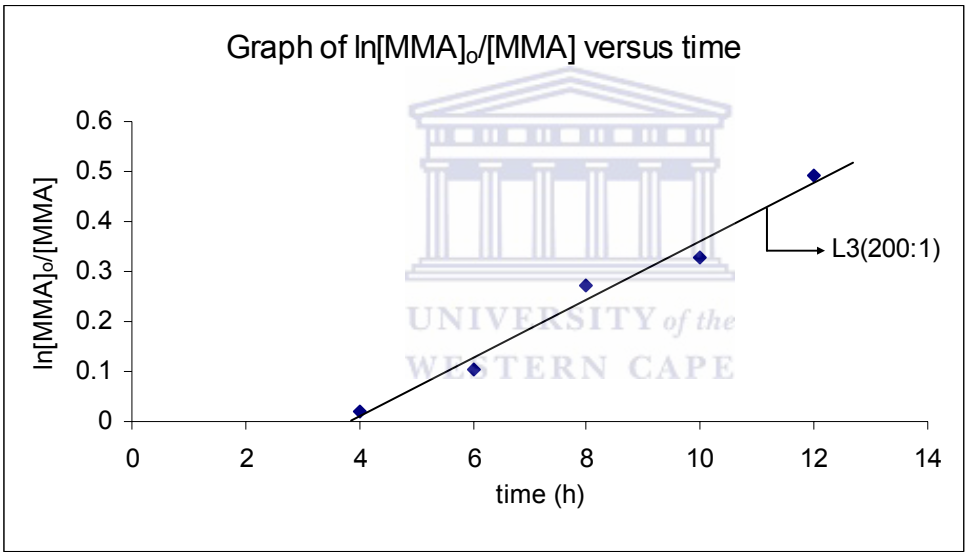

Figure 3.6: *Semilogarithmic kinetic plot for the polymerization of MMA with 2-Ethyl-bromoisobutylrate as an initiator and CuBr/**L3** in p-xylene (33% v/v) at 90°C at ratio of [MMA]/[initiator]/[CuBr][**L3**] = 200:1:2:1.*

This behaviour is often associated with bulkiness of the ligand. A similar observation was also made by Ibrahim and coworkers where they used bulky and rigid amine ligands such as the one displayed in Figure 3.7 with phenyl groups attached to the nitrogen atoms which makes the overall structure more

rigid and bulky.[18] These researchers obtained very similar results to those observed in our study of **L3** see Table 3.4. It should be emphasized that we are only comparing the bulky nature of the two systems. The Ibrahim ligand is a tertiary amine while ours is a secondary amine.

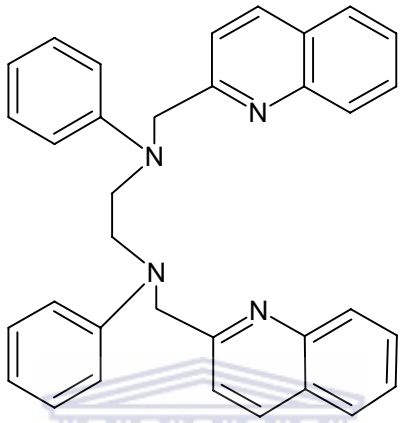

Figure 3.7: *The structure of N, N' diphenyl-N,N'(quinoline-2methyl)-1,2 ethylenediamine*

Table 3.4: Results of the ATRP polymerization of MMA[9] (literature)

Entry	time (h)	conv(%)	$M_{n(cal)}$	$M_{n(GPC)}$	M_w/M_n
1	10	16	3200	15000	1.27
2	20	27	5400	23000	1.36
3	30	43	8600	27000	1.55
4	40	53	10600	61500	2.4

Conditions: T = 90 ^{o}C, solvent, o-xylene (33%, v/v), [monomer]:[initiator]:[catalyst]:[ligand] = 200:1:1:1

If the literature results in Table 3.4 are compared with those of **L3** in Table 3.3 it is observed that in both cases the experimental molecular weight ($M_{n(GPC)}$) are far higher than the theoretical molecular weight ($M_{n(cal)}$). The reason for this poor control has been already explained earlier on.

*3.2.1.1. 3. **L5** in copper mediated ATRP*

The results for **L3** were not much different from those for **L1**. The ligand **L5** was thus synthesized with the hope that it would lead to better solubility than that observed for **L3**. This was because of the tertiary butyl substituents on the benzene ring as shown in Figure 3.3. The ATRP of MMA was performed with **L5** as ligand at 90^{o}C in freshly dried p-xylene as a solvent under the normal conditions of ATRP. It was indeed observed that complete solubility of the catalyst components occurred yielding a deep green homogeneous solution. The ratio of ligand to metal to initiator to monomer was 1:1:1:100. The reaction mixture formed a gel in less than 40 minutes reaction time. The polymerization was repeated with the ratio of ligand to metal to initiator to monomer changed to 1:2:1:100. In this instance there was an observable change in viscosity as polymerization progressed and samples were withdrawn periodically over a 15 hour period. The results are displayed in Table 3.5. Several attempts were made with other ratios but no polymers were obtained especially when the ratio of initiator to monomer was 1:100.

Table 3.5 *Conversions of MMA and GPC data for **L5** as ligand in mma polymerization*

[L5]:[Mt]:[Monomer]	time(h)	conv(%)	$^{a}M_{n(cal)}$	$^{b}M_{n(GPC)}$	Mw/Mn
1:2:100	5	20	2215	52647	2.62
	8	27	2865	55287	2.28
	10	33	3495	55897	2.47
	15	55	5685	60011	2.50

^{a}Mn(cal) = theoretical molecular weights, ^{b}Mn(GPC) = experimental molecular weight. Conditions: 33%(v/v) p-xylene, 90^{o}C:[2-EBiB]$_{o}$/[CuBr]$_{o}$/[ligand]$_{o}$ = 1/2/1

It can be observed from Table 3.5 that the highest conversions were obtained after fifteen hours reaction time, an indication of how slow this polymerization was compared to the reaction where **L1** was used as the ligand**.** The representative results are displayed in Figure 3.8 after several experiments performed. According to the literature, steric hindrance discourages easy exchange of the halogen atom or it retards the exchange allowing termination reactions to be dominant.[7] The concentration of propagating radicals was not as constant and this is evident in the graph in Figure 3.8. In addition, molecular weight distribution is broad. Steric hindrance is proposed to be a contributing factor to the loss of control of molecular weights in these systems as is shown in Table 3.4[18] when a bigger as well as flexible ligand was used and compared to the ligands in this work. It is clear that the results in Table 3.5 are in many ways similar to that obtained with **L3** (Table 3.3).

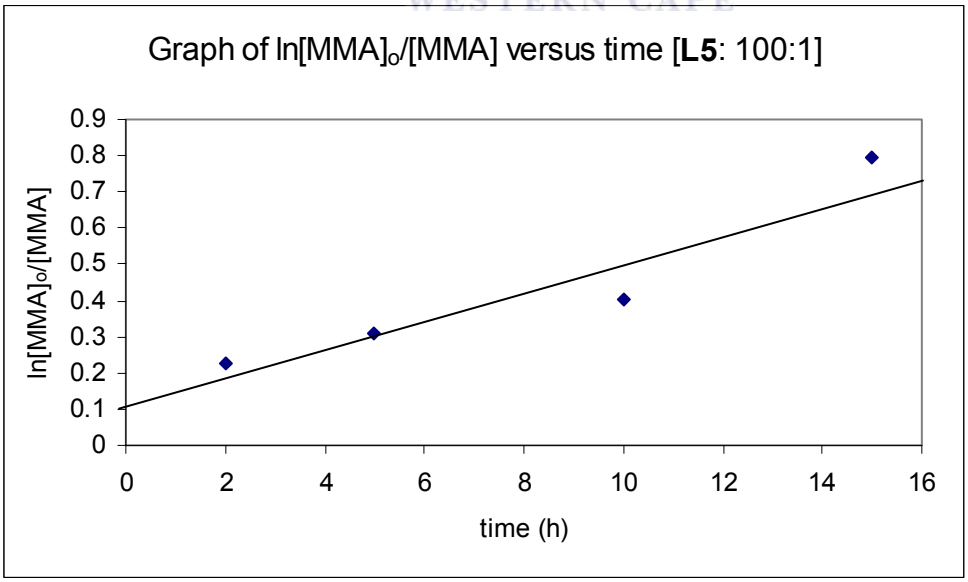

Figure 3.8: *Semilogarithmic kinetic plot for the polymerization of MMA with 2-Ethyl-bromoisobutylrate as an initiator and CuBr/L5 in p-xylene (33% v/v) at 90°C at ratio of [MMA]/[initiator]/[CuBr]/[**L5**] = 100:1:2:1.*

3.2.1.2 Imine dendrimers as ligands (L2 and L4) in copper mediated ATRP

*3.2.1.2.1. **L2** in copper mediated ATRP*

In this section we investigated the behavior of imine ligands in copper mediated ATRP. Imines have previously been employed successfully in ATRP reactions. It was for this reason, ligand **L2** was prepared. **L2** is essentially the imine version of **L3** (see Figure 3.3). The functionalities in **L2** are also known to promote controlled ATRP as reported by Haddleton.[6] As the structure of **L2** dictates, the ratio of metal to ligand was 2:1 and monomer was used at ratio 100:1 monomer to initiator. However, a 200:1 ratio was also attempted and the results are displayed in Table 3.6 and discussed thereafter. The polymerization was conducted in freshly distilled p-xylene at 90^{o}C with **L2** as the ligand. CuBr was used as catalyst and 2-ethylbromoisobutyrate as initiator under ATRP conditions. The solubility of the ligand was very not very good. The colour of the solution was light brown at the beginning of the reaction and became dark brown with visible change in viscosity as the reaction progressed for both ratios but the change was noted to occur after a longer period in the case of 200:1 reaction. The molecular weights of the resulting polymers are shown in Table 3.6.

Table 3.6 *Conversions of mma and GPC data for **L2** as ligand in mma polymerization*

[L2]:[Mt]:[monomer]	time(h)	conv(%)	$^{a}M_{n(cal)}$	$^{b}M_{n(GPC)}$	Mw/Mn
1:2:100	2	20.4	2235	36451	2.90
	4	30.4	3235	53048	2.67
	5	49.2	5115	73071	3.76
	7	56.4	5835	80919	2.71
	9	63.2	6515	86154	3.65
1:2:200	6	7.5	1695	30694	2.05
	8	15.0	3195	34575	4.22
	10	22.0	4595	40674	1.88
	12	32.0	6595	56278	2.79

^{a}Mn(cal) = theoretical molecular weights, ^{b}Mn(GPC) = experimental molecular weight. Conditions: 33%(v/v) p-xylene, 90^{o}C:[2-EBiB]o/[CuBr]o/[ligand]o = 1/2/1

As can be observed from the Table 3.6 the molecular weights obtained from GPC were not good. The experimental molecular weights are much higher than theoretical molecular weights values. The bulkiness of the ligand can potentially stabilize the metal in +2 state as observed by Matyjaszewski and coworkers.[7] Ideally, the high concentration of Cu(II) oxidation state and low concentration of initiator should promote the production of uniform polymers.[7] In the case under investigation, steric factors might have prevented the formation of Cu(II) although the initiator concentration was low. This explains why there was a linear growth of conversion with time although high molecular weights are obtained.

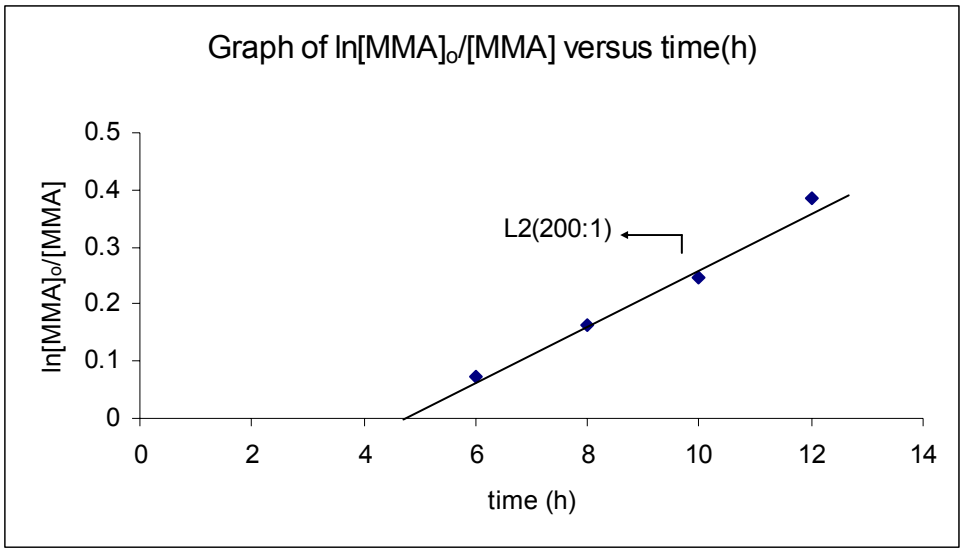

Figure 3.9: *Semilogarithmic kinetic plot for the polymerization of MMA with 2-Ethyl-bromoisobutylrate as an initiator and CuBr/L2 in p-xylene (33% v/v) at 90°C at ratio of [MMA]/[initiator]/[CuBr]/[**L2**] = 200:1:2:1*

The graph in Figure 3.9 shows a perfectly straight line which indicates a first-order semilogarithm plot. This indicates that there was constant concentration of propagating radicals but the higher molecular weights than predicted show loss of control of this system. This can be attributed to mainly bulkiness and rigidity of the ligand as already mentioned. A long induction time can be associated with poor solubility of the ligand-metal complex which leads to slow formation of the active species. In our case we observed that the reaction mixture was distinctly heterogeneous in nature. The slow formation of active species may also be a result of poor initiation as reported by some researchers.[19] The linker between the two coordinating nitrogen atoms of ligand **L2** seem to have an effect even though the imine functionalities on the surface of the dendrimer ligand are known to promote ATRP. In a paper published in 2004[18] a ligand with a similar imine functionality to that of **L2** but with a cyclic linker between the two coordinating

nitrogen atoms (see Figure 3.10) was found to be inactive for ATRP. In this case, the inert nature of the catalyst system based on this ligand was caused not only by the bulkiness and rigidity of aromatic group of the ligand but also the bulkiness of the linker between the two donor nitrogen centers. Cyclic amines produced traces of polymers and show lower conversions as reported by Haddleton *et al.* [17] This was largely attributed to steric hindrance.

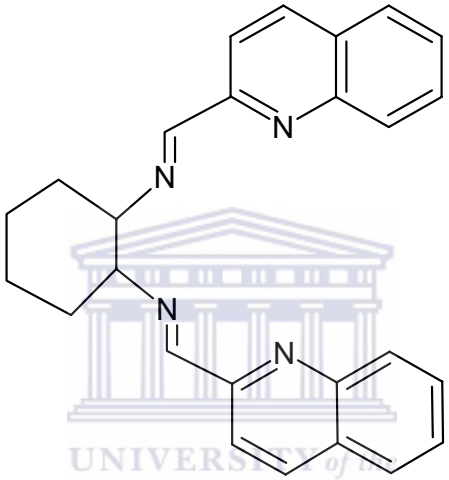

Figure 3.10: *The structure of (1R,2R)-(-1)-N,N'-Di(quinoline-methyl) di-imino-cyclohexane*

3.2.1.2.2. L4 in copper mediated ATRP

In the process of chemically modifying the dendritic ligands we also used the imine version of **L5**. Again in this case we hoped that the presence of the tertiary butyl substituents on the benzene ring would improve the performance of this ligand. The structure of this ligand is displayed in Figure 3.3. The polymerization reaction was performed in 33% v/v of freshly dried p-xylene at 90^{o}C with **L4** as a ligand, CuBr as a catalyst and ethyl-2- bromoisobutyrate as an initiator under ATRP conditions. This ligand unlike other ligands (all other ligands were oils) was

a white solid/powder. The ligand was dried under vacuum for two days before use. The polymerization solution became orange-red at the beginning of the reaction and changed to reddish-brown as time progressed. There was no visible change in viscosity until late in the reaction. The only ratio that gave meaningful results was 100:1:2:1. The ratio of 200:1 (monomer to initiator) failed to produce any polymer throughout the reaction period even after 27hrs. This observation is similar to what was seen for **L5**. Both ligands did not produce polymers easily as that can be observed from the data presented. The results of this polymerization reaction are displayed in the Table 3.7.

Table 3.7 *Conversions of mma and GPC data for **L4** as ligand in mma polymerization*

[L4]:[Mt]:[monomer]	time(h)	conv(%)	$M_{n(ca)}$	$M_{n(SEC)}$	Mw/Mn
1:2:100	5.00	10.5	1245	26525	1.34
	8.00	24.0	2595	22812	1.55
	12.00	44.3	5685	30498	1.89

[a]Mn(cal) = theoretical molecular weights, [b]Mn(GPC) = experimental molecular weight. Conditions: 33%(v/v) p-xylene, 90^{o}C:[I]/[CuBr]/[ligand] = 1/2/1

In Table 3.7 above it can be observed that the molecular weights ($M_{n(GPC)}$) are much higher than expected and the polydispersities are also high. This may be attributed to factors such as rigidity of the ligand. In addition to the rigid aromatic rings, the bulkiness provided by the presence of tertiary butyl substituents could have affected the performance of the ligand negatively even though they may have helped in solubility. This could only be confirmed if the rigid aromatic rings are replaced with flexible substituents and that is objective of the next chapter.

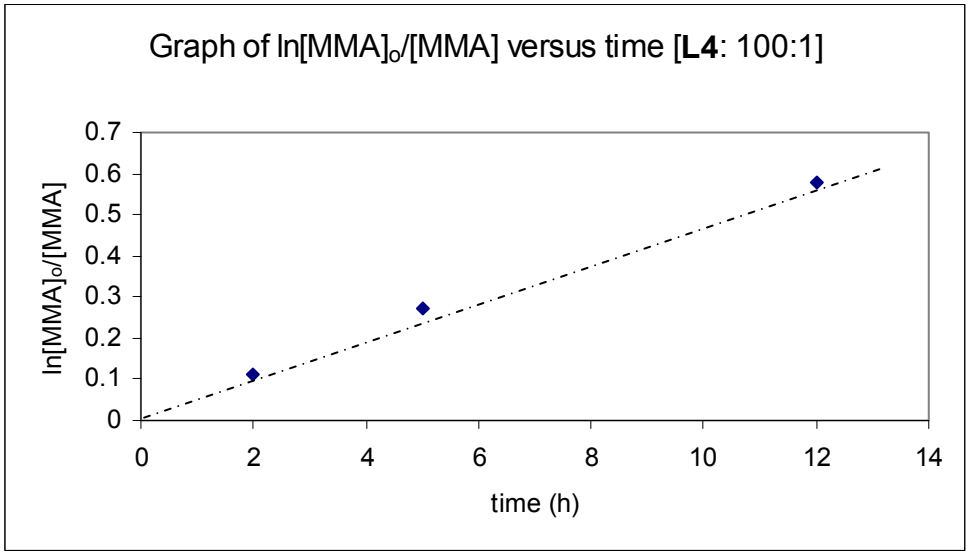

Figure 3.11: *Semilogarithmic kinetic plot for the polymerization of MMA with 2-Ethyl-bromoisobutylrate as an initiator and CuBr/**L4** in p-xylene (33% v/v) at 90°C at ratio of [MMA]/[initiator]/[CuBr]/[**L4**] = 100:1:2:1*

The kinetic results in Figure 3.11 did not show a conclusive trend as required by ATRP. Although we had a straight line graph the reaction was still not controlled as evidenced by the high experimental molecular weights for the polymers isolated.

3.3. General discussion and conclusion

In section 3.1 we have accounted for the behavior of each ligand under ATRP conditions. In this section we conclude by presenting the results for all the ligands used at a particular ratio on the same kinetic plot in order to make a clearer comparison of their behavior. This comparison should help ascertain where the chemical modifications had improved or failed in terms of the ATRP

process. This section will also help in drawing conclusions about the behavior of these ligands and most importantly provide guidance with respect to deciding whether we should continue with the modification of the ligands for application in the ATRP or opt for the use of these ligands for other applications.

3.3.1 ATRP at ratio of 100:1, monomer to initiator

All the ligands used at this ratio managed to produce polymers. All of the ligands achieved higher molecular weights than expected as well as high polydesipersities. As far as kinetic analysis are concerned, the polymerization at the ratio 100: 1, monomer to initiator showed high rates with very little induction time as shown in Figure 3.12 .

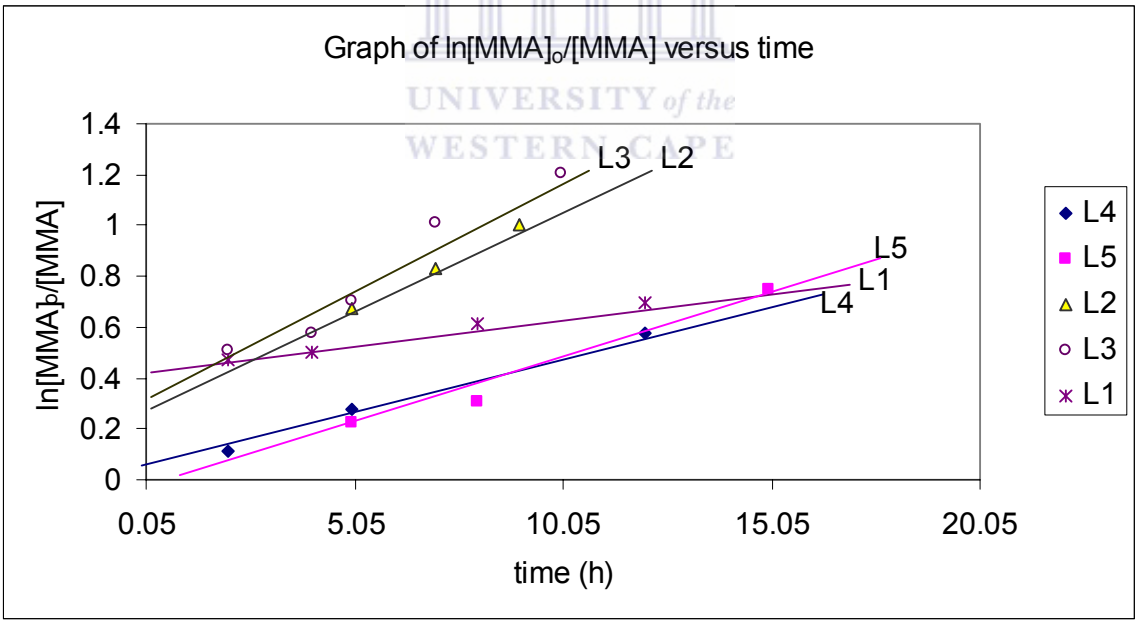

Figure 3.12: *Semilogarithmic kinetic plots of the polymerization of MMA with 2-Ethyl-bromoisobutylrate as an initiator and CuBr/L in p-xylene (33% v/v) at 90°C at ratio of [MMA]/[initiator]/[CuBr]/[L] = 100:1:2:1 where L =* ***L1- L5***

The high rate of reaction as shown in the plots above is an indication of fast initiation of polymerization that may generally be attributed to the fact that there is high concentration of the initiator. In most of the plots especially for **L1** a first order straight line was observed indicative of a constant propagating radical concentration. The fact that this kind of observation only occurs with ligands that possess aromatic rings leads to the conclusion that rigidity on the ligands had affected the performance of the ligands an easy halogen exchange. In addition, these ligands possessing aromatic functionalities also showed lower polymerization rates as observed from the low conversions compared to **L1.** This was further evidence that indeed steric hindrance may have played an inhibiting role. What can also be learnt from this kinetic plot is that the structural nature was more influential than the electronic properties. This effect can be clearly observed from the curve of **L2** and **L3** which both have their points slightly scattered although the behavior is more pronounced for **L3**. This is also observable in the case of **L4** and **L5** which both have low rate of polymerization and their curves are almost the same. **L4** and **L5** are much bulkier than **L2** and **L3**.

3.3.2 ATRP with ratio of 200:1, monomer to initiator

The ratio of 200:1 monomer to initiator serves to support the conclusion made above about the negative effect of the bulkiness of ligands possessing aromatic substituents. As can be observed from the graph in Figure 3.13 ligands **L3** and

L2 both show long induction times whereas **L4** and **L5** did not produce any polymer at this ratio.

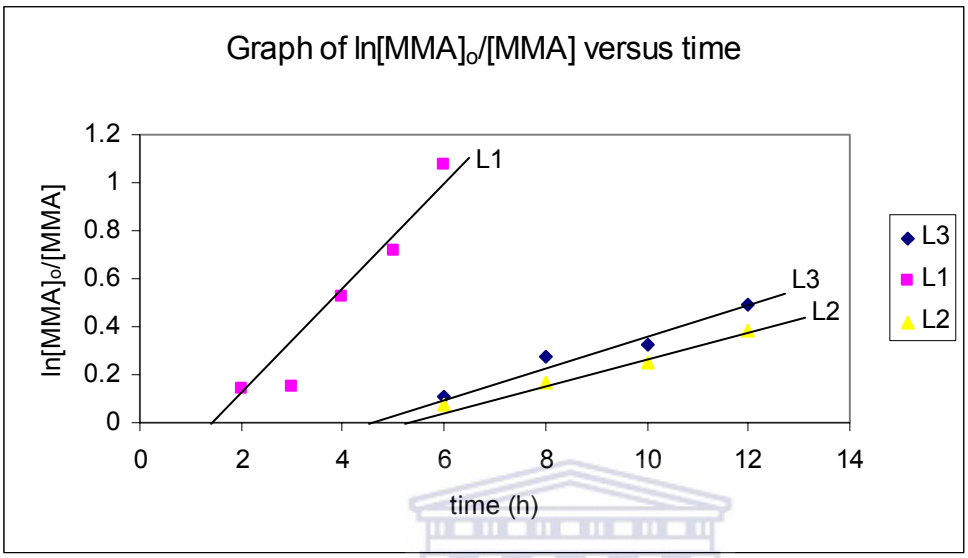

Figure 3.13: *Semilogarithmic kinetic plot for the polymerization of MMA with 2-Ethyl-bromoisobutylrate as an initiator and CuBr/L in p-xylene (33% v/v) at 90°C at ratio of [MMA]/[initiator]/[CuBr]/[L = 100:1:2:1 where L =* ***L1****,* ***L2****, and* ***L3****.*

The only positive observation in Figure 3.13 is the fact that both **L2** and **L3** show a first order kinetic plot indicative of constant production of active species but the polydispersities and the molecular weights were high which undermines the essence of this result as far as ATRP is concerned. The graph in Figure 3.13 serves to confirm the statement that the structural design of the ligand had more influence on the overall performance of the ligands in these reactions. **L1** is bulky but flexible compared to the other ligands and it is smaller in size in this family of dendrimers. If compared to the structures given in Figure 3.5 this may mean that the contributing factors to poor performance of **L1** under ATRP condition are the

effect of more two methylene carbons between two coordination nitrogens atoms as reported by Matyjaszewski and the fact that this ligands has peripheral primary amine groups which are not useful in ATRP.[14] It is in the objectives of the next chapter to replace or remove the primary amine groups at surface of the dendritic ligands **L1**. The 200:1 ratio shows clearly that it is the most preferred composition compared to 100:1 monomer to initiator. Although also negative these results of L1 served as encouragement to further modify the ligand with strictly flexible functionalities as it reported in Chapter four.

3.4. Experimental Method

3.3.1 Material

All experimental manipulations were conducted under an argon atmosphere using Schlenk line techniques. All solvents were freshly distilled before use. Toluene and *p*-xylene were purchased from Kimix Chemicals and dried over sodium/benzophenone ketyl under argon atmosphere. 2-Bromo-ethylisobutylrate was purchased from Sigma-Aldrich and distilled before use. Methyl methacrylate was purchased from Sigma-Aldrich and passed through a column of basic alumina and distilled twice over calcium hydride before use. Methanol was purchased from Kimix Chemicals and used as received. Tetrahydrofuran (HPLC grade) was purchased from Anatech and was used as received. Cu(I)bromide (98%) was purchased from Sigma-Aldrich and purified according to literature procedures.[20] Nylon membrane solvent filters were purchased from Anatech. DAB-(Am) 4 was purchased from Symochem, Netherlands.

3.3.2 Instruments

The monomer conversions were monitored using Gas Chromatography (Varian CP-3800:column: HP-PONA 50 m x 0.200 mm (agilent technologies Inc)). Molecular weights were determined using Gel Permeation chromatography {Agilent 1100 series: columns : PLgel 10 µm 500 Å, PLgel 5 µm Mixed-C(300 x 7.5 mm), PLgel 5µm Mixed-D (300 x7.5 mm) and guard PLgel 5 µm(50 x 7.5 mm)}.

3.3.3. General polymerization procedure.

An oven dried Schlenk tube equipped with a magnetic stirrer bar was charged with purified CuBr, ligand, freshly distilled MMA (10 ml) and freshly distilled and dried solvent (33% vol). The tube was sealed under vacuum before performing three freeze-pump-thaw cycles followed by addition of freshly distilled ethyl 2-bromoisobutyrate. The mixture was placed in an oil bath at 90 ^{o}C and the vessel sealed under vacuum. After certain time intervals, the tube was opened under positive pressure of argon and a 1ml sample was withdrawn and transferred into a vial containing THF (9 ml).

-*General characterization of polymer samples*: The samples were analyzed by GC analysis using 1-decene as internal standard to determine the conversion. The samples were then passed through the column of basic alumina before precipitation with methanol. The polymers obtained were dried under vacuum for

at least a 24 hours before the molecular weight determination using GPC. Molecular weights of polymethyl methacrylate were calibrated with polymethyl methacrylate standards purchased from Polymer Laboratories.

3.5. References:

1. Xia, J. ; Matyjaszewski, K.; *Macromolecules.* **1997**, 30, 7697.
2. Percec, V.; Kim, H.J.; Barboiu, B.; *Macromolecules.* **1997**, 30, 8526.
3. Granel, C.; Dubois, Ph.; Jerome, R.; Teyssie. Ph. *Macromolecules.* **1996**, 29, 8576.
4. Wang, J.; Matyjaszewski, K.; *Macromolecules*, **1995**, 28, 7901.
5. Destarac, M.; Bessiere, J.M.; Boutevin, B.; *Macromol Rapid commun*, **1997**. 18 .967.
6. Haddleton, D.;Jasieczek, C.B.; Hannon, M.J. Schooter, A.J.; *Macromoleculas*. **1997**, 30, 2190.
7. Kickelbick, G.; Matyjaszewski, K.; *Macromol Rapid Commun*. 1999, 20, 341.
8. Uegaki, H. ; Kotani, Y. ; Kamigaito, M. ; Sawamoto, M. *Macromolecules*. **1997**, 30, 2249.
9. Uegaki, H. ; Kotani, Y. ; Kamigaito, M. ; Sawamoto, M. *Macromolecules.* **1998**, 31, 6756.
10. Haddleton, D.M. ; Crossman, M.C. ; Dana, B.H. ; Duncalf, D.J. ; Heming, A.M; Kukulj, D.; Shooter, A.J.; *Macromolecules*, **1999**. 32. 2110.

11. O'Reilly, K.R.; Shaver, M.P.; Gibson, V.C.; *Inorganica Chimica Acta.* **2006,** 359, 4417.

12. Britovsek, G.J.P.; Gibson, V.C.; Kimberley, B.S.; Maddox, P.J.; McTavish, S.J.; Solan, G.A..; White, A.J.P.; Williams, D.J. *Chem. Commun*. **1998**, 849.

13. Johnson, L.K.; Killian, C.M.; Brookhart, M.; *J. Am. Chem. Soc*. **1995**, 117, 6414.

14. Xia, J. ; Zhang, X.; Matyjaszewski, K.; *Polym. Mater.Sci. Eng*, **1999**, 80, 453.

15. Kozuka, M.; Tsuchida, T.; Mitani. M. *Tetrahedron Letters*, **2005**, 46, 4527.

16. Dubber, M.; Lindhorst, T.K.; *Org. Letters*, **2001**. 3. 4019.

17. Clark, J.A.; Battle, G.M.; Heming, A.M.; Haddleton, D.M.; Bridge, A.; *Tetrahedron Letters*, **2001**. 42, 2003

18. Ibrahim, K,; Yliheikkila, K.; Abu-Surrah, A.; Lofgren, B.; Lappalainen, K.; Leskela, M.; Repo, T.; Sepala, J.*; Eur. Pol*, *J*. **2004**, 40, 1095.

19. Xue, Z.; Lee, W.B.; Noh, S.K.; Lyoo, W.S. *Polymer.* **2007**, 48, 4704.

20. Keller, R.N.; Wycoff, H.D.; *Inorg. Synth*. **1947**,2,1.

Chapter 4:

Contents *Pages*

4.1. Introduction

In Chapter 3, it was mentioned that the ligand structure which carries a propyl chain or a longer chain of carbons between two coordinating nitrogen atoms may not be able to induce polymerization that yield well-defined polymers under ATRP conditions[1]. Also in Chapter 3, it was suggested that there was a possible reaction between the primary amine groups on the dendrimer surface of **L1** and the methyl methacrylate monomer which occurs *via* a Michael addition reaction[2,3] but this was not proven conclusively. In Chapter 3 it was concluded that aromatic peripheral groups had a negative effect on the performance of these dendrimers as ligands in ATRP. In 2006, Frey and coworkers reported a reaction between a primary amine and an acrylate monomer which occurred *via* a Michael addition reaction to produce hyper-branched ligands.[3] These hyper-branched macro ligands were employed as catalyst components that promoted ATRP. The polymers produced by these hyper-branched macro-ligand systems were well-defined polymers with low polydispersities. As can be observed from the chemical structure of these hyper-branched ligands the length of the carbon chain between two nitrogen atoms is less than three carbon atoms (see Figure 4.1).[3,1] The only possible challenge faced with these hyper-branched macroligands was the difficulty in removing free copper ions from the polymer if the incorrect ratio of copper to ligand is used. This resulted in the polymers produced using these macroligands having a greenish colour attributed to trapped copper ions.

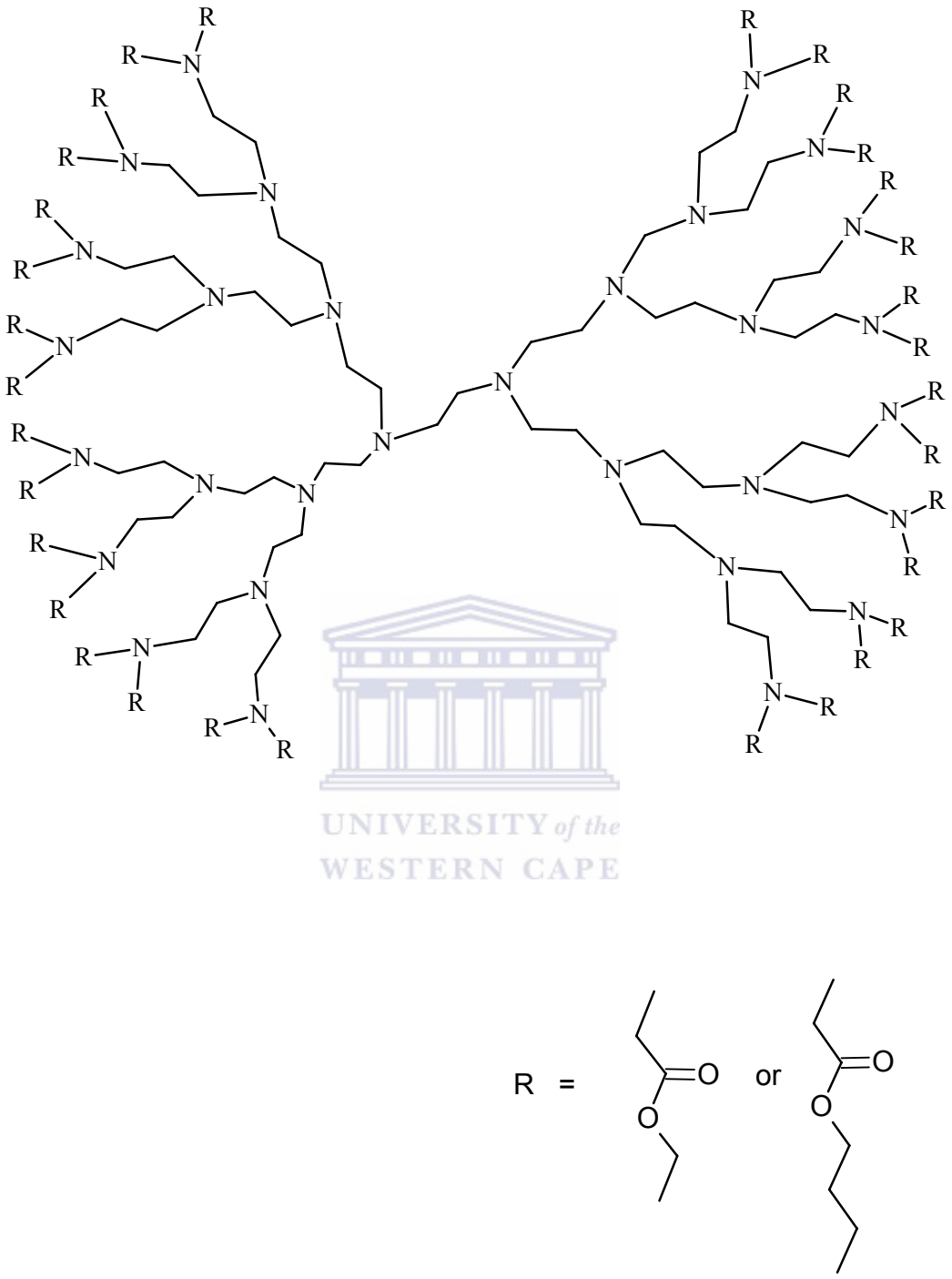

Figure 4.1: *The structure of hyperbranched polyethylenime macroligands*

The chemical structure of these hyperbranched polyethylenimine macroligands in Figure 4.1 represents a good example of a bulky and flexible structure which was

predicted to give very good results under ATRP conditions by Matyjaszewski and coworkers. [1]

4.2. Results and Discussions

Different ligands were used under ATRP conditions in Chapter 3 and the results obtained did not exactly meet the requirements of ATRP. Although all the ligands (**L1**-**L5**) gave reasonable plots of $\ln[MMA]_o/[MMA]$ versus time, the molecular weights of polymers obtained as well as their polydispersities were much higher than expected. All these ligands used in the previous chapter were derived from the DAB based ligand (**L1**) by incorporating aromatic substituents at the surface of the dendrimer ligand **L1**. Some of the ligands obtained were further modified by converting the imine functional groups to amine. Based on the results obtained after employing these ligands (**L2**-**L5**) under ATRP conditions, it was concluded that aromatic substituents did not have the positive or expected influence, especially when compared with the results obtained when unmodified **L1** was used under the same conditions. The main focus of this chapter is to employ modified **L1** with flexible functionalities under ATRP conditions. The modification of **L1** resulted in bulky and flexible ligands **L6** and **L7** which were successfully synthesized and characterized as reported in Chapter 2. The ATRP reactions were performed using **L6** and **L7** as a ligands with purified copper(I) bromide salt as a catalyst in the presence of methyl methacrylate as the monomer in freshly dried 33% p-xylene. The reaction was performed under argon atmosphere at 90^{o}C. Like all the amines studied in this work, the colour of the reaction solution was dark green. Several polymerization reactions were

performed at different ratios of monomer to initiator and the results are discussed in the next section. Each experiment was repeated at least three times in order to test consistency and reproducibility. All the experiments produced white polymers which simply means that there was low level of trapped copper ions if not absent.

4.2. 1. L6 as a ligand in copper mediated ATRP

4.2.1.1. L6 in copper mediated ATRP at ratio of 200:1 (monomer to initiator)

The first polymerization reactions were performed at a ratio of 1:1:2:100 of initiator to ligand to metal to monomer. The reaction mixture formed a gel within 30 minutes. The ratio was then changed to 1:1:2:200 of initiator to ligand to metal to monomer and the reactions were performed under vacuum for twelve hours. The color of the mixture changed from green to brownish-green and there was an observable change in viscosity. At different time intervals, a 1 ml sample was withdrawn to determine the conversions and the molecular weights. The conversions and molecular weights data are displayed Table 4.1.

Table 4.1 *GPC and percentage conversion data for **L6** at 200:1 monomer to initiator*

[L6]:[M_t]:[Monomer]	time (h)	conv (%)	$^{a}M_{n(cal)}$	$^{b}M_{n(GPC)}$	M_w/M_n
1:2:200	2	20	4195	4342	1.12
	4	30	6195	5616	1.12
	7	49	9995	8161	1.09
	10	56	11395	10764	1.07
	12	63	12795	13143	1.07

[a]$M_{n(cal)}$ = calculated or theoretical molecular weight, [b]$M_{n(GPC)}$ = experimental or measured molecular weights. Polymerization of MMA was conducted at 90°C in 33% p-xylene.

After 12 hours the reactions were commonly viscous making it difficult to withdraw further samples. The experimental molecular weights ($M_{n(GPC)}$) of the first sample and the last sample in Table 4.1 exceeded the calculated value slightly. Although these two molecular weights are slightly higher than expected they are still within acceptable limits. The data in Table 4.1 also displays very low polydispersities for the polymers, which is indicative of narrow molecular weight distribution due to minimal or no termination reactions occurring during the polymerization. In Table 4.1 it is shown that there is a linear relationship between M_n and increasing conversion which is characteristic of a controlled ATRP system. The linear semilogarithmic plot of $\ln[MMA]_o/[MMA]$ versus time in Figure 4.2 shows that the polymerization rate is first order with respect to monomer. This linear relationship is indicative of the constant concentration of propagating radicals and low occurrence or absence of termination reactions. The absence of any induction time in this graph is evidence for a high rate of polymerization compared to reactions performed at the same ratio for some of the ligands previously discussed in Chapter 3. The visible homogeneity of the **L6** solution is an encouraging factor observed in these systems, the flexibility of the ligands may have play a positive role in this solubility. The graph in Figure 4.2 further shows that conversion increases with time as expected.

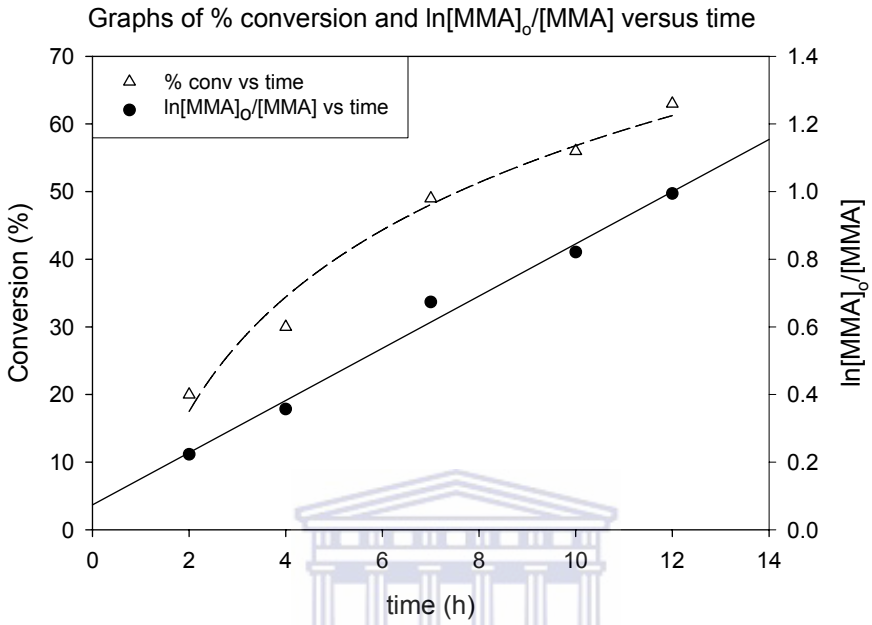

Figure 4.2: *Conversion and Semilorgarithimic kinetic plot versus time of polymerization of MMA with 2-ethylbromoisobutylrate as an initiator and CuBr/**L6** in p-xylene (33% v/v) at 90°C at ratio [MMA]/[initiator]/[CuBr]r/[**L6**] = 200:1:2:1.*

Although the semilogarthimic plot shows that the reaction has a relatively high initial rate, the overall polymerization reaction took a longer period of time to reach its highest conversion (63%) after 12 hours. This decrease of rate with time was attributed to the increase of viscosity as the reaction progressed. This graph indicates that the reaction exhibits all the properties of a controlled ATRP system. The graph in Figure 4.3 shows the relationship between the experimental molecular weights and conversion as well as polydisperisities against conversions. The graph further shows that the experimental molecular weight

($M_{n(GPC)}$) grows linearly with conversion while the molecular weight distribution (M_w/M_n) remains narrow. These results also confirm the absence of or a low level of termination reactions as represented by the straight line graph shown in Figure 4.2.

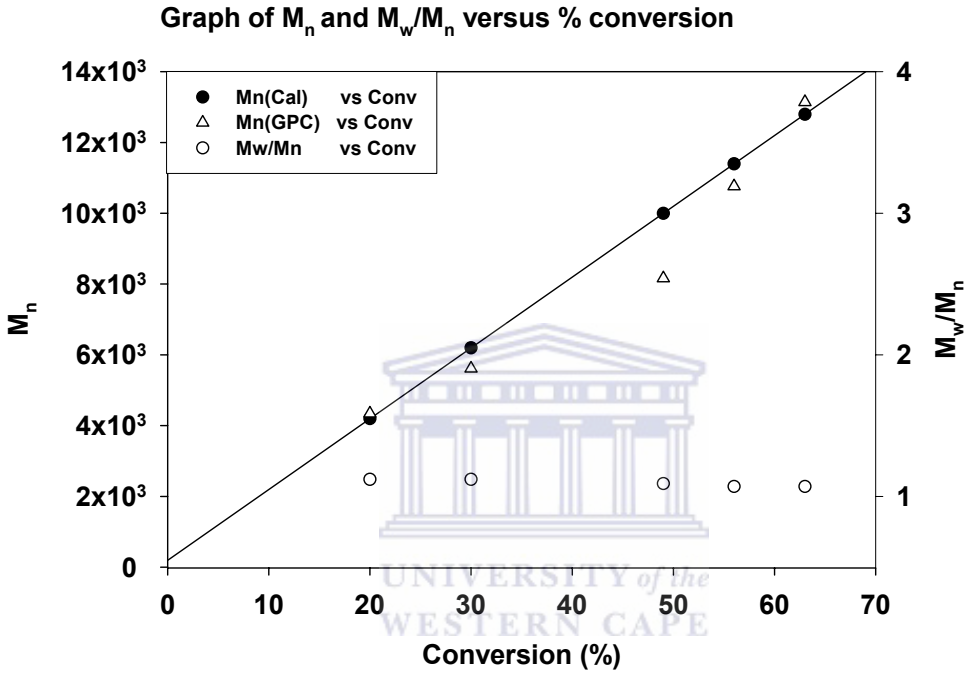

Figure 4.3: *The graph of $M_{n(GPC)}$ and M_w/M_n versus % conversion of polymerization of MMA with 2-ethylbromoisobutylrate as an initiator and CuBr/**L6** in p-xylene (33% v/v) at 90°C at ratio [MMA]/[initiator]/[CuBr]/[**L6**] = 200:1:2:1.*

To satisfy the requirements of ATRP, the experimental molecular weight should not exceed the predicted or theoretical molecular weights. This is observed from the data in Table 4.1. The graph in Figure 4.3 also shows that **L6** at ratio 200:1 of monomer to initiator complied with requirements of ATRP. The $M_{n(GPC)}$ is lower than $M_{n(cal)}$ and the molecular weight shows uniform growth with conversion.

4.2.1.2. L6 in copper mediated ATRP at ratio of 300:1 of monomer to initiator

Given that Ligand **L6** excelled at a ratio 200:1 of monomer to initiator under ATRP conditions this led to exploring other ratios including the ratio of 300:1 of monomer to initiator. The results of this are displayed in Table 4.2 and discussed thereafter.

Table 4.2 *GPC and percentage conversion of mma data for **L6** at 300:1 monomer to initiator*

[L6]:[M_t]:[Monomer]	time(h)	conv(%)	$^aM_{n(cal)}$	$^bM_{n(GPc)}$	M_w/M_n
1:2:300	4	9	2895	4600	1.10
	7	19	5895	5388	1.13
	10	28	8595	6084	1.10
	15	36	10995	7676	1.10

^aM_n(cal) = calculated or theoretical molecular weight, $^bM_{n(GPC)}$ = experimental or measured molecular weights. M_w/M_n = polydispersity. Polymerization of MMA was conducted at 90^oC in 33% p-xylene.

Table 4.2 shows the conversion data for reaction performed at a ratio of 1:2:300 (ligand:metal:monomer) and this is compared with the data in Table 4.1. It is observed that for the reaction at 1:2:200 a conversion 56% was obtained after 10 hours whereas with the 1:2:300 ratio conversion was only 28%. Although the conversions are low using the 300:1 ratio, molecular weight distributions are still narrow. Again the experimental molecular weight ($M_{n(GPC)}$) of the first sample is

higher than the theoretical molecular weight. The low conversions in the case of the ratio of 300:1 compared to the 200:1 ratio could be associated with the low concentration of the catalyst components in the presence of higher monomer concentration. A plot of $\ln[MMA]_o/[MMA]$ and conversion versus time for the reaction times 300:1 depicts a linear progression with time

(Figure 4.4).

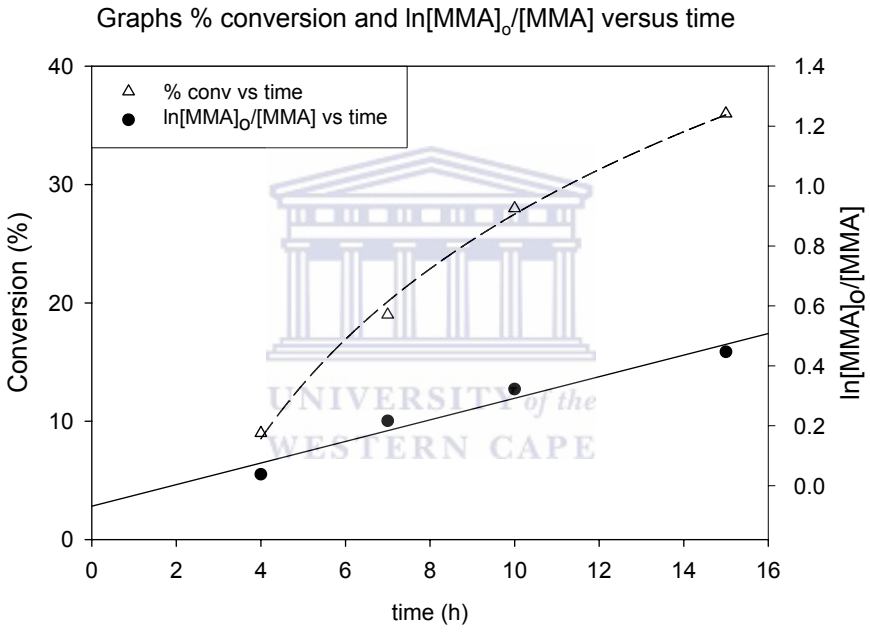

Figure 4.4: *The % conversions and semilorgarithimic kinetic plot versus of polymerization of MMA with 2-ethylbromoisobutylrate as an initiator and CuBr/**L6** in p-xylene (33% v/v) at 90°C at ratio [MMA]/[initiator]/[CuBr]/[**L6**] = 300:1:2:1.*

As mentioned earlier when the monomer concentration is higher and the catalyst components including the initiator are lower in concentration this result in slow chain propagation of the polymer and therefore longer periods of polymerization are observed (Figure 4.4). The linear semilogarimithic graph in Figure 4.4

suggests that there was a constant concentration of propagating radicals and minimal termination reactions. According to the equation $M_w/M_n = 1 + k_p[RX]_o/k_d[M_t^{II}X]\{(2/p -1)\}$ which was discussed in Chapter 3, the high concentration of the copper(II) complex results in uniform polymers being obtained. According to this equation the low polydispersities can be indicative of high concentration of copper(II) complex .The graph in Figure 4.5 confirms that a high concentration of copper(II) complex also stimulates the formation of uniform polymers as predicted by the formula above. In this graph (Figure 4.5) a linear relationship between experimental molecular weights ($M_{n(GPC)}$) and percentage conversion is observed.

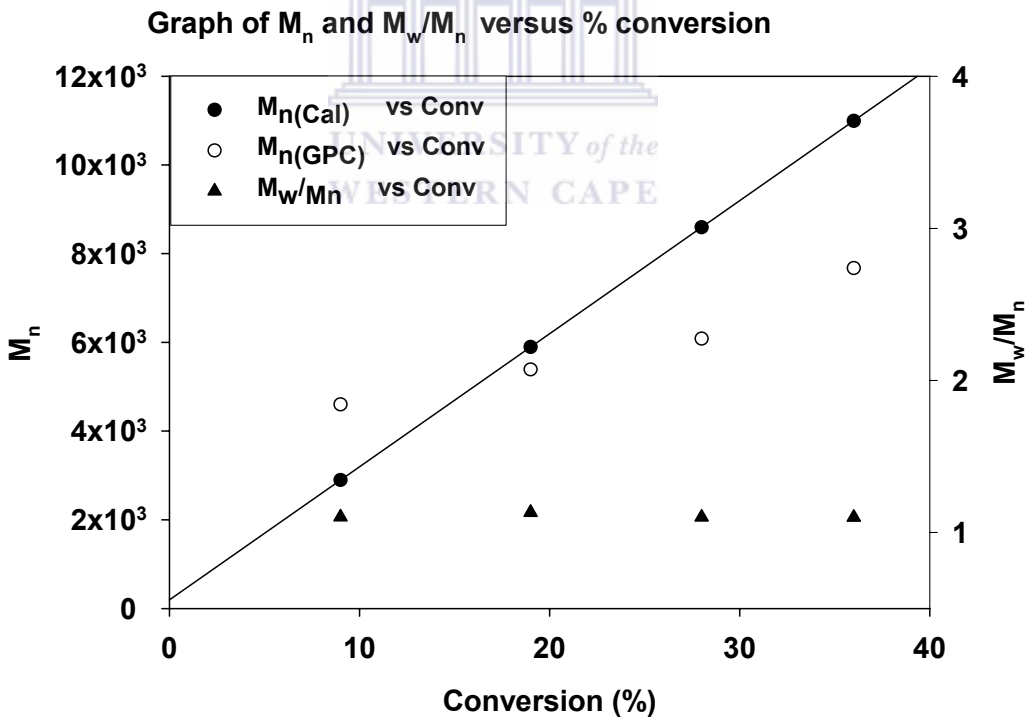

Figure 4.5: *The graph of $M_{n(Cal)}$, $M_{n(GPC)}$ and M_w/M_n versus % conversion of polymerization of MMA with 2-ethylbromoisobutylrate as an initiator and CuBr/**L6** in p-xylene (33% v/v) at 90°C at ratio [MMA]/[initiator]/[CuBr]/[**L6**] = 300:1:2:1.*

There is also an observable decrease of polydispersities with conversion which further indicates that there could be high concentration of a copper(II) complex. The good behaviour of **L6** as a ligand in ATRP catalysis is confirmed by minimal deviation of experimental molecular weight ($M_{n(GPC)}$) from calculated molecular weights ($M_{n(cal)}$) as shown in (Figure 4.5).

In addition uniform polymers were obtained as a result of the minimal number of side reactions being limited (Figure 4.5). Since these results indicate that **L6** is a good ligand for ATRP, there was an interest to know what would happen if a higher generation analogue of **L6** were to be used in ATRP. This question arose not only because generation one ligand, **L6** performed well but also because the hyperbranched macroligands (Figure 4.1) used by Frey and coworkers[3] were much bigger than generation one dendrimer **L6**. These macro-ligands produced polymers within the acceptable limits with narrow molecular weight distributions at high conversion and at very short reaction times. A comparison between these ligands is discussed under the conclusion section but Frey's macroligand is used in that discussion only because both **L6** and **L7** were synthesized based on the procedure which was similar to that used by Frey and coworkers. Both ligand systems carry acrylate functionalities on the periphery. It must be pointed out that the reaction conditions in which **L6** and **L7** were used are completely different to those used by Frey in his polymerizations. Our objectives were to evaluate new dendrimeric ligands in ATRP. There was no direct attempt to

reproduce Frey's work. It should also be pointed out that most of the work reported in this thesis was initiated long before Frey's publication.

4.2.2. L7 as a ligand in copper mediated ATRP

4.2.2.1. L7 in copper mediated ATRP at ratio of 200:1 monomer to initiator

The polymerization reactions of methyl methacrylate using **L7** as a ligand with copper(I)bromide as a catalyst in the presence of 2-bromoethylisobutyrate as initiator were conducted in freshly distilled p-xylene at 90^{o}C under an argon atmosphere. The ratio of the mixture was 1:200:1:4 initiator to monomer to ligand to metal. At the beginning of the reaction a completely homogeneous solution with a dark green colour which changed to a greenish dark-brown color as the reaction progressed was observed. There was no visible change in viscosity during the polymerization process. Samples were withdrawn at different time intervals over an 18 hour period.

Table 4.3 *GPC and percentage conversion of MMA data for **L7** at 200:1 monomer to initiator*

[L7]:[M_t]:[Monomer]	time (h)	conv (%)	$^{a}M_{n\ (cal)}$	$^{b}M_{n(GPC)}$	M_w/M_n
1:4:200	4	16	3395	6298	1.24
	8	26	5395	6821	1.15
	12	32	6595	7979	1.08
	18	38	7795	8450	1.08

$^{a}M_{n(cal)}$ = calculated or theoretical molecular weight, $^{b}M_{n(GPC)}$ = experimental or measured molecular weights, M_w/M_n = polydispersity. The polymerization was conducted at 90^{o}C in 33% p-xylene.

Table 4.3 shows that the polymerization was very slow and conversions were also very low. The molecular weight distributions were narrow and the PDI values decreased as conversion increased. The low conversions were accompanied by low experimental molecular weights. The graphical representation of the results show that the concentration of propagating radicals was constant which means there were minimal termination reactions as displayed in Figure 4.6.

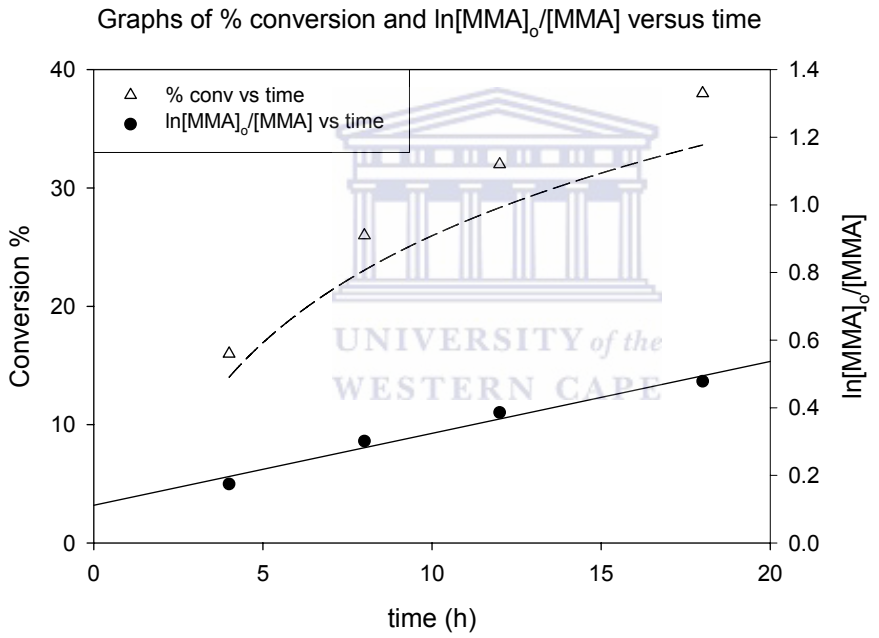

Figure 4.6: *The % conversion and semilorgarithimic kinetic plot versus time of polymerization of MMA with 2-ethylbromoisobutylrate as an initiator and CuBr/**L7** in p-xylene (33% v/v) at 90°C at ratio [MMA]/[initiator]/[CuBr]/[**L7**] = 200:1:4:1*

Figure 4.6 also shows that there was a gradual increase of conversion with time. Similar to the case of **L6** the semilogarithimic plot of $ln[MMA]_o/[MMA]$ versus time

shows linearity and absence of an induction period which is an indication of rapid formation of the active species. The decrease of initiation efficiency as the generation of the dendrimer increased can be attributed to the increase of the number tertiary amine functional groups at the periphery of the ligand. This has previously been observed with other multi-amine ligands.[4] The experimental molecular weights obtained were also graphically interpreted as shown in Figure 4.7.

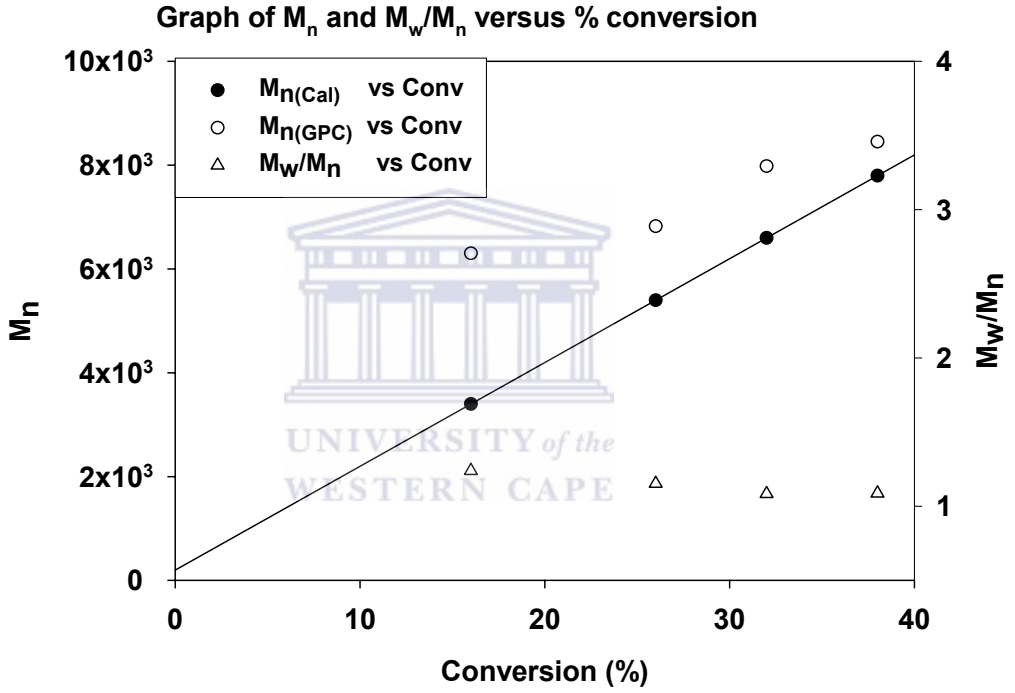

Figure 4.7: *The $M_{n(Cal)}$, $M_{n(GPC)}$ and Mw/Mn versus % conversion of polymerization of MMA with 2-ethylbromoisobutylrate as an initiator and CuBr/**L7** in p-xylene (33% v/v) at 90°C at ratio [MMA]/[initiator]/[CuBr]/[**L7**] = 200:1:4:1*

The two graphs above (Figure 4.6 & 4.7) suggest that **L7** promoted a system that complies with ATRP requirements because the plot in Figure 4.7 shows a linear variance of experimental molecular weights with monomer conversion. There is also a decrease of molecular weight distribution with conversions. The narrow

molecular weight distribution confirms the hypothesis that this system had minimal termination reactions. However, the reason for low overall conversions and longer reaction time is not entirely clear. The bulkiness of the ligand as discussed in the literature and mentioned in Chapter 3 affects the equilibrium between the two oxidation states of the metal by blocking the active species from accessing the metal center and therefore delaying the inter-change of copper between the two different oxidation states. This increase in the number of amines affected the efficiency of the initiation as observed from the graph of theoretical and experimental molecular weights (see Table 4.3). The experimental molecular weights ($M_{n(GPC)}$) are slightly higher than the calculated molecular weights (Table 4.3) and this is confirmed by the graph in Figure 4.7. The polymerization reactions at ratio of 300:1 (monomer to initiator) were attempted, yielding very good results which were reproducible. These results are discussed in the next section.

4.2.2.2. L7 in copper mediated ATRP at ratio of 300:1 (monomer to initiator)

The same experimental procedure as described previously was followed. As expected a green colour was observed at the beginning which turned brown towards the end of the reaction. The reaction at (300:1) ratio gave very low conversions at the beginning of the reaction but as the reaction progressed, the conversion improved until a change in viscosity was observed towards the end of the reaction (Table 4.4). At this ratio of 300:1 slightly better conversions were obtained than those of reactions at 200:1 ratio (Table 4.4). A good performing

system is observed from the kinetic plot of $\ln[MMA]_o/[MMA]$ versus time in Figure 4.8 which give a straight line showing that the polymerization rate was first order with respect to monomer.

Table 4.4 *GPC and percentage conversion of mma data for **L7** at 300:1 monomer to initiator*

[L1]:[M_t]:[Monomer]	time (h)	conv (%)	$^{a}M_{n\,(cal)}$	$^{b}M_{n\,(GPC)}$	M_w/M_n
1:4:300	5	12	3885	3869	1.36
	9	33	10035	9772	1.16
	13	39	11895	12106	1.16
	18	42	12675	13105	1.13

$^{a}M_{n(cal)}$ = calculated or theoretical molecular weight, $^{b}M_{n(GPC)}$ = experimental or measured molecular weights, M_w/M_n = polydispersity. The polymerization was conducted at 90°C in 33% p-xylene.

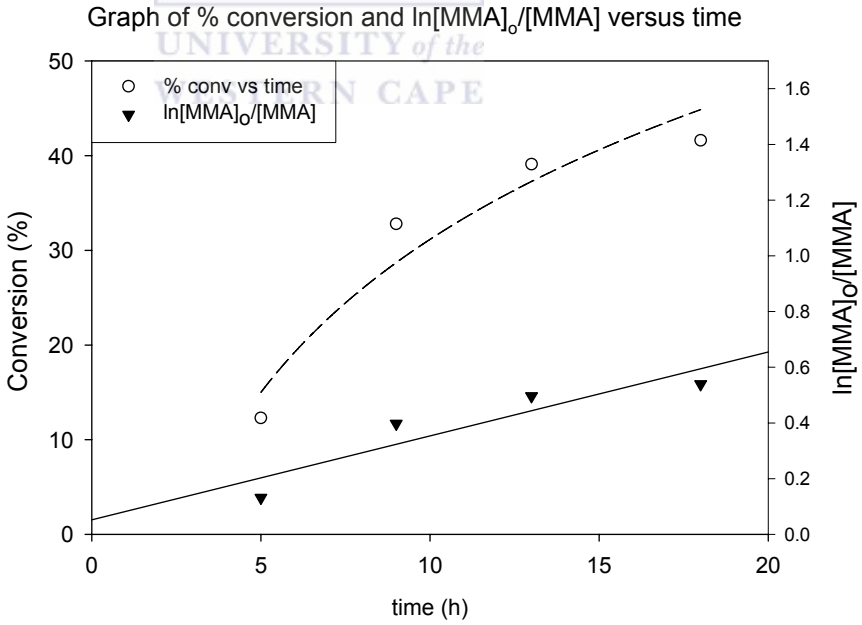

Figure 4.8: *The % conversion and semilorgarithimic kinetic plot versus time of polymerization of MMA with 2-ethylbromoisobutylrate as an initiator and CuBr/**L7** in p-xylene (33% v/v) at 90°C at ratio [MMA]/[initiator]/[CuBr]/[**L7**] = 300:1:4:1*

Figure 4.8 also shows an increase of conversion with time whereas the graph in Figure 4.9 a linear increase of molecular weight with conversion is observed. The graph confirms that polymerization using **L7** at 300:1 monomer to initiator although shown slightly higher conversion than at 200:1, the molecular weight distribution remained narrow. The initiator efficiencies are close to 1, similar to those of 200:1. This can be observed also in Figure 4.9 where experimental molecular weights almost equal theoretical ones.

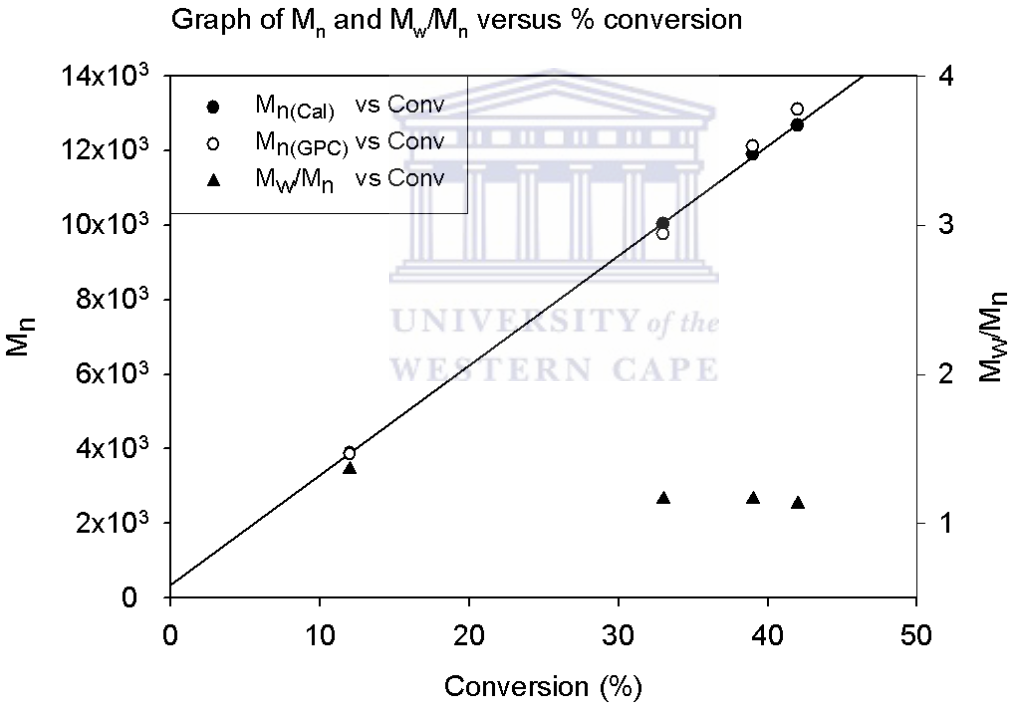

Figure 4.9: *The $M_{n(GPC)}$ and M_w/M_n versus % conversion of polymerization of MMA with 2-ethylbromoisobutylrate as an initiator and CuBr/**L7** in p-xylene (33% v/v) at 90°C at ratio of [MMA]/[initiator]/[CuBr]/[**L7**] = 300:1:4:1*

4.3. General discussion and conclusion

In the foregoing sections the outcome of ATRP reactions for each of the two ligands **L6** and **L7** was discussed in detail. In this section we now compare the performances of these ligands at their different reaction ratios under ATRP conditions. These comparisons will help us draw pertinent conclusions about the behavior of these ligands. We also tried to compare results from this research with similar literature systems.

4.3.1 The kinetic results of ligands L6 and L7

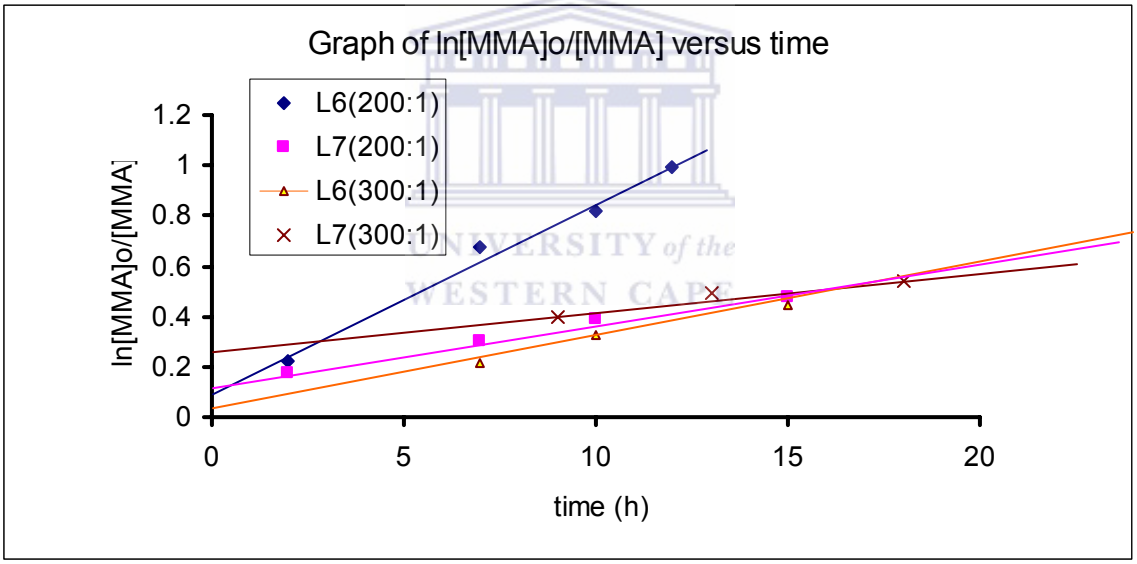

Figure 4.10: *Semi-logarithmic kinetic plot of polymerization of MMA with 2-ethylbromoisobutylrate as an initiator and CuBr/**L6** in p-xylene (33% v/v) at 90°C at ratio of [MMA]/[initiator]/CuBr/[**L6**] = 200:1:2:1*

The semilogarithimic plots of $\ln[MMA]_o/[MMA]$ versus time show straight lines for **L6** and **L7** at 200:1.The other curves for **L7** and **L6** at 300:1 are also linear but not as perfect. The graph for the **L7** at 200:1 is the one that showed the highest

polymerization reaction rate of all the other systems. It took a little longer for the **L7** systems to achieve percentage conversion of above 30%. These graphs are proof of the efficiency of aliphatic substituents and they clearly show that these ligands have managed to overcome the difficulties exhibited by the ligands discussed in Chapter 3. Similar behaviour was observed with the hyperbranched polyethylenimine ligands reported by Frey and coworkers.[3] These hyperbranched macroligands are similar in structural design to **L6** and **L7** except for the fact that they have an ethylene chain between two adjacent nitrogen atoms. Also, the structure of the hyperbranched polyethylenimine macroligands is less regular than that for **L6** and **L7**. The linear polymerization shown in the semilogarithimic plots above is a behavior common to all working systems of ATRP. This includes the systems based on common nitrogen containing ligands such as those employed by Matyjaszewski and coworkers.[5,6] Most nitrogen based ligands of Matyjaszewski were also simple tertiary amines They were also bulky but smaller compared to the ligands in this chapter. It was noted that 1,1,4,7,10,10-hexa-methyl tri-ethyl tetra-amine (HMTETA) which is one of these simple tertiary amine ligands gave faster polymerization rates than those of bipyridine ligands. This was due to the fact that the complex formed between copper and simple amines have lower redox potentials than the copper-bipyridine complex[5]. Based on these discussion it is concluded that kinetic results of **L6** and **L7** are in agreement with the literature results as discussed earlier.

4.3.2. Conversions and molecular weights of L6 and L7

To further compare the performance of **L6** and **L7** with the literature systems, it made sense to use the results of the hyperbranched polyethylenimine (HPEI) macroligand reported by Frey and coworkers.[3] This ligand HPEI has a similar structural design as ligands in this chapter in that it has butyl acrylate functionality and **L6** and **L7** have methyl methacrylate at the periphery and they are all synthesized in a similar fashion that making them essentially belong to the same class of compounds.

Table 4.5. The GPC and percentage conversion for HPEI, **L6, L7** for comparison reasons

[**L**:][Monomer]: [initiator]	time(h)	conv(%)	$M_{n(cal)}$	$M_{n(GPC)}$	M_w/M_n
HPEI(254:1)	3	79	$2.03x10^4$	$2.63x10^4$	1.27
HPEI(254:1)	4	90	$2.31x10^4$	$2.89x10^4$	1.24
L6(200:1)	4	30	$6.20x10^4$	$5.62x10^4$	1.12
L6(200:1)	12	63	$12.79x10^4$	$13.14x10^4$	1.07
L6(300:1)	8	21	$6.49x10^4$	$6.08x10^4$	1.10
L6(300:1)	10	28	$8.59x.10^4$	$7.68x10^4$	1.10
L7(200:1)	12	32	$6.59x10^4$	$7.98x10^4$	1.08
L7(200:1)	18	38	$7.79x10^4$	$8.45x10^4$	1.08
L7(300:1)	13	39	$11.89x10^4$	$2.16x10^4$	1.16
L7(300:1)	18	42	$12.67x10^4$	$13.11x10^4$	1.13

$M_{n(cal)}$ = calculated or theoretical molecular weight, $M_{n(GPC)}$ = experimental or measured molecular weights. HPEI was performed at ratio 1:254 initiator to monomer in dioxane as a solvent at 80^{o}C and **L6** and **L7** were both performed in p-xylene as a solvent at 90^{o}C.

The results in Table 4.5 show clearly that HPEI achieved high conversions over a shorter reaction time compared to **L6** and **L7** but polydispersities were higher than those of **L6** and **L7** ligands although all of them meet the ATRP requirements. **L7** (200:1) had the lowest conversions and the reaction proceeded much slower than all other systems. At first, this could be attributed to the bulkiness of this ligand compared to **L6**. However, bulkiness of **L7** could not be the reason for lower conversion because **L7**(300:1) is even better than **L6**(300:1) which is smaller in size than **L7.** The reason therefore is not entirely clear. The HPEI ligand is even bigger in size than both **L6** and **L7** but it still managed to produce high conversions in shorter period. The possible reasons for the lower conversions achieved with **L6** and **L7** could be attributed to the reaction conditions such as the solvent and temperature.[12] These polymerization reactions were performed at exactly the same conditions as the polymerization in Chapter 3 for reason of comparison and also because the original idea was to modify **L1** and observe the effect. The HPEI reactions were performed at completely different conditions but they were only quoted in this chapter was just to do comparison based on the structural make up where there some similarities. Although HPEI is similar in structure to the two ligands under investigation it has an ethylene chain linker between the nitrogen atoms. This could impact on the performance of the ligand as mentioned in Chapter 3. Despite the lower conversions and slower reaction rates showed by **L6** and **L7**, all the systems complied with the requirements of ATRP. Therefore, **L6** and **L7** results are in

some agreement with literature results. The narrow molecular weight distribution of these polymers can be clearly observed from their GPC traces (Figure 4.11),

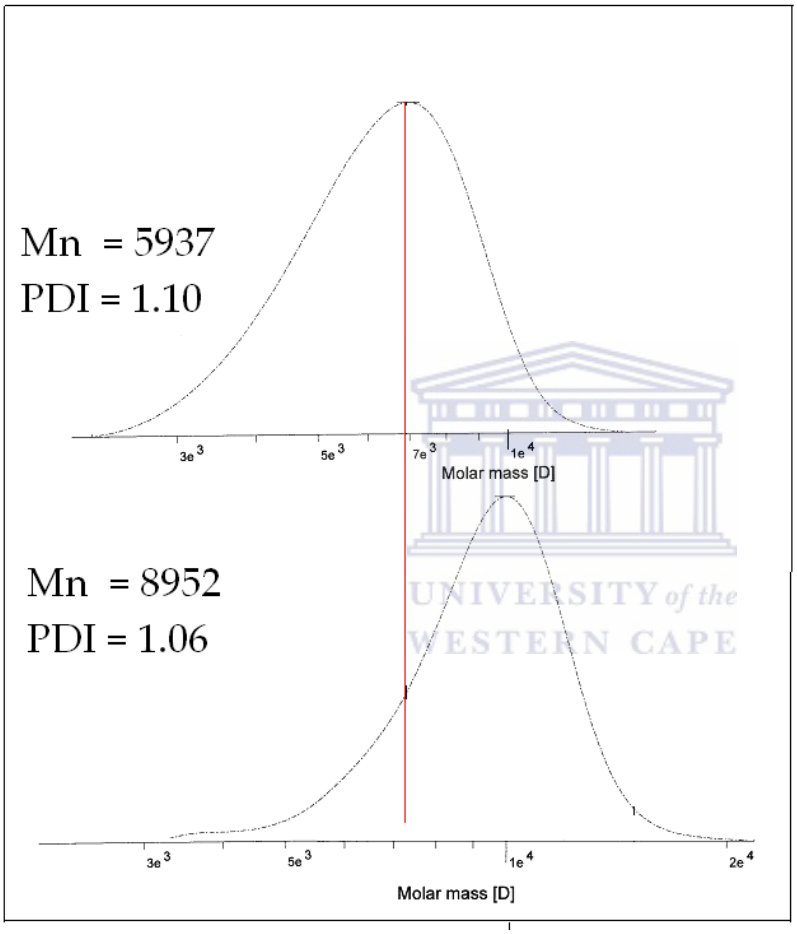

Figure 4.11: *GPC trace taken from* ***L6****(200:1) top and* ***L7****(200:1) bottom at 30% and 39% conversion respectively.*

4.4. End group analysis

The polymers produced via ATRP have a unique characteristic in that the resulting polymers resemble the initiator especially if the initiator is an alky halide.

Normally the alkyl and the halide groups of the initiator are observed at the α and ω terminal ends of the polymer chain.[7-11] If the polymer chain produced via an ATRP mechanism carries these characteristics described in this section, then it is expected to behave as an alkyl halide macro-initiator to re-initiate polymerization, since it is supposed to be a living polymer. Polymerization that produce living polymers will usually follow the general mechanism of ATRP as given in Scheme 1.2 of Chapter 1. In order to see if our polymers satisfy the above condition of a living polymer a proton NMR spectrum of the polymer was recorded to analyze the end groups of our polymer chains. As can be observed from the spectrum in Figure 4.13, there is a multiplet at δ = 4.10 ppm associated with methylene protons **1** (see Figure 4.12) of the ethoxy group at the α-terminal end. The peaks at δ = 3.80 ppm belonged to the methyl ester protons **5** (see Figure 4.12) adjacent to the terminal bromide atom at the ω-terminal end. The strong peak at δ = 3.60 ppm was assigned to the protons **4** of methoxy group of the polymer backbone which shifted to δ = 3.80 ppm in the presence of the terminal bromide as mentioned for protons **5**. The strong peaks δ = 0.85 ppm and δ = 1.03 ppm were associated methyl protons **3** on the polymer backbone and the methyl protons **7** at the ω-end of the polymer chain. The less intense peaks observed at δ = 1.25 ppm was attributed to methyl protons **6** of the ethoxy group at ω-terminal of the polymer chain. The strong peak at δ = 1.8 ppm was assigned to methylene protons **2** at the backbone of the polymer. From this analysis it can be concluded that we did not only obtained a living polymer but also a well-defined polymer.

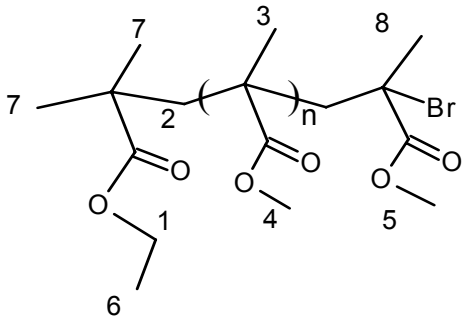

Figure 4.12: *The chemical structure of terminally functionalized ATRP produced MMA polymer.*

The structural designation in Figure 4.12 corresponds with the assignments on the ^{1}H NMR spectrum in Figure 4.13 .

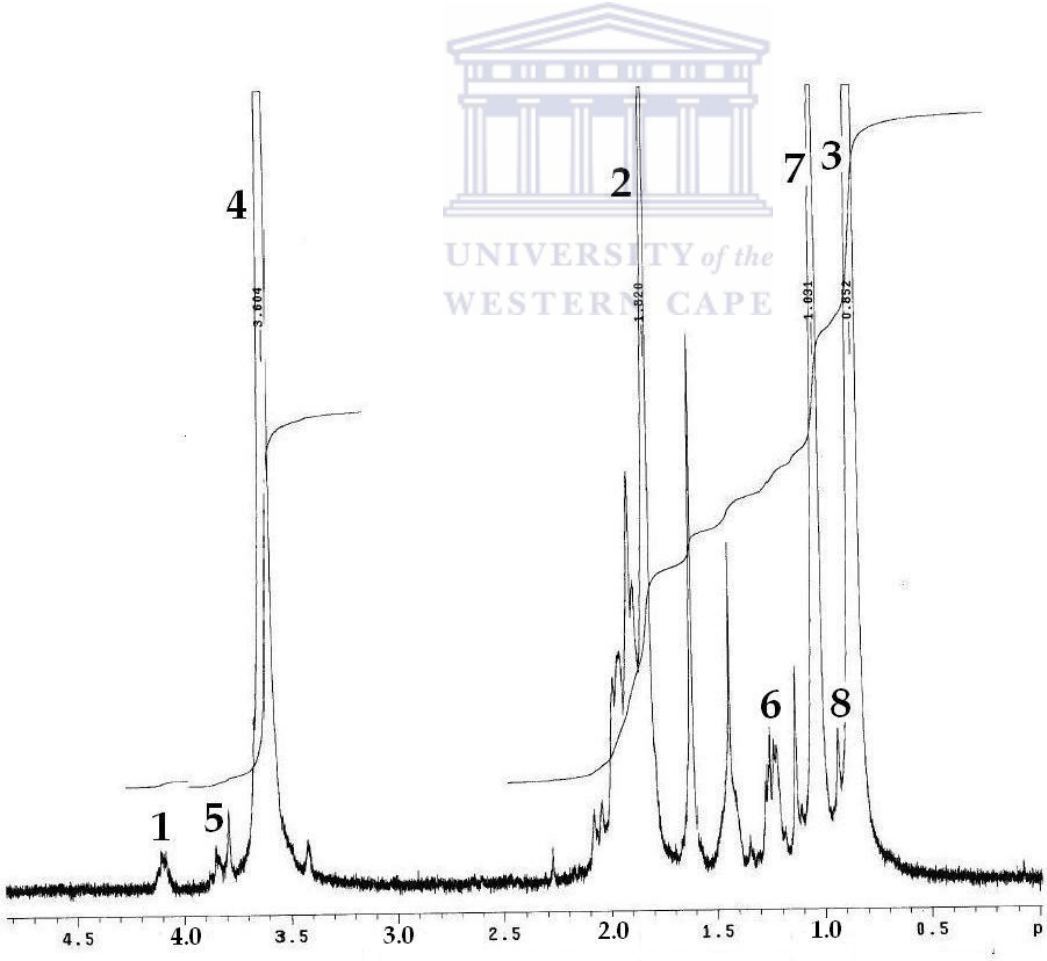

Figure. 4.13: *The ^{1}HNMR spectrum of bromide and ethyl isobutyrate terminated ATRP produced MMA polymer.*

4.5 Preliminary studies of copper mediated ATRP of styrene using L6 and L7 as ligands

In the previous sections of this Chapter, the best performance by *methyl methacrylate functionalized DAB (**L6** and **L7**)* as ligands in the ATRP of methyl methacrylate was reported. One of the most important characteristics of ATRP above and beyond its living and controlled nature is the ability to polymerize a wide range of monomers which cannot be polymerized by known living ionic polymerization methods.[12-16] Although the focus of this work was limited to studying the performance of the newly synthesized ligands in the ATRP of methyl methacrylate, the good results obtained in this Chapter encouraged us to do a preliminary investigation of the ligands (**L6** and **L7**) in the polymerization of styrene.

As indicated at the beginning of Chapter 3 the nickel complex (Ni{ o,o'-$(CH_2NMe_2)_2$- C_6H_3 }Br was unable to polymerize styrene at high temperature but managed to polymerize methyl methacrylate when the temperature was lowered. This observation suggested that it is possible for a catalyst system to work for one monomer but fail to polymerize another. We thus wondered whether the catalyst system used this Chapter would polymerize styrene given the fact that it would require higher temperatures especially since the polymerization is metal

chloride-mediated.[12] It is known that each monomer has a specific equilibrium property and has different optimal polymerization conditions, which include temperature, type of catalyst and nature of the solvent.[17] As was mentioned in previous chapters of this work, ATRP relies on the reversible reaction of a low-oxidation state metal complex with an alkyl halide generating radicals and the corresponding high oxidation state metal complex.[17,18] In most cases bromide containing copper-catalysts are said to be more efficient radical deactivators compared to chloride containing copper catalysts and therefore bromide based catalysts are preferred.[19-21] However, in special cases such as the ATRP of styrene in the presence of a nucleophilic solvent, the chloride based copper catalyst proved to be essential.[19] Mixed halide initiation systems are known to produce better control over molecular weight in the ATRP of methyl methacrylate especially in a nonaqueous medium.[19] The loss of molecular weight control in copper mediated ATRP of styrene in nonaqueous medium was observed by Gibson and co-workers.[22] This loss of control of molecular weight occurred when a bromide based initiator was used in conjunction with a bromide metal salt. This situation was attributed to side reactions promoted in the bromide initiator systems. This could be overcomed by the use of a mixed halide based catalyst. The improved molecular weight control observed when these mixed halide based catalysts were used was due to the faster initiation because of the weaker carbon halide bond of the alkyl bromide initiator and slower propagation due to the stronger carbon-chloride bond.[22,23] The polymer produced in the reactions promoted by these mixed halide based catalyst systems had chloride chain ends

because of the high strength of carbon-chloride bond.[22,23] As we were aiming to achieve improved catalytic systems with better control of molecular weight of the polystyrene polymer, we were forced to use a mixed halide based catalyst systems as our initiation system. In the attempt to polymerize styrene under ATRP conditions, copper chloride as a catalyst was used instead of the copper bromide used in Chapter four. The alkyl halide initiator used was 1-ethylphenyl bromide. This was thus a mixed halide based catalyst system because our initiator was an alkyl bromide and the salt was copper chloride (Scheme 4.1). The advantages of having the polymer chains terminated by chloride instead of bromide chain ends is that as mentioned above that carbon-bromide bond is very susceptible to side reactions which lead to unwanted chain branching.

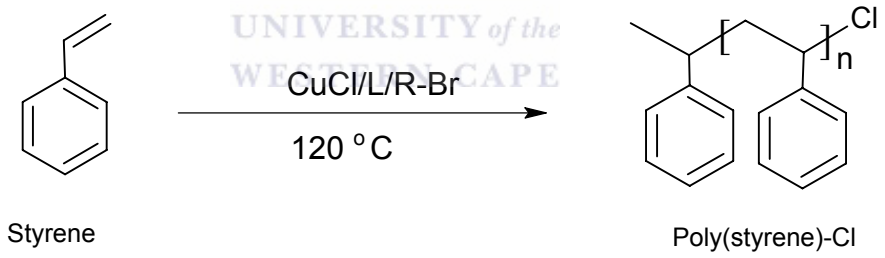

Styrene

Poly(styrene)-Cl

R-Br = 1-phenylethyl bromide

Scheme 4.1: *ATRP of styrene using a mixed halide based catalyst system*

4.5.1 Results and Discussion

As already indicated in the introduction polymerization of styrene was performed at 120 °C using a mixed halide catalyst system mainly consisting of copper

chloride as a catalyst and 1-ethylphenylbromide as an initiator in 33% of p-xylene as a solvent in the presence of **L6** and **L7** as ligands. The outcome of these reactions is discussed below.

4.5.1.1. L6 in ATRP of styrene at ratios 100:1 and 200: 1 of monomer to initiator

According to the data in Table 4.6 which shows the results of the reaction performed at 100:1 ratio of (monomer to initiator), about 47% conversion was achieved in 13 hours.

Table 4.6 *GPC* data *and percentage conversion of styrene for **L6** at 100:1 monomer to initiator*

[L6]:[M_t]:[Monomer]	time (h)	conv (%)	$^{a}M_n$(cal)	$^{b}M_{n(GPC)}$	M_w/M_n
1:2:100	4	34	3595	5483	5.44
	7	39	4095	7428	5.59
	10	44	4595	8300	3.13
	13	47	4895	10271	2.63

$^{a}M_{n(cal)}$ = calculated or theoretical molecular weight, $^{b}M_{n(GPC)}$ = experimental or measured molecular weights, M_w/M_n = polydispersity. The polymerization was conducted at 120^{o}C in 33% p-xylene.

Table 4.7 shows that a 200:1 monomer to initiator ratio gives a maximum conversion of 43% in 13 hours which is reasonable. The reaction periods for reactions done at both ratios are long compared to the best performing catalyst system. However, what is normally important is the nature of the polymer

produced. In both of the above cases a gradual increase of experimental molecular weight with conversion was observed. These experimental molecular weights when compared with theoretical molecular weight ($M_{n(cal)}$) are slightly high for ratio of 100:1 whereas in the case of 200:1 only the last two samples show slightly higher molecular weights.

Table 4.7 *GPC data and percentage conversion of styrene for **L6** at 200:1 monomer to initiator*

[L6]: $[M_t]$:[Monomer]	time (h)	conv (%)	$^{a}M_n$ (cal)	$^{b}M_{n\ (GPC)}$	M_w/M_n
1:2:200	4	26	5395	4107	4.25
	7	29	5995	4802	4.74
	10	33	6795	6602	4.11
	13	43	8795	10271	2.21

$^{a}M_{n(cal)}$ = calculated or theoretical molecular weight, $^{b}M_{n(GPC)}$ = experimental or measured molecular weights, M_w/M_n = polydispersity. The polymerization was conducted at 120^{o}C in 33% p-xylene

These slightly high molecular weights are accompanied with fairly high polydispersities. The reason for the high polydispersities is not well understood but the nature of GPC traces show polymodal molecular weight distributions. Such polymodality was previously observed by Tsarevsky and Matyjaszewski in the ATRP of 4-vinylpyridine.[20,21] This was attributed to chain branching resulting from the reaction of the bromide terminated polymer chain with the nitrogen atom in pyridine ring of the monomer. [20,21] To suppress this chain branching they used

mixed halide based catalyst systems consisting of copper chloride as a catalyst. In our case a mixed halide based catalyst system was used and the monomer was different in that it did not contain N-atom.

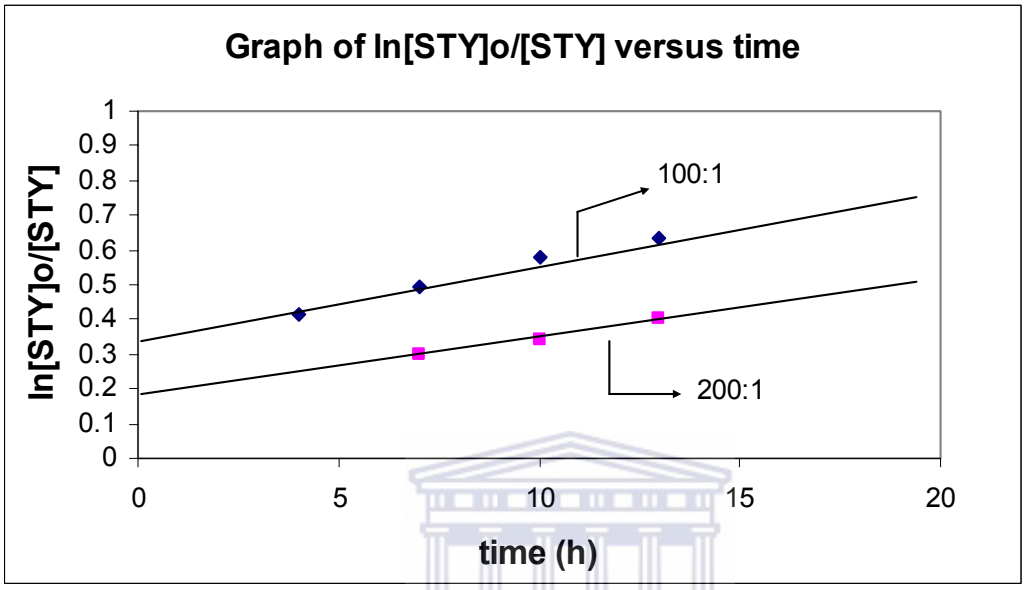

Figure 4.14: *Semilogarithimic kinetic plot versus time of polymerization of styrene with 1-phenylethyl bromide as an initiator and CuCl/**L6** in p-xylene (33% v/v) at 120°C at ratios [styrene]/[initiator]/[CuCl]/[**L6**] = 100:1:2:1 and 200:1:2:1.*

In the semilogarithimic kinetic plots, at different ratios show a perfect straight line which indicates low concentration of active radicals produced which minimizes or the chances of termination reactions occurring. This is not unexpected for the mixed halide base catalyst systems. This theory states that the high strength of the bond between the terminal carbon of the polymer chain and chloride should cause the slow propagation of the growing chain. The slow propagation leads to

a uniform polymer. In addition, the strength of the carbon chloride bond limits the possibility of side reactions.

4.5.1.2 L7 in ATRP of styrene at ratios 100:1 and 200:1 of monomer to initiator ratio

The data in Table 4.8 show the percentage conversions and the molecular weights of the polymer obtained using the mixed halide based catalyst system with **L7** as a ligand at ratio of 100:1 (monomer to initiator). The percentage conversion reached 63% which is the best for this type of ligand in a relatively short reaction period compared with **L6** above. The conversion as well as experimental molecular weight ($M_{n\ (GPC)}$) increases with time. At a ratio 100:1, **L7** produced high molecular weight (higher than the targeted values) polymer with high polydispersities which indicates loss of control over molecular weight.

Table 4.8 *GPC data and percentage conversion of styrene for **L7** at 100:1 monomer to initiator*

[L6]: $[M_t]$:[Monomer]time (h)		conv(%)	$^{a}M_n$(cal)	$^{b}M_{n(GPC)}$	M_w/M_n
1:4:100	5	29	3095	4141	4.03
	8	40	4195	8903	2.87
	12	63	6495	11136	2.95

$^{a}M_{n(cal)}$ = calculated or theoretical molecular weight, $^{b}M_{n(GPC)}$ = experimental or measured molecular weights, M_w/M_n = polydispersity. The polymerization was conducted at 120^{o}C in 33% p-xylene

In the case of the 200:1 ratio in Table 4.9, the maximum percentage conversion is lower than that of the reaction done at 100:1 ratio but the conversion increases with time and molecular weight. Although the experimental molecular weights are within the acceptable range according ATRP requirements, the polydispersities are very high. The same explanation as above about the polydispersities for **L6** also applies in this case.

Table 4.9 *GPC data and percentage conversion of styrene for **L7** at 200:1 monomer to initiator*

[L7]:[M_t]:[Monomer]	time(h)	conv(%)	[a]$M_{n(cal)}$	[b]$M_{n(GPC)}$	M_w/M_n
1:4:200	5	25	5195	5286	7.77
	8	36	7395	9906	3.21
	12	43	8795	9956	3.24
	16	46	9395	10734	2.50

[a]$M_{n(cal)}$ = calculated or theoretical molecular weight, [b]$M_{n(GPC)}$ = experimental or measured molecular weights, M_w/M_n = polydispersity. The polymerization was conducted at 120^oC in 33% p-xylene

The semi-logarithimic plot of the reaction at 200:1 shows a perfect straight line indicative of the first order polymerization rate with respect to the monomer. The one disappointing aspect about this data is the polydispersities which disqualifies these systems as controlled living ATRP. The reason for this behaviour is not entirely understood.

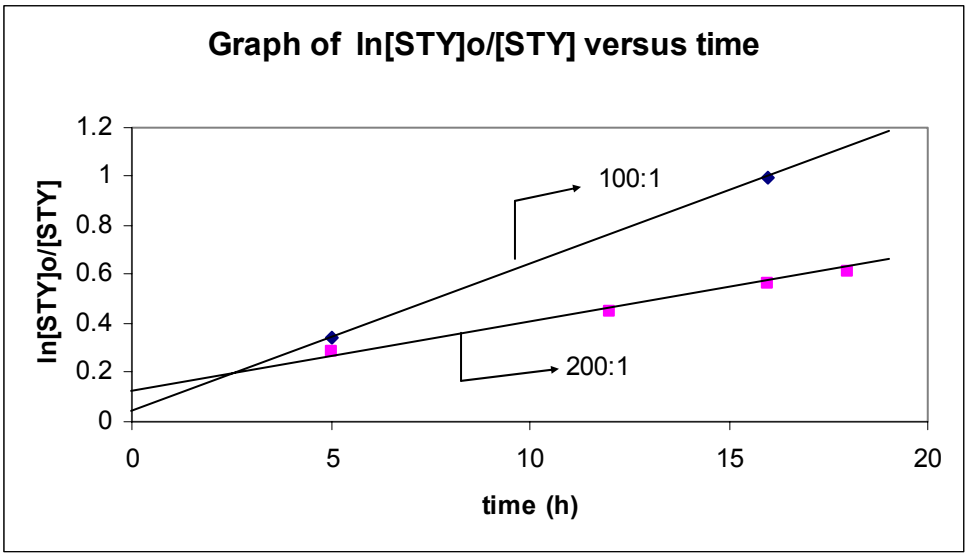

Figure 4.15: *Semilogarithimic kinetic plot versus time of polymerization of styrene with 1-phenylethyl bromide as an initiator and CuCl/**L7** in p-xylene (33% v/v) at 120°C at ratios [styrene]/[initiator]/[CuCl]/[**L7**] = 100:1:4:1 and 200:1:4:1.*

In Figure 4.16, a sample of a GPC trace (B) shows the definite polymodal nature for the molecular weight distribution of these polymers. The GPC trace for polymethyl methacrylate is included for comparison. When compared to the GPC trace (A) for polymethyl methacrylate using a similar catalyst system, it can be seen that A is fairly smooth without a low molecular weight trail. The distribution is narrow which explains its low polydipersity index. The graph for polystyrene shows a shoulder of higher molecular weight. The broadness of these peaks also gives a clear indication that high polydispersity index will be obtained.

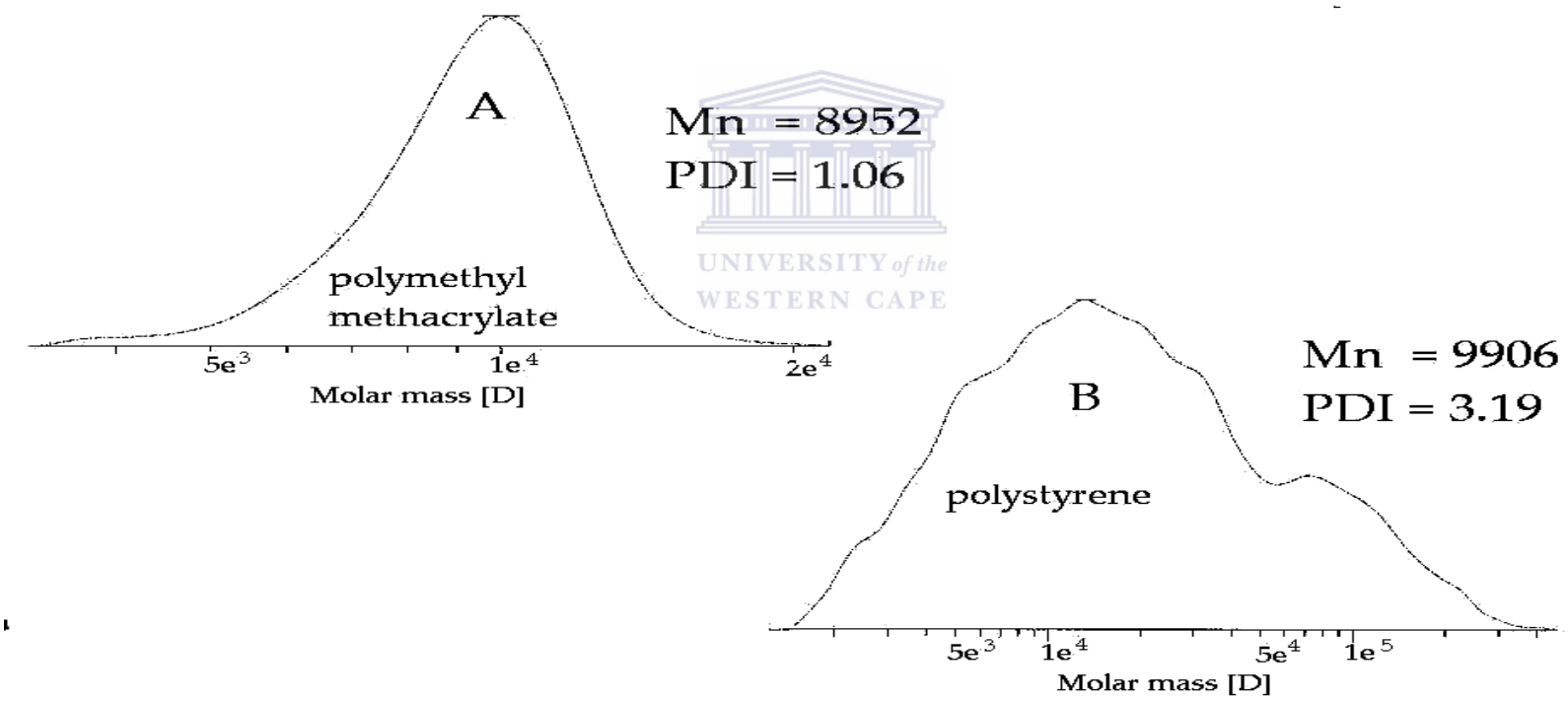

Figure.4.16: *GPC traces for polymethyl methacrylate and polystyrene at different molecular weights.*

4.5.2 Conclusions

The performance of **L6** and **L7** as ligands in ATRP of styrene was not as good as was observed for methyl methacrylate, although the semi-logarithimic plots were very promising in their nature. Based on the statement that each monomer has a specific equilibrium constant and optimal polymerization conditions which include concentration, temperature, type of catalyst and solvent, further investigation should be conducted by changing the conditions.[14] It is clear that the type of catalyst which involved a *mixed halide based catalyst system* may not be good for this reaction. It is therefore suggested the same catalyst system used in Chapter four should be tested. It is also known that to achieve low polydisperisities with styrene low temperature are ideal because there will be less chances of thermal self-initiation by styrene.[14] Therefore temperature as well as the nature of the solvent should also be varied when changing the type of catalyst. In conclusion, it can be said that the investigation performed in this work has laid groundwork for further investigation of these two ligands in ATRP of styrene and other monomers.

4.6 Experimental Method

4.6.1 Material

All experimental manipulations were conducted under argon atmosphere using standard Schlenk line techniques. All solvents were freshly distilled before use. P-xylene was purchased from Kimix Chemicals and dried over sodium/benzophenone ketyl under

argon atmosphere. 1-ethylpheylbromide was supplied by Sigma-Aldrich and distilled before use. Styrene and methyl methacrylate were purchased from Sigma-Aldrich and passed through a column of basic alumina and distilled twice over calcium hydride before use. Methanol was purchased from Kimix Chemicals and used as received whereas Tetrahydrofuran (HPLC grade) was obtained from Anatech and was used as received. Cu(I) Chloride (99%) and Cu(I) Bromide were purchased from Sigma-Aldrich and purified according to the literature.[24] Nylon membrane solvent filters were source from Anatech.

4.6.2. Instrumentation

The monomer conversions were monitored using Gas Chromatography (Varian CP-3800:column: HP-PONA 50 m x 0.200 mm (agilent technologies Inc)). Molecular weights were determined using Gel Permeation chromatography {Agilent 1100 series: columns : PLgel 10 µm 500Å, PLgel 5 µm Mixed-C (300 x 7.5 mm), PLgel 5µm Mixed-D (300 x7.5 mm) and guard column PLgel 5 µm (50 x 7.5 mm)}.

4.6.3. General polymerization procedure of methyl methacrylate

An oven dried Schlenk tube equipped with a magnetic stirrer bar was charged with purified CuBr, ligand, freshly distilled MMA (10 ml), and freshly distilled and dried solvent (33% vol). The tube was sealed under vacuum before performing three freeze-pump-thaw cycles followed by addition of freshly distilled ethyl 2-bromoisobutyrate. The mixture was placed in an oil bath at 90^{o}C and the vessel sealed under vacuum. After certain time intervals, the tube was opened under positive pressure of argon and a 1ml sample was withdrawn and transferred into vial containing THF.

-*General characterization of polymer samples*: The samples were then taken for GC analysis using 1-decene as internal standard to determine the conversion. The samples were then passed through the column of basic alumina before precipitation with methanol. The polymers obtained were dried for least a day before the molecular weight determination using GPC. Molecular weights of polymethyl methacrylate were calibrated with polymethyl methacrylate standards purchased from Polymer Laboratories

4.6.4. General polymerization procedure of styrene.

An oven dried Schlenk tube equipped with a magnetic stirrer bar was charged with purified CuCl, the ligand, freshly distilled styrene (10.ml), and freshly distilled and dried solvent (33% vol). The tube was sealed under vacuum before performing three freeze-pump-thaw cycles followed by addition of freshly distilled ethyl 2-ethylphenylbromide. The mixture was placed in an oil bath at 120 ^{o}C and the vessel was sealed under vacuum. After certain time intervals, the tube was opened under positive pressure of argon and a 1 ml sample was withdrawn and transferred into vial containing THF (9 ml) and the vessel sealed under vacuum to continue with experiment. The procedure was carried out until the last sample was withdrawn.

-*General characterization of polymer samples*: The samples were then analyzed by GC using 1-decene as an internal standard to determine the conversion. The samples were then passed through a column of basic alumina before precipitation with methanol. The polymers obtained were dried for least 24hrs before the molecular weight determination using GPC. Molecular weights of polystyrene were calibrated with polystyrene standards purchased from Polymer Laboratories.

4.7. References:

1. Xia, J. ; Zhang, X.; Matyjaszewski, K. *Polym. Mater.Sci. Eng*. **1999**, 80, 453.
2. Dubber, M.; Lindhorst, T.K. *Org. Letters*. **2001**, 3, 4019.
3. Shen, Z.; Chen, Y.; Frey, H.; Stiriba, S.E. *Macromolecules*. **2006**, 39, 2092.
4. Kumar, K.R.; Kizhakkedathu, J.N.; Brook, D.E. *Macromol. Chem. Phys*. **2004**. 35. 4849
5. Xia, J. ; Gaynor, S.G. ; Matyjaszewski, K. *Macromolecules*. **1997**, 30, 7697.
6. Karlin, K.D.; Zubeita, J. **1993**. Copper Coordination Chemistry: Biochemical and Inorganic Perspective: Adernine Press, New York.
7. Haddleton, D.M. ; Crossman, M.C. ; Dana, B.H. ; Duncalf, D.J. ; Heming, A.M; Kukulj, D.; Shooter, A.J. *Macromolecules*. **1999**, 32, 2110.
8. Granel, C.; Dubois, Ph.; Jerome, R.; Teyssie. Ph. *Macromolecules*. **1996**, 29, 8576.
9. Ibrahim, K,; Yliheikkila, K.; Abu-Surrah, A.; Lofgren, B.; Lappalainen, K.; Leskela, M.; Repo, T.; Sepala, *J. Eur. Pol*. J. **2004**, 40.,1095.
10. Ando, T. ; Kato, M. ; Kamigaito, M. ; Sawamoto, M. *Macromolecules*. **1996**, 29, 1070.
11. Chen, X.P.; Qui, K.Y.; *Macromolecules.* **1999**. 32. 8711.
12. Matyjaszewski, K.; Patten, T.; Xia, J. *J. Am. Chem. Soc*, **1997** 119, 674.
13. Percec, V.; Barboiu, B.; Neumann, A.; Ronda, J.C.; Zhao, M.; *Macromolecules*, **1996**, 29, 3665.

14. Grubbs, R.B.; Hawker, CJ.; Dao, J.; Frechet, J.M.J. *Angew. Chem. Int. Ed. Engl*. **1997**, 36, 27.

15. Matyjaszewski, K*. Macromolecules*, **1997** 30, 2216.

16. Matyjaszewski, K.; Wang, J-L.; Grinaund, T.J.; Shipp, D.A. *Macromolecules*. **1998**, 31, 1527.

17. Matyjaszewski, K.; Xia, J.; *Chem. Rev*, **2001**, 101, 2921.

18. Kamigaito, M.; Ando, T.; Sawamoto, M. *Chem. Rev*. **2001**, 101, 3689.

19. Jewrajka, S.K,; Chatterjee, U.; MandaL, B.M. *Macromolecules,* **2004,** *37,* 4325.

20. Tsarevsky, N. V.; Pintauer, T.; Matyjaszewski. K. *Macromolecules,* **2004,** *37, 9768*.

21. Tsarevsky, N. V.; Braunecker, W.A.; Brooks, S.J.; Matyjaszewski. K. *Macromolecules.* **2006,** *39,* 6817.

22. O' Reilly, R.K.; Shaver, M.P.; Gibson, V.C.; White, A.J.P. *Macromolecules.* **2007**, 40, 7441.

23. Matyjaszewski, K.; Wang, J-L.; Grinaund, T.J.; Shipp, D.A.; Patten, T. *Macromolecules*. **1998**, 31, 6836.

24. Keller, R.N.; Wycoff, H.D.; *Inorg. Synth*. **1947**, 2,1.

CHAPTER 5:

5.1 Overall conclusions:

The main aim of this study was to design new polyfunctional ligands based on the polypropyleneimine dendrimer DAB-$(NH_2)_4$ referred to as **L1** in this work, to be used in copper mediated atom transfer radical polymerization (ATRP) of vinyl monomers. These ligands were synthesized by modifying DAB-$(NH_2)_4$ with aromatic and aliphatic substituents on the nitrogen atoms at the periphery of **L1**.

Two classes of ligands viz. imines (**L2** and **L4**) and tertiary amines (**L3** and **L5**) were successfully synthesized and fully characterized suing a range of spectroscopic techniques. These ligands were then evaluated in the copper mediated ATRP of methyl methacrylate at monomer to initiator ratios of 100:1 and 200:1. All the ligands produced polymers at a ratio of 100:1 monomer to initiator. Ligands **L1** to **L5** however did not conform to all ATRP requirements even at a ratio of 200:1(monomer to initiator). Of the ligands **L1**-**L5**, **L1** performed the best at the ratio 200:1 (monomer : ligand)

Although some of the ligands evaluated yielded promising results in terms of giving active catalysts, the experimental molecular weights of polymers obtained in these reactions were far higher than the theoretical molecular weights. The molecular weight distribution (MWD) of the polymers produced using these ligands (**L1-L5**) were also rather broad. This led us to conclude that these catalytic systems based on the above mentioned ligands failed to produce polymers that met the requirements of controlled living radical polymerization which should normally yield polymers with polydispersity

values of less than 1.5. This was also the case when styrene polymerization was attempted with the same ligands. Once again the polymerization results were not encouraging. As the styrene polymerization results were similar to those of obtained for MMA they are not reported here. Although **L1** also did not completely satisfy the ATRP requirements, the degree of deviation from expected ATRP behaviour, its performance was better than the other ligands. From this it can be concluded that aromatic peripheral groups which were part of a secondary amine system performed poorly in the ATRP reactions. Attempts were made to prepare 3º amine analogues directly from **L4** and **L5** were not successful.

The noticeable difference between the results of **L1** and other ligands was that the molecular weights of polymers produced from the catalyst systems based on these aromatic functionalized ligands were far higher than theoretical molecular weights whereas for **L1** the target was only exceeded slightly (see Table 3.2 in Chapter 3). This observation supports the conclusion that the aromatic substituents had a negative influence on the performance of these ligands. In addition this observation also suggested that **L1** required a different modification approach for it to be effective in ATRP. This prompted further modification of **L1** by reacting it with methyl methacrylate.

Modification of **L1** using methyl methacrylate led to **L6** which was more flexible in its structure than **L2** – **L5**. In addition it also had 3º amine groups as opposed to 2 º amine groups. The 2nd generation analogue of **L6** was also successfully prepared as **L7**. When these ligands (**L6** and **L7**) were used in the ATRP of methyl methacrylate

acceptable results that met the requirements of controlled living ATRP were obtained. These ligands performed better at ratios of 200:1 and 300:1 (monomer to initiator). The results obtained using these two ligands brought us to the conclusion that flexible structures and tertiary amines have a positive impact on the performance of these ligands in ATRP. It was also clear that **L1**-**L5** were not appropriate ligands to promote ATRP. This conclusion agrees with literature reports that aromatic ring carrying structure of ligands such as bipyridine based ligands were not as good aliphatic tertiary amines in ATRP. A preliminary investigation into the use of these ligands (**L6** and **L7**) in the ATRP of styrene proved to be not effective. However further work is needed to investigate whether the process can be improved by optimizing the reaction conditions.

Conditions such as temperature, solvent, concentration and the nature of the active will significantly influence these types of polymerization reactions. This preliminary study used a mixed halide catalyst system. The reason for adopting this approach of mixed metal halide systems was based on literature precedence as stated previously. Failure of our catalysts to perform effectively in styrene polymerization might mean that the choice of a mixed halide system might not have been the correct one. This would have to be verified in future investigations. It is clear that a fair amount of additional work have to be done before a final conclusion about the efficacy **L6** and **L7** in ATRP of styrene can be made.